CHALMERS
UNIVERSITY OF TECHNOLOGY

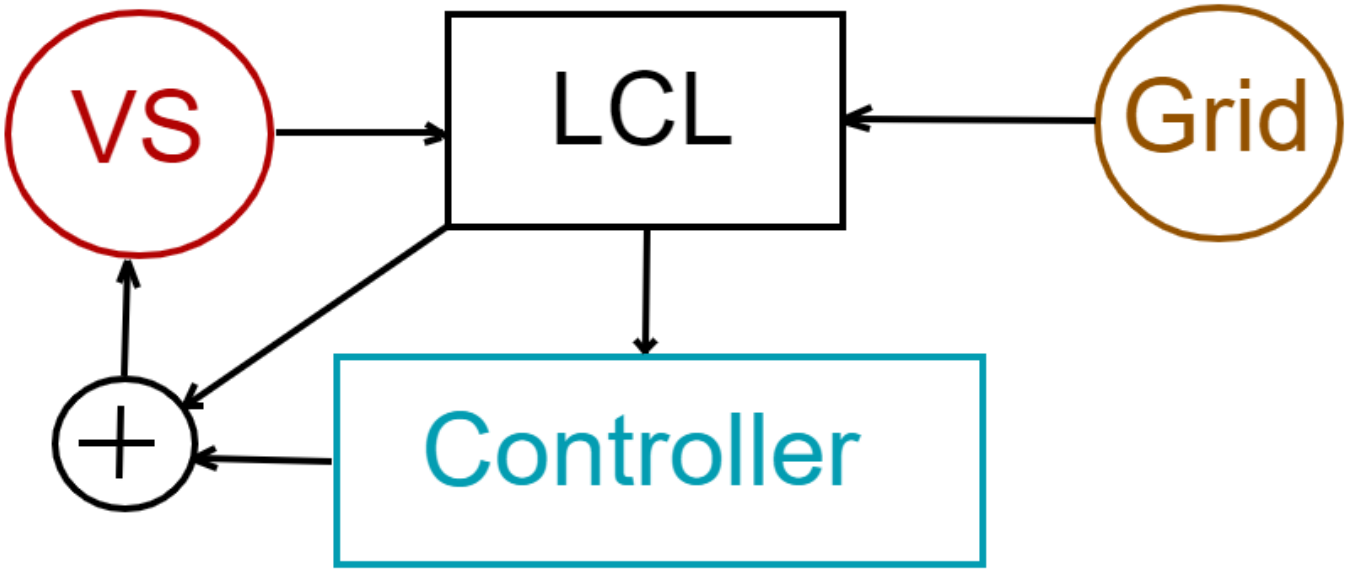

Current control of grid connected converter using LCL filter

An analysis of the performance of differing control methodologies and evaluation of the current behaviour depending on sensor placement

Master's thesis in Systems, Control and Mechatronics

Anna Ferm
Erik Gustavsson

DEPARTMENT OF ELECTRICAL ENGINEERING
CHALMERS UNIVERSITY OF TECHNOLOGY
Gothenburg, Sweden 2023
www.chalmers.se

Master's thesis 2023

Current control of grid connected converter using LCL filter

An analysis of the performance of differing control methodologies and evaluation of the current behaviour depending on sensor placement

Anna Ferm
Erik Gustavsson

CHALMERS
UNIVERSITY OF TECHNOLOGY

Department of Electrical Engineering
Division of Electric Power Engineering
Chalmers University of Technology
Gothenburg, Sweden 2023

Current control of grid connected converter using LCL filter
An analysis of the performance of differing control methodologies and evaluation of the current behaviour depending on sensor placement
Anna Ferm
Erik Gustavsson

Supervisors: Daniel Chädström, Aros electronics AB
Filip Karlsson, Aros electronics AB
Examiner: Torbjörn Thiringer, Department of Electrical Engineering

Master's Thesis 2023
Department of Electrical Engineering
Division of Electric Power Engineering
Chalmers University of Technology
SE-412 96 Gothenburg
Telephone +46 31 772 1000

Cover: The system in question, showing the LCL filter, Grid, VS and controller blocks and their connections.

Typeset in LaTeX
Printed by Chalmers Reproservice
Gothenburg, Sweden 2023

Current control of grid connected converter using LCL filter
An analysis of the performance of differing control methodologies and evaluation of the current behaviour depending on sensor placement
Anna Ferm
Erik Gustavsson
Department of Electrical Engineering
Chalmers University of Technology

Abstract

This report describes how to construct different control schemes and evaluate them in regards to controlling a current in a system using a grid connected converter and an LCL filter. The control schemes in question are a PI controller that controls a DC version of the current as well as a PR, an LQR and an LQG controller operating with the AC currents. The controlled current will be analysed in how well the controllers are able to mitigate peak errors when drastic changes occur, as well as its ability to follow a steady state when the system is noisy. Additionally the controllers are tested with extra harmonic mitigation tactics such as additional integrator terms in the frequency of the harmonic component, changing the placement of the current sensor and the controllers are also tested with a Smith predictor that looks one and two steps ahead.

The conclusion is that for the base system the LQG is the absolute best controller because it follows the reference closely and reacts quickly to great changes while still having very low amounts of oscillation. The LQR is the second strongest controller but it has oscillation problems. The LQG is the most affected controller by changes in the grid impedance. Since it is a model based controller that also uses a model based Kalman filter, it overreacts a lot if the grid impedance is weak. The result is an unacceptable amount of oscillation which leads to the conclusion that a PI might be better when the grid is unknown or that the grid needs to be estimated before using the LQG. The problems discussed for the LQG are the same for the Smith predictor, it gives an overall stronger performance to the system but causes oscillation when it poorly estimates the true grid impedance.

Keywords: LCL filter, current control, grid converter, PI controller, PR controller, LQR, LQG, feed-backward, feed-forward, prediction.

Acknowledgements

First of we would like to thank Aros electronics AB and more specifically our supervisors Daniel Chädström and Filip Karlsson for their invaluable help and support during this master thesis. They have continuously provided insight and knowledge throughout the entire process and it would not have been possible without them.

Secondly we would like to express our outmost gratitude to our examiner Professor Torbjörn Thiringer, who has been vital in providing structural feedback and support. We would also like thank our opposition Daniel Quach for his input and feedback.

Anna Ferm, Gothenburg, June 2023

Erik Gustavsson, Gothenburg, June 2023

List of Acronyms

Below is the list of acronyms that have been used throughout this thesis listed in alphabetical order:

AC	**A**lternating **C**urrent
DC	**D**irect **C**urrent
FF	**F**eed **F**orward
LCL	Inductor Capacitor Inductor
LQE	**L**inear **Q**uadratic **E**stimator
LQG	**L**inear **Q**uadratic **G**aussian
LQR	**L**inear **Q**uadratic **R**egulator
MPC	**M**odel **P**redictive **C**ontrol
PI	**P**roportional **I**ntegral
PLL	**P**hase **L**ocked **L**oop
PR	**P**roportional **R**esonance
PWM	**P**ulse **W**idth **M**odulation
RMS	**R**oot **M**ean **S**quare
SS	**S**tate **S**pace
VSI	**V**oltage **S**ource **I**nverter

Nomenclature

Below is the nomenclature of indices, sets, parameters, and variables that have been used throughout this thesis.

Indices

k	Index for time step
h	Index for harmonic component

Parameters

A_c	State space matrix for continuous time
A_{cont}	A general SS matrix for continuous time
A_d	State space matrix for discrete time
A_{disc}	A general SS matrix for discrete time
B_c	State space matrix for continuous time
B_{cont}	A general SS matrix for continuous time
B_d	State space matrix for discrete time
B_{disc}	A general SS matrix for discrete time
C_1	Capacitor in the LCL filter
C_c	State space matrix for continuous time
C_{cont}	A general SS matrix for continuous time
C_d	State space matrix for discrete time
C_{disc}	A general SS matrix for discrete time
D_c	State space matrix for continuous time
D_{cont}	A general SS matrix for continuous time
D_d	State space matrix for discrete time
D_{disc}	A general SS matrix for discrete time

J	The cost to be reduced in the LQR cost function
K	The Kalman gain for the LQG controller
K_1	Part of integral term in PR and LQR/LQG controllers
K_2	Part of integral term in PR and LQR/LQG controllers
K_I	Integral term in PI and PR controllers
k_{I_1}	Boolean determining whether or not I_1 will be an output of the SS model
k_{I_2}	Boolean determining whether or not I_2 will be an output of the SS model
k_{V_c}	Boolean determining whether or not V_c will be an output of the SS model
K_P	Proportional term in PI and PR controllers
K_{PI}	The combined gain for the PI controller
K_{PR}	The combined gain for the PR controller
L	The LQR/LQG gain
L_1	The inductor closest to the controller in the LCL filter
L_2	The inductor closest to the grid in the LCL filter
M	A vector with one 1 and the rest zero giving the state to be controlled in the LQR controller
N	Matrix giving the intensity and cross correlation of the noise in the state space model
P	The solution to the Riccati equation used to derive the Kalman gain
Q_1	One of the weighting matrices for the LQR controller gain
Q_2	One of the weighting matrices for the LQR controller gain
R	The noise intensity matrix for the state space model
R_1	The noise intensity for the states in the state space model
R_{12}	Determines the cross correlation in the noise intensity matrix for the state space model
R_2	The noise intensity for the input in state space model
R_{L1}	The resistance of the inductor closest to the controller in the LCL filter
R_{L2}	The resistance of the inductor closest to the grid in the LCL filter
S	Matrix used to solve for optimal L gain
s	The Laplace operator variable
T_s	Step time for discrete case

u	Input in the state space models
v_1	White noise
v_2	White noise
ω_0	The frequency an R term compensates at
ω_{0h}	The frequency at harmonic degree h that an R term want to compensate at
ω_c	The bandwidth the R term compensates around ω_0

Variables

I_1	Measured current going through L_1
I_2	Measured current going through L_2
I_{refe}	The estimated reference current for the LQR and LQG
I_{refm}	The measured reference current for the LQR and LQG
V_c	Measured voltage over C_1
V_g	Applied voltage from the grid
V_{in}	Voltage applied by the controller
x	The states in the state space models
$\dot{x}$	The rate of change of the states in the state space models
$\widetilde{x}$	The estimation error of the states in the state space models
$\dot{\widetilde{x}}$	The estimation error of the rate of change of the states in the state space models
$\hat{x}$	The estimated states in the state space models
$\dot{\hat{x}}$	The estimated rate of change of the states in the state space models
z	The z-transforms operating variable
z_c	The state to be controlled in the LQR

Contents

1 Introduction

1.1 Problem background

Todays power-grids use three phase alternating voltage (AV). From this grid it is possible to extract a three phase alternating current (AC) by generating a new AV and matching it with the grid AV. The differences between the two voltage sources will cause a current to flow and it is the control of this current that this thesis will study. The system used for this purpose is a grid connected converter using an LCL filter. This system is a three phase current system but the voltage source inverter (VSI) is unable to handle unsymmetrical voltages well [1, Ch. 3.5, pp. 140-154]. One way to avoid the problem with unsymmetrical currents is to split up and control each individual phase on its own [2]. The one phase base system is shown in Figure 1.1.

There are several aspects that needs to be considered which makes this control problem non-trivial. Firstly there is white noise, harmonic components, phase shifts and grid drops in the grid voltage, all of which needs to be compensated for. In addition there are always errors in the measurements and reading delays which means that the generated voltage will always be sent out some time after it is optimal to generate it.

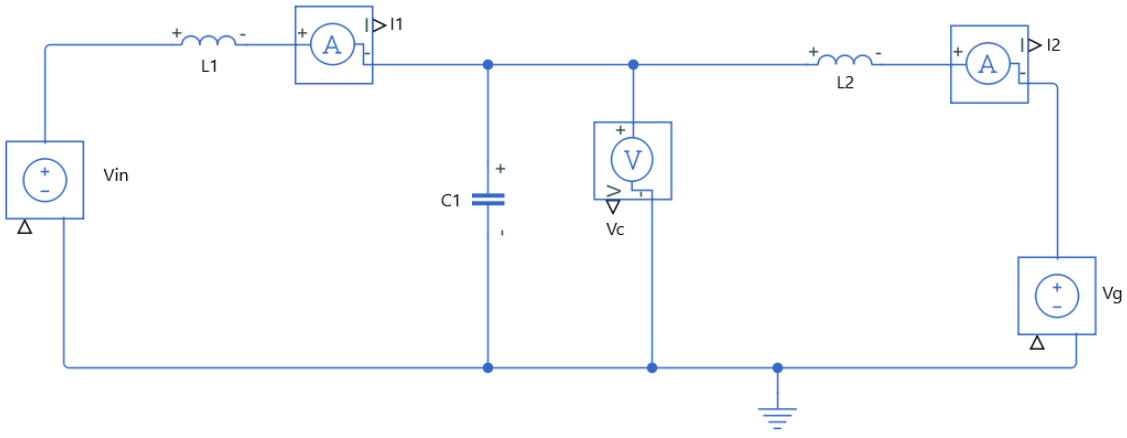

Figure 1.1: The LCL filter implemented in Simscape. The inductor L1 uses has the inductance L_1 and the resistance R_{L1}. Inductor L2 has an inductance L_2 as well as a resistance, R_{L2}. The capacitor does have a resistor in reality but it is so small that it is assumed to be zero.

Figure 1.1 shows the two inductances, L_1 and L_2, as well as the capacitance C_1. The voltage over the capacitance will always be measured and that voltage will be referred to as V_c. There are two possible points to measure the current, I_1 and I_2, where the major difference is on what side of the capacitor the current is measured on. I_2 is the current that is important in the sense that it is what will be sent out to or from the grid. I_1 is more expensive to measure but it is important to have knowledge of. If the current in I_1 oscillates then the components of the chip will be damaged.

1.2 Previous work

Several single phase LCL filters have been implemented previously, often with proportional integral (PI) controllers for the current control. Most control schemes uses both the I_1, I_2 as well as V_c but there was a request from Aros to only measure one of the currents in order to be more cost effective. Additionally the measured V_c signal is used in a feed forward (FF) fashion. The base current used for measurements is the I_1 current. These methods and implementations will be used as the base for the thesis work.

1.3 Purpose

The purpose of this thesis is to find alternative control solutions to the control problem. These control solutions are meant to be evaluated based on the performance of the LCL filter and controller in regards to:

- Following of reference current in a timely manor.
- Suppressing influence from non ideal voltage, meaning amplitude differences and phase shifts.
- Avoidance of unwanted behaviour and mitigation of undesired current components in the measured LCL current.
- Handling of the unknown grid inductance and resistance.
- The advantages and disadvantages of reading current from I_2 instead of from I_1. Where I_2 is the current closest to the grid and I_1 affects the components of the LCL the most. It is therefore important to mind any oscillations reading from I_2 rather than I_1 might cause.

1.4 Delimitation

- 1) Only one phase of the three phase system will be analysed.
- 2) The outer loop that would exist in a real system will not be considered here.
- 3) Pulse width modulation (PWM) will not be implemented and approximations will be used instead.
- 4) Clock speeds and computational power of chips and the computational need of the different control methods will not be considered.

- 5) Since a complete model was not provided by Aros, one was made instead. Some assumptions and possible simplifications has therefore been made.
- 6) It is assumed that the measurement of the voltage V_c is fast and accurate enough that its derivative is usable in estimation.

These delimitations have been evaluated and deemed appropriate for the thesis work:

1) The implementation of a three phase system is rather complex and small errors in the controllers may lead to larger errors since the controllers are used multiple times. If instead one phase is implemented and controlled properly then it is simple to duplicate the controllers to each of the three phases in the equivalent three phase system. Using only one phase also gives a focus on the entirety of one signal instead of the combination of several.

2) Not taking into account the effect the outer loop may have on the system and the controllers performances is a simplification which affects the results of this thesis. The missing outer loop might have had a positive effect on some results, which will not be taken into account in this thesis and is therefore a delimitation which is vital to take into account when using this thesis as a guide for choosing a possible control method.

3) Instead of implementing a PWM, a sinusoidal signal will be run through a zero order hold to approximate the same thing. This is to decreases the amount of work and research needed into areas not directly concerning the thesis task.

4) While the cost of using different chips with different clock speeds is important in a practical application, it will not be considered here. The reason for that is that the time and effort needed to do a complete and accurate evaluation would limit the time different control schemes could be analysed. In addition it is mainly the performance of different schemes that are of interest in this report not the cost of implementation.

5) Conversations with Aros were ongoing but assumptions were still made.

6) It may not be possible to, in practise, estimate the I_c current using the derivative of V_c. To take the derivative, over a small amount of time, of a signal with a large amount of noise could in practise cause larger disturbances in the result than is seen in this report.

2

Theory and Methodology

This chapter contains the theory and methodology of this report, where the system in question as well as the control techniques are explained.

2.1 3 phase and grid

The LCL system is usually operating towards a three phase voltage system and used to exchange power to ordinary grids and a three phase voltage is visualised in Figure 2.1. It is simpler to control a single phase sinusoidal instead so the signal will be split up into 3 parts and sent into 3 identical systems. This means that the only thing that the system needs to handle is the single phase shown in Figure 2.2 instead of the output voltage [1, Ch. 2.4, pp. 54-60].

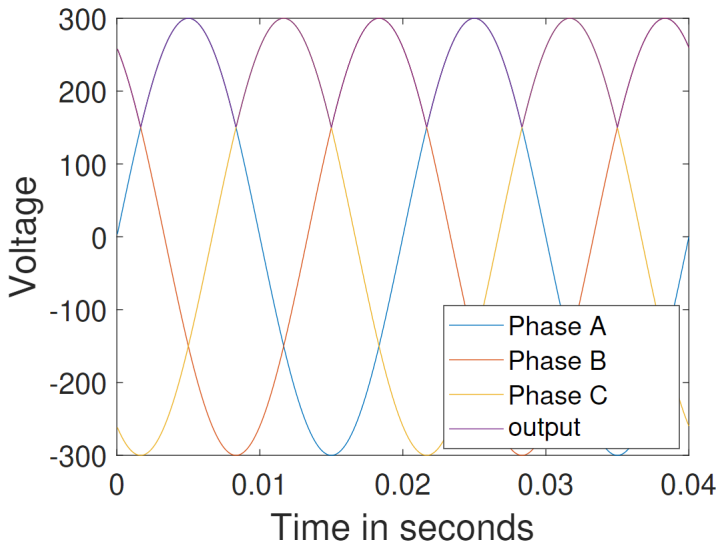

Figure 2.1: A simple rendition of a three phase voltage and output voltage

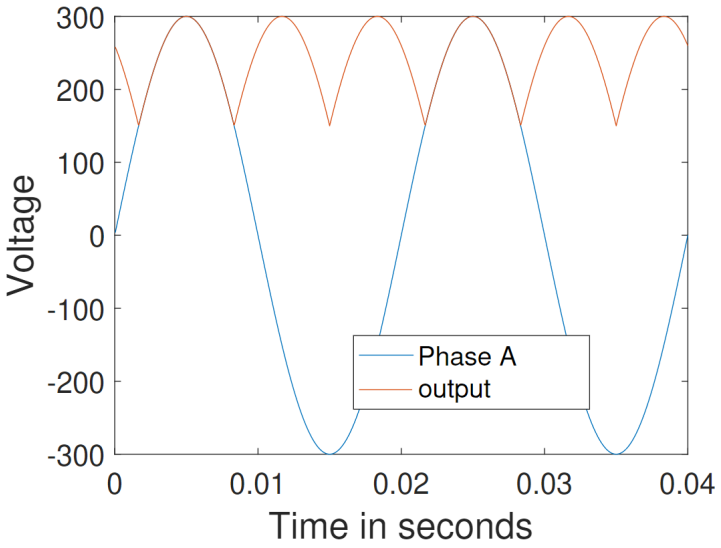

Figure 2.2: A simple rendition of a one phase voltage and the output voltage of the three phase system

Since it is easier to work with the phases separately there are three sets of controllers for each control scheme showed in this report. The three separate voltages will later be combined into one three phase signal again but that will not be explored further in this report [1, Ch. 2.4, pp. 54-60].

2.1.1 Harmonics

Any three phase system is prone to have harmonics. The harmonics that are multiples of 3 are zero-sequence components, meaning that they are seen as invisible and can be excluded from being considered. The remaining harmonics do have to be taken into consideration, since they may cause oscillations and unwanted behaviour despite decent control being implemented. These harmonic components follows into all single phase versions as well so these will be focused on in this report [1, Ch. 2.4, pp. 59-60].

2.2 Overview of the system

While many different controllers have been implemented they are all a part of the same base system.

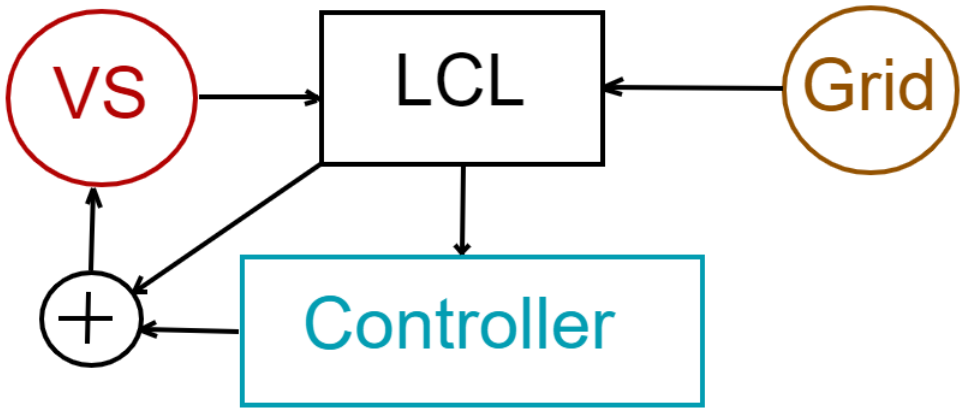

Figure 2.3: A simplified overview of the system that was implemented. There are two voltage sources. The first is the grid voltage and the other one is the controller voltage source here referenced to as the VS. The controller gets information about the LCL system and the output is added with additional information in a FF fashion.

The system in Figure 2.3 consist of an LCL filter that, on one side, has an voltage input from the grid and, on the other side, the controlled voltage source. The controller receives information regarding the current flow either right before or right after the capacitor and generates a voltage output from this information. Afterwards that signal adds the voltage that is measured at the capacitor as a FF signal and this voltage is what the voltage source outputs. The reason for why the measured voltage over the capacitor is used as an FF is that if the voltage from the voltage source and the grid were identical, then no current would flow. Using this logic the controller may only need to work on fixing the error in current and not on generating the entire signal.

2.3 The reference method

A base reference method was created in order to compare the different results and to use as a base to build upon. This method uses PI control which uses DC values in steady state with a FF reference from the capacitor voltage.

2.4 LCL filter

Often when converting from direct current (DC) to alternating current (AC) an LCL filter is used, see Figure 2.4. The reason to use an LCL filter is twofold. The first is that it can take a signal of square waves and soften it to a sinusoidal signal such as when using a PWM. The other reason is that an LCL reduces the harmonics that naturally occur when converting between the two current types [3]. The filter consists of two inductors and one capacitor.

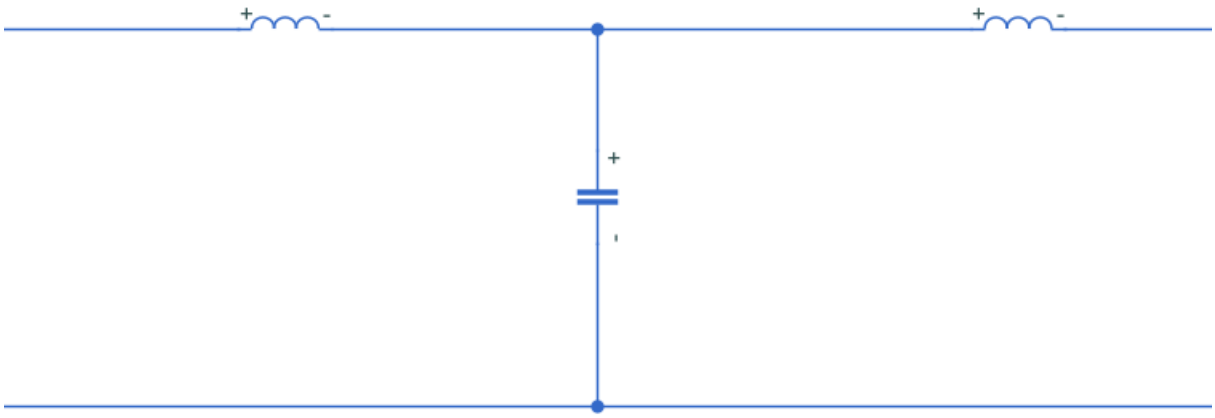

Figure 2.4: Basic LCL filter using one capacitor and two inductors

The LCL filter was implemented in Simscape and it is presented in Figure 1.1. The values for the components in the LCL filter are seen in Table 2.1.

Table 2.1: The values of L_1, L_2, R_{L1}, R_{L2} and C_1 in the LCL-filter

L_1	120 μH
R_{L1}	40 mΩ
L_2	300 μH
R_{L2}	300 mΩ
C_1	(5 + 2.2)·3 μF

The filter consists of two voltage sources as well, as seen in Table 2.2.

Table 2.2: The two voltage sources V_{in} and V_{g} in the LCL-filter.

V_{in}	Voltage source to be controlled
V_{g}	Voltage source representing the grid

The measurements that can be taken in this LCL-filter are presented in Table 2.3.

Table 2.3: The three possible measurements in the LCL-filter, although it is stated that I_1 and I_2 cannot both be measured at the same time due to costs.

I_1	Current measured after L_1
I_2	Current measured after L_2 and before grid
V_{c}	Voltage measured over the capacitor

Two different currents can be measured, I_1 and I_2, however they cannot both be measured due to the financial costs this would cause. In the current implementation, the I_1 current is measured and used for control. Part of the aim of this project

is to shift from measuring I_1 to measuring I_2. The voltage is measured over the capacitor, given by V_c. R_{L1} cannot be seen in Figure 1.1 due to that it is included in the inductance L_1. There is a resistance in the other inductance L_2 as well which is given the name R_{L2}. The L_2 in this report is a combination of the grid inductance, which is unknown, and the known inductance of a inductor right before the grid. L_2 is unknown but for the sake of this report an average value will be used, as seen in Table 2.1. V_{in} is the voltage that is meant to be controlled, and the control of this will result in a change in the current flowing trough the filter. The grid voltage is represented by V_g and is neither controlled nor measured.

2.5 Single phase grid artifact

The capacitor in the LCL system has a reactive current, which is subtracted from the I_1 current and this causes artifacts that needs to be compensated for [2]. These artifacts are compensated for by using an estimation of the current flowing through the capacitor

$$I_c = V_c j\omega_0 C_1 \tag{2.1}$$

with a phase shift of 90° to the reference current in question. This is meant to mitigate the problem and reduce these oscillations, because without this fix, any control solution implemented would be difficult to fully evaluate.

2.6 Phase-Locked Loop (PLL)

The phase-locked loop or phase lock loop is a control scheme used to generate a signal that has the same phase as the input signal. The PLL is normally used to generate a new voltage signal but in this case it will instead be used only to extract the phase of the input using the phase detector that is used in the PLL [4, Ch. 1-2, pp. 1-29].

2.7 PI controller

The PI controller is often used in linear systems where the reference should be constant over some period of time. The input to a PI controller is the measured data of what is to be controlled subtracted from the reference signal. The proportional term takes the input, scales it by a constant and then outputs the answer. This term is used in order to get a high settling speed and to react to rapid changes in the input signal. The integral term on the other hand is used to reduce errors over time and may only do so effectively when the reference is constant [5]. The transfer function of a basic PI controller is

$$K_{PI} = K_P + \frac{K_I}{s} \tag{2.2}$$

where K_P is the proportional gain and K_I is the integral gain [6].

In order for a PI controller to work well it needs to have a signal that is constant over time, therefore the PI controllers use DC values in steady state.

2.7.1 FF connection to the grid

Something that was implemented in the current method in use is that the controller output is adjusted to the grid [7, Ch. 1, pp. 12]. This is something that perhaps is not the most commonly used method, however this will have to be taken into consideration when developing new implementations.

2.8 Disturbances

Different disturbances will have to be taken into consideration in order to be able to test the proposed solution to the various problems that can occur. These disturbances includes voltage drops, phase shifts and harmonics components as major errors. There are also more nuanced errors such as constant white noise in the grid and measurements [2].

2.9 PR controller

A Proportional Resonance (PR) controller is in many way similar to a PI controller. They both use the proportional aspect in the same way. The difference is in the use of the Integral term. The PR expands the Integral part of the PI by adding a bandpass filter for a specified frequency. This effectively allows the PR to work only with signals that are of a constant, or close to constant, rotational speed without reacting to noise of a different rotational speed [8]. In the ideal case the equation of the PR is described as

$$K_{PR} = K_P + \frac{K_I s}{s^2 + \omega_0^2} \tag{2.3}$$

where K_P is the proportional gain, K_I the integral gain and ω_0 the frequency that is to be controlled.

In practice this is not adjustable enough and a cut off term is added and it acts like a bandwidth. This term specifies the range of frequencies around the base frequency that should be handled by the integral term. This term becomes important in the modeling since noise is to be minimized but if the base frequency does not match the frequency of the control signal, then it may not be controlled. When updating the ideal PR (2.3) the new equation becomes

$$K_{PR} = K_P + \frac{2K_I\omega_c s}{s^2 + 2\omega_c s + \omega_0^2} \tag{2.4}$$

where ω_c is the cut of frequency, ω_0 is the base angular speed. The resulting Simulink implementation is seen in Fig 2.5.

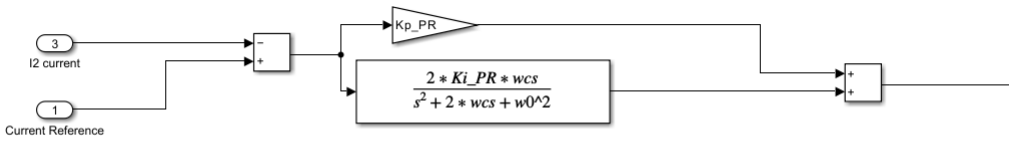

Figure 2.5: The PR controller showing how the K_P and the K_I are used together in order to get compensation for a specific frequency range.

2.9.1 Harmonic compensation

The R term only works with the frequency that is specified in the bandwidth around the base frequency but that gives the possibility of using several R terms at once. This works since the integral terms dampens everything that is not in the band pass meaning that each term may control a different frequency without conflicting with each other. This only holds for as long as the R terms do not control frequencies to close to each other in regards to bandwidth. This is therefore often used to control specific harmonics as well as the base frequency. The equation for the PR gain may then be updated once more and it becomes

$$K_{PR} = K_P + \sum_{h=1,3,5,\ldots} \frac{2K_{Ih}\omega_{ch}s}{s^2 + 2\omega_{ch}s + \omega_{0h}^2} \tag{2.5}$$

where the different integral terms all act on a specific frequency range [8].

2.9.1.1 Harmonic compensators in this system

As previously discussed the R term may be expanded upon in order to control several different ranges of frequencies. Since there are several harmonics that should be removed, several harmonic compensators were implemented. These focused on the 5th and 7th harmonics where the 3rd and 9th disappear since all harmonics that are a multiple of 3 do not affect the current. These harmonic compensators closely resembles the resonant part of the PR controller, but has been modified to match each of the harmonics. Each new compensator needs a new K_I, a ω_0 set to the harmonic frequency and a ω_c adapted to give a reasonable bandwidth. An updated Simulink model can be seen in Fig 2.6.

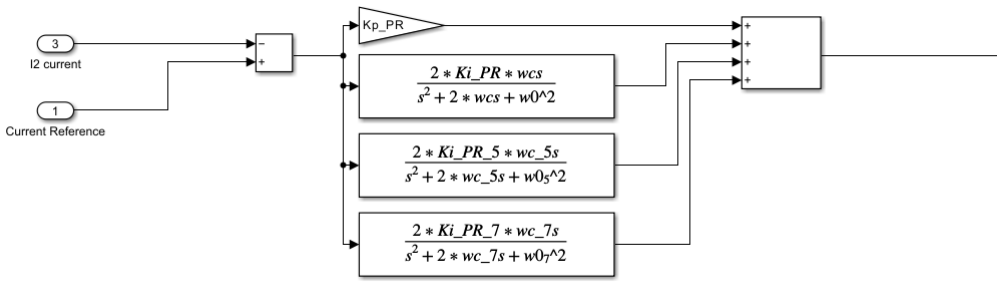

Figure 2.6: PR controller with added Harmonic compensators. Any number of additional terms may be added.

ω_0 for each harmonic, such as ω_{05}, is calculated by multiplying the original ω_0 with the number of the harmonic. Meaning that for each harmonic h holds $\omega_{0h}{=}h \cdot \omega_0$ where ω_0 is set to 314 rad/s originally. No such equation is used to calculate the K_I for each harmonic, these are trimmed instead to be able to compensate for the specific harmonic and aid in producing a good result.

2.9.2 Modified PR controller with harmonic mitigation

In order to be able to adjust the controller even further, a term was added to the numerator of the R-term of the PR controller. This new term is meant to be adjusting the controller vertically. The PR controller with harmonic mitigation remains the same as described in (2.5) and as visualized in Figure (2.6). The modified PR controller with harmonic mitigation is best described as

$$K_{PR} = K_P + \sum_{h=1,3,5,\ldots} \frac{K_{Ih1}s + K_{Ih2}}{s^2 + 2\omega_{ch}s + \omega_{0h}^2} \tag{2.6}$$

2.10 Model based control

Implementing model based control involves describing the system in question mathematically, thereby deciding the state space (SS) model. This involves deciding upon the input and outputs, as well as what the state space includes,

$$\dot{x}(t) = Ax(t) + Bu(t) + De(t) \tag{2.7}$$

$$y(t) = Cx(t) \tag{2.8}$$

where x is the states of the system, $\dot{x}$ is the rate of change in the states and y is the system output. A, B, C and D are state space matrices. Equations (2.7) and (2.8) are used to describe the system in question to be controlled, note that this is described in continuous time. In order to use the state space model in a discrete system the matrices has to be discretized in the following way [9]

$$A_{disc} = e^{A_{cont}T_s} \tag{2.9}$$

$$B_{disc} = -A_{cont}^{-1} \cdot (I - A_{disc}) \cdot B_{cont} \tag{2.10}$$

$$C_{disc} = C_{cont} \tag{2.11}$$

$$D_{disc} = -A_{cont}^{-1} \cdot (I - A_{disc}) \cdot D_{cont} \tag{2.12}$$

where T_s is the systems step time.

2.10.1 SS Model

The first part of constructing an model based controller is to model the system mathematically. This includes deciding on inputs, outputs and the state space. V_{in} is the variable that the controller is supposed to affect, meaning it is the output. For this case it is known that I_2 or I_1 is measured and supposed to be used as an input

along with measured voltage V_c. The LCL system can be described mathematically as

$$\frac{dI_1(t)}{dt} = -\frac{I_1 R_{L1}}{L_1} - \frac{V_c}{L_1} + \frac{V_{in}}{L_1} \tag{2.13}$$

$$\frac{dI_2(t)}{dt} = -\frac{I_2 R_{L2}}{L_2} + \frac{V_c}{L_2} - \frac{V_g}{L_2} \tag{2.14}$$

$$\frac{dV_c(t)}{dt} = \frac{I_1 - I_2}{C_1} \tag{2.15}$$

This results in the following state space models to describe the system

$$\dot{x} = \begin{bmatrix} \frac{dI_1(t)}{dt} \\ \frac{dI_2(t)}{dt} \\ \frac{dV_c(t)}{dt} \end{bmatrix} = \underbrace{\begin{bmatrix} -\frac{R_{L1}}{L_1} & 0 & -\frac{1}{L_1} \\ 0 & -\frac{R_{L2}}{L_2} & \frac{1}{L_2} \\ \frac{1}{C_1} & -\frac{1}{C_1} & 0 \end{bmatrix}}_{\mathrm{A}_c} \cdot \begin{bmatrix} I_1(t) \\ I_2(t) \\ V_c(t) \end{bmatrix} + \underbrace{\begin{bmatrix} \frac{1}{L_1} \\ 0 \\ 0 \end{bmatrix}}_{\mathrm{B}_c} \cdot \Big[V_{in}(t)\Big] + \underbrace{\begin{bmatrix} 0 \\ -\frac{1}{L_2} \\ 0 \end{bmatrix}}_{\mathrm{D}_c} \Big[V_g(t)\Big] \tag{2.16}$$

$$y = \underbrace{\begin{bmatrix} k_{I_1} & 0 & 0 \\ 0 & k_{I_2} & 0 \\ 0 & 0 & k_{V_c} \end{bmatrix}}_{\mathrm{C}_c} \cdot \begin{bmatrix} I_1(t) \\ I_2(t) \\ V_c(t) \end{bmatrix} \tag{2.17}$$

Where the boolean variables k_{I_1}, k_{I_2} and k_{V_c} decides which sensors are being used, meaning that if the variable is set to 1 that specific sensor is being used. These systems were discretized using (2.9), (2.10), (2.11) and (2.12) and thus creating the discrete matrices A_d, B_d, D_d and C_d which has the following values

$$A_d = \begin{bmatrix} 0.9179 & 0.0751 & -0.1602 \\ 0.0300 & 0.9503 & 0.0636 \\ 0.8900 & -0.8840 & 0.8943 \end{bmatrix} \tag{2.18}$$

$$B_d = \begin{bmatrix} 0.1619 \\ 0.0017 \\ 0.0756 \end{bmatrix} \tag{2.19}$$

$$D_d = \begin{bmatrix} -0.0017 \\ -0.0653 \\ 0.0301 \end{bmatrix} \tag{2.20}$$

$$C_d = \begin{bmatrix} k_{I_1} & 0 & 0 \\ 0 & k_{I_2} & 0 \\ 0 & 0 & k_{V_c} \end{bmatrix} \tag{2.21}$$

These equations result in a discrete state space model with the following composition

$$x_{k+1} = \begin{bmatrix} I_{1,k+1} \\ I_{2,k+1} \\ V_{c,k+1} \end{bmatrix} = A_d \begin{bmatrix} I_{1,k} \\ I_{2,k} \\ V_{c,k} \end{bmatrix} + B_d \Big[V_{in,k}\Big] + D_d \Big[V_{g,k}\Big] \tag{2.22}$$

$$y_{k+1} = C_d \begin{bmatrix} I_{1,k} \\ I_{2,k} \\ V_{c,k} \end{bmatrix} \tag{2.23}$$

2.10.2 Observability

If the observability matrix

$$O(A,C) = \begin{bmatrix} C \\ CA \\ . \\ : \\ CA^{n-1} \end{bmatrix} \tag{2.24}$$

is of full rank the system is deemed to be observable [10, Ch. 3.2, pp. 44-45]. The observability shows if the states can be estimated using measurements and is therefore a good test for if the estimations of the states and variables are possible. Using the already calculated SS model matrices (2.18) and (2.21) results in an observability matrix of rank 3 and the system is therefore deemed observable.

2.10.3 Controllability

The system is deemed to be controllable if the controllability matrix

$$S(A,B) = \begin{bmatrix} B & AB & ... & A^{n-1}B \end{bmatrix} \tag{2.25}$$

is of full rank [10, Ch. 3.2, pp. 44-45]. If calculating the controllability matrix using the previously calculated SS model with the specific matrices (2.18) and (2.19) the controllability matrix is found to be of rank 3 and the system is therefore controllable.

2.10.4 Estimation of current and voltage

Given the previously calculated state space model (2.16) and (2.17), estimations of the unknown currents or voltages can be made from the known ones. Due to the limitation of only being able to measure one of the currents as well as the voltage over the capacitor in the LCL filter it is vital to be able to estimate the non-measured current and voltage, in order to do prediction as well as model based control of the system. The estimations are given by

$$I_1 = I_2 + \frac{V_c - z^{-1}V_c}{T_s} \cdot C_1 \tag{2.26}$$

$$I_2 = I_1 - \frac{V_c - z^{-1}V_c}{T_s} \cdot C_1 \tag{2.27}$$

$$V_{in} = L_1 \cdot \frac{I_1 - z^{-1}I_1}{T_s} + I_1 R_{L1} + V_c \tag{2.28}$$

$$V_g = -L_2 \cdot \frac{I_2 - z^{-1}I_2}{T_s} - I_2 R_{L2} + V_c \tag{2.29}$$

which are basically (2.13), (2.14) and (2.15) but rewritten. These equations are meant to guide the estimation, however some does not result in a good estimation

and has therefore been used as a guide rather than the actual true values. This holds for the estimated currents (2.26) and (2.27) which are instead estimated as

$$I_1 = I_2 + (V_c - z^{-1}V_c) \cdot \frac{1}{1.05} \tag{2.30}$$

$$I_2 = I_1 - (V_c - z^{-1}V_c) \cdot \frac{1}{1.05} \tag{2.31}$$

in the actual Simulink model of the system. These estimations proved to be the most accurate when comparing to the true signal.

2.10.5 Smith predictor

Smith predictor is a simple form of prediction that uses the knowledge of the systems SS to create the new update. It does not have any control built in to it so a control scheme is needed in addition to the smith predictor. It is used when there is a delay in reading or outputting data were the goal of the Smith predictor is to guess what the systems states will be in the future and thereby effectively eliminating the problems arising from using old data [11]. In theory it is possible to perfectly estimate the future but in practice this is impossible. The Smith predictor is visualized in Figure 2.7.

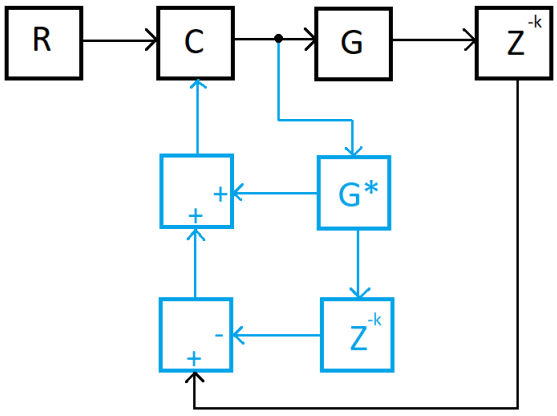

Figure 2.7: Smith predictor (in blue) as part of the system (in black) where R is the reference, C is the controller, G is the plant, G^* is the estimated plant, Z^{-k} is the discrete time delay in k steps.

2.10.5.1 One step ahead

The prediction was created using the discrete SS model (2.22) along with (2.26), (2.27) and (2.29). One of the currents are measured along with the voltage over the capacitor, the previously calculated control output V_{in} is saved and used in the predictor while the V_g and the non-measured current are estimated as described in 2.10.4. The estimation allows for the prediction to occur, since the SS model relies on that these variable have known values meanwhile there are certain restrictions on how many sensors can be used.

2.10.5.2 Two step ahead

The two step ahead prediction simply repeats the one step ahead prediction method, except using the already predicted values as input to the prediction. This can be described with the following prediction model

$$x_{k+2} = \begin{bmatrix} I_{1,k+2} \\ I_{2,k+2} \\ V_{c,k+2} \end{bmatrix} = A_d \begin{bmatrix} I_{1,k+1} \\ I_{2,k+1} \\ V_{c,k+1} \end{bmatrix} + B_d \begin{bmatrix} V_{in,k+1} \end{bmatrix} + D_d \begin{bmatrix} V_{g,k+1} \end{bmatrix} \tag{2.32}$$

This means that the two step ahead predictor relies heavily on estimations of the variables in question as well as predictions. There are high demands on the SS model to be accurate, since the predictions from the one step ahead are used as the input to the two step ahead. A large deviation from the true value in the prediction from one step ahead will only increase after using the second step ahead.

Even though (2.32) as well as (2.22) contains enough information to predict all of the states it is still possible and valid to use the prediction of only one of the states. The reasoning behind this is due to the uncertainty that too many predicted values could cause. The uncertainties could be due to the modelling of the system in question as well as due to any disturbances the signals could be affected by when being measured or errors in estimation of the signals. This reasoning holds for both one step ahead as well as for two steps ahead.

2.10.6 Linear Quadratic Regulator

The standard SS system to be controlled by an LQR as done in [10, Ch. 9, pp. 241-242]. The continuous state change is described by

$$\dot{x} = Ax + Bu + Nv_1 \tag{2.33}$$

where x is the states, u is the input and v_1 is white noise. Next the controlled variable is described as

$$z_c = Mx \tag{2.34}$$

where M is a row matrix. Lastly the output is described as

$$y = Cx + v_2 \tag{2.35}$$

where v_2 is white noise as well. The intensity of the white noise $\begin{bmatrix} v_1 \\ v_2 \end{bmatrix}$ is $\begin{bmatrix} R_1 & R_{12} \\ R_{12}^T & R_2 \end{bmatrix}$.

The Linear Quadratic Regulator (LQR) is a model based controller which uses a cost function as an aid in controlling the system. The aim with an LQR is to control a dynamic system with the lowest cost possible and optimize the control based on this cost function. The cost function in question has the following appearance in continuous time [10, Ch. 9, pp. 245]

$$J = \int_0^\infty (z_c^T Q_1 z_c + 2x^T Q_{12} u + u^T Q_2 u) dt \tag{2.36}$$

but since the cross correlation is assumed to be zero that means that $Q_{12} = 0$ and the actual equation becomes

$$J = \int_0^\infty (z_c^T Q_1 z_c + u^T Q_2 u)dt. \tag{2.37}$$

where Q_1 and Q_2 are the weighting matrices. These are used to determine the trade off between control effort and control error. The LQR controller is defined by Glad and Ljung [10, Ch. 9, pp. 242] where the control gain is given by

$$L = Q_2^{-1} B^T S \tag{2.38}$$

where S is the solution to the equation

$$A^T S + SA + M^T Q_1 M - SBQ_2^{-1} B^T S = 0 \tag{2.39}$$

and is unique, positive semidefinite and a symmetric solution.
The equations (2.33)-(2.39) are all for a continuous system but for this application a discrete model is needed. The thought process is the same and is explained in [10, Ch. 9, pp. 264-266]. The discrete system is described by

$$x(t+1) = Ax(t) + Bu(t) + Nv_1(t) \tag{2.40}$$

$$z_c(t) = Mx(t) \tag{2.41}$$

$$y(t) = Cx(t) + v_2(t) \tag{2.42}$$

where the equations now focus on time steps. The new cost function to be minimized is

$$min \sum_{t=1}^{\infty} z_c^T(t) Q_1 z_c(t) + 2x^T(t) Q_{12} u(t) + u^T(t) Q_2 u(t) \tag{2.43}$$

which is the minimization over all time steps for the given criterion. Once again $Q_{12} = 0$ and that leads to the new equation

$$min \sum_{t=1}^{\infty} z_c^T(t) Q_1 z_c(t) + u^T(t) Q_2 u(t). \tag{2.44}$$

The LQR gain L is calculated using

$$L = (B^T SB + Q_2)^{-1} B^T SA \tag{2.45}$$

where S needs to be solved. S is the answer to the equation

$$S = A^T SA + M^T Q_1 M - A^T SB(B^T SB + Q_2)^{-1} B^T SA. \tag{2.46}$$

By finding the best cost matrices Q_1 and Q_2 the cost function will be minimized. In the LCL system that this report handles, the LQR controller is added in Matlab as follows in Figure 2.8.

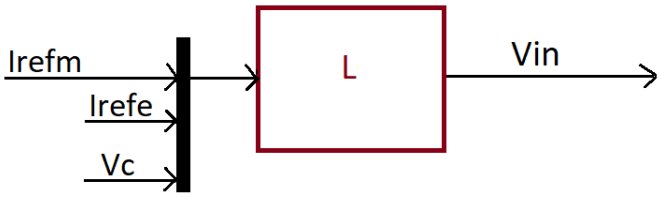

Figure 2.8: LQR block

The LQR needs all states as inputs but only one of the currents are measured at a time. This means that the other one is estimated using one of the equations (2.26) and (2.27). In the figure I_{refm} is the measured reference current and I_{refe} is the current reference that is estimated. To improve the systems control response further an integral term was added in the form of a resonance controller in addition to the LQR and the new control scheme is shown in figure 2.9.

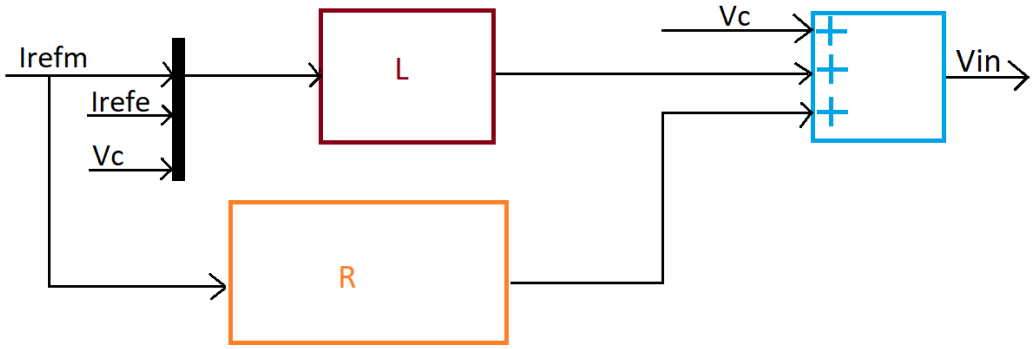

Figure 2.9: LQR with R-term and FF

The LQR is extended with an R-term to compensate for delays and other long term problems such as phase shifts. In addition this control scheme, as all others in this report, uses a feed forward of the voltage over the capacitor and adds it to its output. These extensions are done in order to complement any shortcomings the LQR may have on its own.

2.10.7 Observers and Kalman Filter

In many applications it is known that noise will be present and make it so that the true states are unknown. To mitigate this the states may be estimated or reconstructed. One way of doing these estimations is by using an observer that uses observed data from y and u to estimate x [10, Ch. 5, pp. 124]. To understand this lets start by looking at the known system

$$\dot{\hat{x}}(t) = A\hat{x}(t) + Bu(t) \tag{2.47}$$

where $\dot{\hat{x}}$ is the estimated $\dot{x}$ and $\hat{x}$ is an estimation of x. How well the estimation $\hat{x}$ is performing may be assessed by computing $y(t) - C\hat{x}(t) - Du(t)$ since this equation

will go towards zero as $\hat{x}(t)$ approaches $x(t)$. By using this measure of the quality in a feedback loop the following observer is obtained

$$\dot{\hat{x}} = A\hat{x}(t) + Bu(t) + K(y(t) - C\hat{x}(t) - Du(t)) \tag{2.48}$$

where K is a matrix [10, Ch. 5, pp. 124]. The purpose of the observer is to minimize the estimation error of the states and the formalized version of this [10, Ch. 5, pp. 125] is

$$\widetilde{x}(t) = x(t) - \hat{x}(t) \tag{2.49}$$

where $\widetilde{x}(t)$ is the estimation error. By combining (2.49) with (2.33-2.35) the following is obtained

$$\dot{\widetilde{x}}(t) = (A - KC)\widetilde{x}(t) + Nv_1(t) - Kv_2(t). \tag{2.50}$$

By analysing 2.50 it is clear that K affects the estimation error in two ways. Firstly it affects the matrix $A - KC$ which affects the speed at which the old errors die out [10, Ch. 5, pp. 125]. This matrix should have its eigenvalues as far into the stable region as possible. Secondly the measurement error v_2 increases when K does. An optimal observer is therefor an observer that balances the state error mitigation with the measurement error correctly for the given system.

The Kalman filter is a version of an observer that uses the knowledge of the characteristics of the disturbances in order to calculate an observer gain [10, Ch. 5, pp. 126]. To get the Kalman gain, the Riccati equation

$$AP + PA^T - (PC^T + NR_{12})R_2^{-1}(PC^T + NR_{12})^T + NR_1N^T = 0 \tag{2.51}$$

needs to be solved for P. The Kalman gain is then achieved by solving

$$K = (PC^T + NR_{12})R_2^{-1} \tag{2.52}$$

using the previously solved P [10, Ch. 9, pp. 242].
For the purposes of this thesis a discrete system is used which means that other equations are used [10, Ch. 9, pp. 265]. Once again the Riccati equation

$$P = APA^T + NR_1N^T - (APC^T + NR_{12})(CPC^T + R_2)^{-1}x(APC^T + NR_{12})^T \tag{2.53}$$

needs to be solved for P which in turn means that the discrete Kalman equation

$$K = (APC^T + NR_{12})(CPC^T + R_2)^{-1} \tag{2.54}$$

is solvable.

2.10.8 Linear Quadratic Gaussian controller

The Linear Quadratic Gaussian (LQG) controller is a controller which has a lot of similarities with LQR except it also assumes that there is some white Gaussian noise in all inputs and states and tries to compensate for it by using a Linear Quadratic state Estimator (LQE) in the form of a Kalman filter [10, Ch. 9, pp. 243]. The LQG is an optimal solution to the linear problem of minimizing the expected quadratic

cost by generating the best output feedback law. An LQG controller generates a dynamic control law and is not computationally heavy but one important aspect to consider when using an LQG is that the LQG optimally does not guarantee robustness and so it must be checked separately [10, Ch. 9, pp. 243].

The LQG implemented in this project is visualized in Figure 2.10.

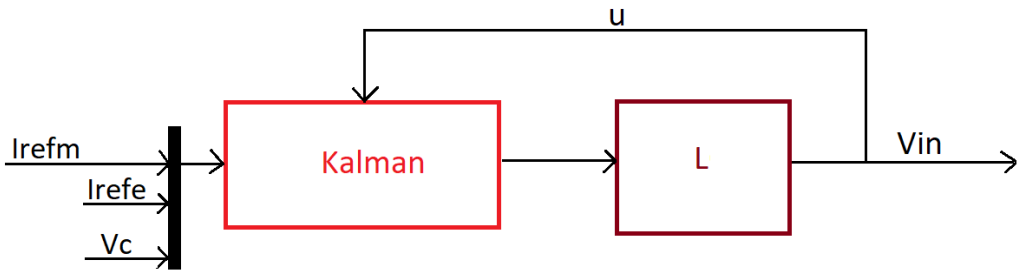

Figure 2.10: The LQG controller

The control signal u is fed back into the Kalman filter, where new states are estimated that are used in the LQR in an attempt to minimize the error.
The version of the LQG described above is however the basic version and it was expanded in this project. There is a resonant term added as in the LQR but it is used in the feedback loop to inform the Kalman filter of the full control action being applied. In addition the feedforward signal is once again applied to the output and this expanded version is seen in Figure 2.11.

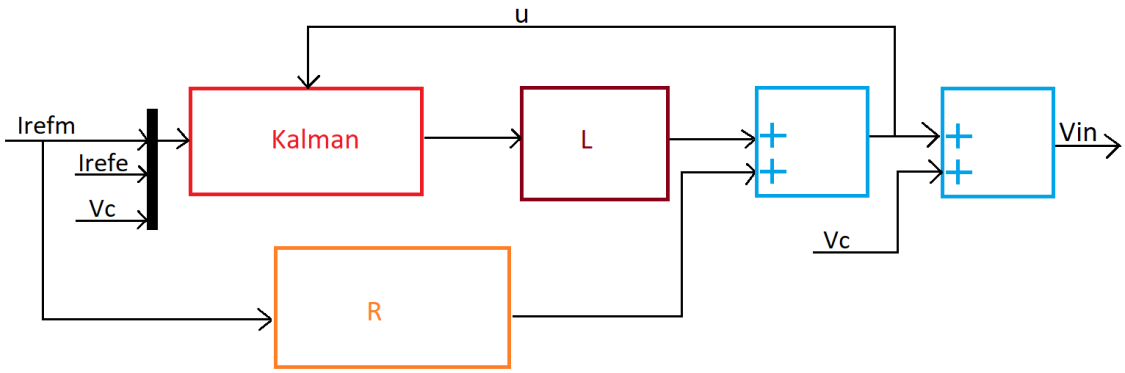

Figure 2.11: The LQG controller with R-term and FF

This implementation of an LQG also contains a R-term, which is meant to function as an aid in preventing a delay to happen. The R-term was chosen instead of a simple I-term since it can specify which frequency the signal is supposed to have as well as the bandwidth best suited for this signal. Feed forward is used in this controller as well, where the measured voltage over the capacitor is added onto the calculated control signal from the LQG and R-term.

3
Case Setup

This chapter will describe the cases used for testing alongside with all the parameter data needed to recreate the experiments. As well as the controllers constructed based on the discoveries in previous chapters.

3.1 Controllers

The controllers will be split up into two categories. The slow controllers, which have a rise time of 1 ms which is the same as the base PI controller and the fast controllers which have a rise time of 0.25 to 0.6 ms. The reason for this split is to have a base line where all controller types are set to have the same rise time (1 ms). Thereafter, the controllers were tuned up until the errors stopped decreasing and instead the controllers started to become oversensitive. All controllers do use the FF V_c signal and adds it to the output of the controller.

3.1.1 Slow controllers

Here all the slow controllers are described as they will be run in tests together.

3.1.1.1 PI

This is the base reference controller and the one future results will be compared against. The signal is controlled by a PI controller and the output is then added to the FF voltage measured from the capacitor.

Table 3.1: The variable values of the slow PI controller

Variable	Value	Explanation
Kp	0.12	Proportionat response
Ki	0.0008	Integral response

3.1.1.2 PI with harmonic compensation but slowed down

This PI controller is an expanded version of the *PI* controller. To reduce harmonic influences, the angle of the V_c is estimated using a PLL and multiplied with the grade of the harmonic component to be compensated for. Adding more control components adds to the speed of the controller. Therefore the original components were slowed down in order to once again reach 1 ms of rise time.

Table 3.2: The variable values of the slow PI with harmonic compensation controller

Variable	Value	Explanation
Kp	0.1008	Proportionat response
Ki	0.000672	Integral response
Kp 5 harm.	0.012	Proportionat response
Ki 5 harm.	8e-05	Integral response
Kp 7 harm.	0.012	Proportionat response
Ki 7 harm.	8e-05	Integral response

3.1.1.3 PR

This controller works with AC currents and voltages, in addition it uses an R-term instead of an I-term.

Table 3.3: The variable values of the slow PR controller

Variable	Value	Explanation
Kp	0.11999095	Proportionat response
Kr_1	50.22582	Integral response of order 1
Kr_2	-1240.8129	Integral response of order 0

3.1.1.4 PR with harmonic compensation but slowed down

To compensate for harmonic overtones new R-terms are added and changed to only react on signals of a faster type. This just as in the PI case adds to the speed of the controller so all R-terms are slowed down.

Table 3.4: The variable values of the slow PR with harmonic compensation controller

Variable	Value	Explanation
Kp	0.090709823	Proportionat response
Kr_1	71.751172	First order integral response
Kr_2	-1772.5898	second order integral response
Kr_1 harm 5	7.1751172	First order integral response harm 5
Kr_2 harm 5	-177.25898	second order integral response harm 5
Kr_1 harm 7	7.1751172	First order integral response harm 7
Kr_2 harm 7	-177.25898	second order integral response harm 7

3.1.1.5 LQR(-R)

This controller is the same as the original PR controller but it replaces the P term with an LQR controller instead. As mentioned in the theory section this requires I_1, I_2 as well as V_c. Since one of the currents never will be measured it is instead estimated.

Table 3.5: The variable values of the slow LQR controller

Variable	Value	Explanation
Kr_1	64	First order R
Kr_2	3360	second order R
L_1	0.12785543	LQR gain 1
L_2	-0.017987875	LQR gain 2
L_3	-0.0011181418	LQR gain 3

3.1.2 Fast controllers

Faster controllers are described here and they will be used in the same test scenarios at a later time.

3.1.2.1 PI and harmonic compensation

This controller functions as *PI with Harmonic compensation but slowed down* but does not have the limitation on the speed of the controller. Therefore this controller has a faster rise time.

Table 3.6: The variable values of the fast PI controller

Variable	Value	Explanation
Kp	0.12	Proportionat response
Ki	0.0008	Integral response

3.1.2.2 PR harmonic compensation

This controller works the same as *PR with harmonic compensation but slowed down*, 3.1.1.4, but the speed of the R and P components are instead changed to be as fast as possible without introducing an abundance of instability.

Table 3.7: The variable values of the fast PR with harmonic compensation controller

Variable	Value	Explanation
Kp	0.18141965	Proportionat response
Ki 1	143.50234	First order integral response
Ki 2	-3545.1796	second order integral response
Ki 1 harm 5	71.751172	First order integral response for 5 harm
Ki 2 harm 5	-1772.5898	second order integral response for 5 harm
Ki 1 harm 7	71.751172	First order integral response for 7 harm
Ki 2 harm 7	-1772.5898	second order integral response for 7 harm

3.1.2.3 LQR(-R) fast

This is the same as *LQR(-R)* but the speed is changed to be faster.

Table 3.8: The variable values of the fast LQR controller

Variable	Value	Explanation
Kr_1	400	First order R
Kr_2	120000	second order R
L_1	0.8326389084	LQR gain 1
L_2	-0.005033464123	LQR gain 2
L_3	-0.005727706974	LQR gain 3

3.1.2.4 LQG(-R)

This controller adds a feedback loop that takes the error values and adds the control output from the previous time step and sends it into a Kalman filter. This Kalman filter then estimates new currents and voltage and these new values are used in the controller. Importantly the R term is also used in the feedback and not only the LQR output.

Table 3.9: The variable values of the fast LQG controller

Variable	Value	Explanation
Kr_1	400	The first R component
Kr_2	250000	The second R component
L_1	0.6371078964	LQR gain 1
L_2	-0.1327706252	LQR gain 2
L_3	-0.02122311864	LQR gain 3
Q_{11}	0.01	Weighting matrix 1, first diagonal value
Q_{12}	0.1	Weighting matrix 1, second diagonal value
Q_{13}	0.02	Weighting matrix 1, third diagonal value
Q_2	0.15	Weighting matrix 2
Qn	15	Kalman filter weighting matrix

3.2 Cases

The test cases which are executed are explained in this section of the chapter. They will also all use an input and output delay of 20 μs.

3.2.1 Case 1

The first case is to evaluate the steady state performance of the control schemes. There is an A and a B case. A is steady state at a constant 0. B is steady state when following an sinusoidal reference of 30A at 50Hz as seen in Figure 3.2. The grid voltage is a 300V signal at 50Hz without disturbances for both cases shown in Figure 3.1.

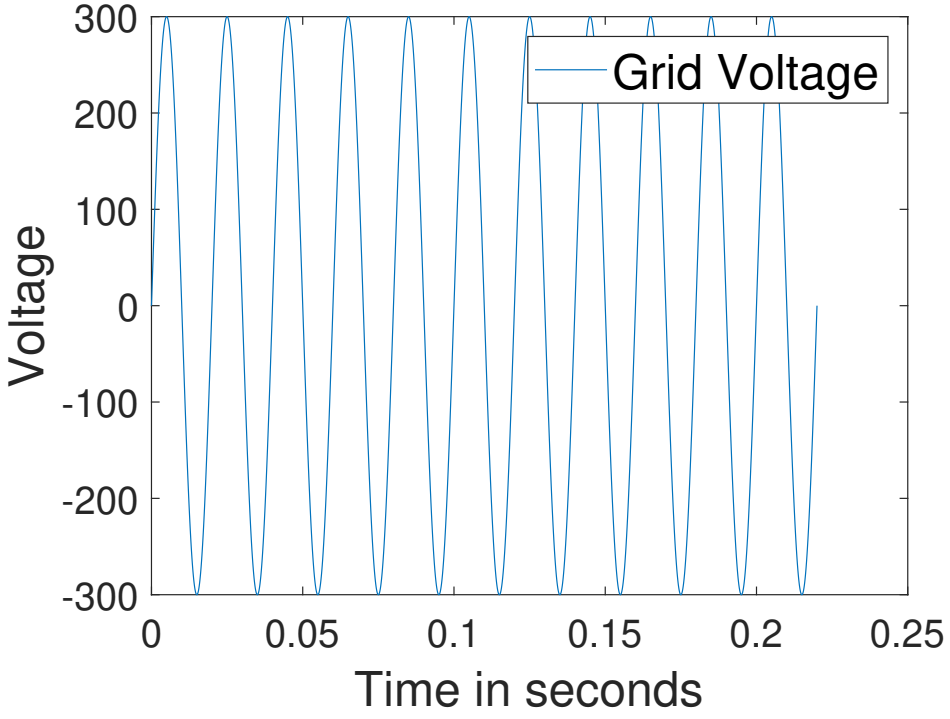

Figure 3.1: The voltage coming from the grid in the most ideal case

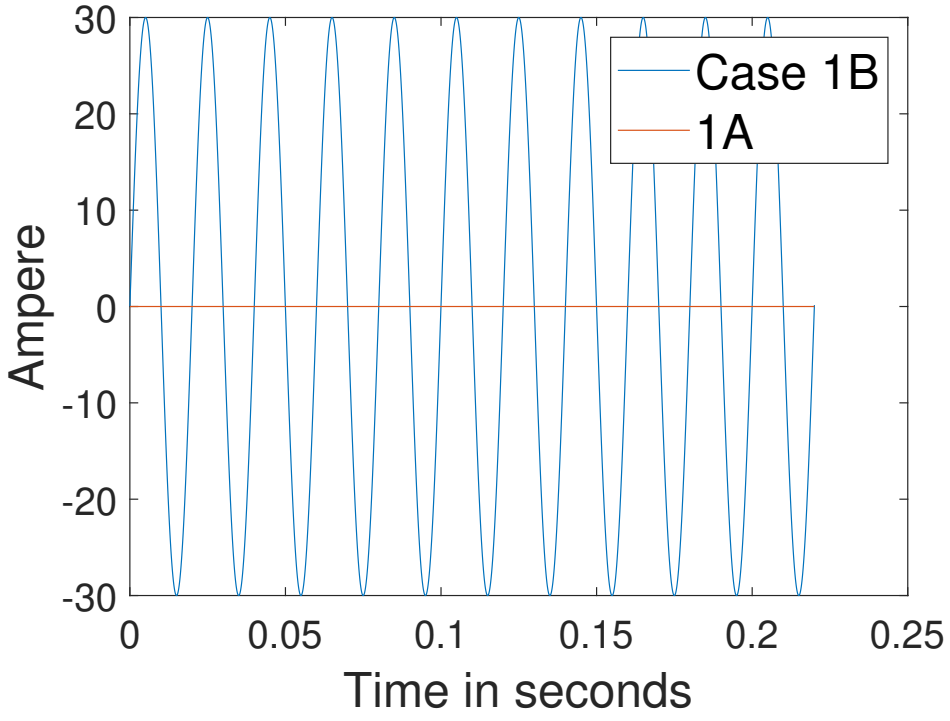

Figure 3.2: The reference for stead state at both 0 and 30 A

3.2.2 Case 2

The second test case starts of as 1A with having a reference current of 0 A but at time 75 ms this reference is instantaneously switched to match that of the reference current in Case 1B 3.2.1. Importantly the switch happens when the sinusoidal is at a peak in order to create a worst case scenario and the reference is shown in Figure 3.3. The grid voltage is the same as in Case 1 seen in chapter 3.2.1. This test is used to show the rise and settling time when drastic changes in the output is desired.

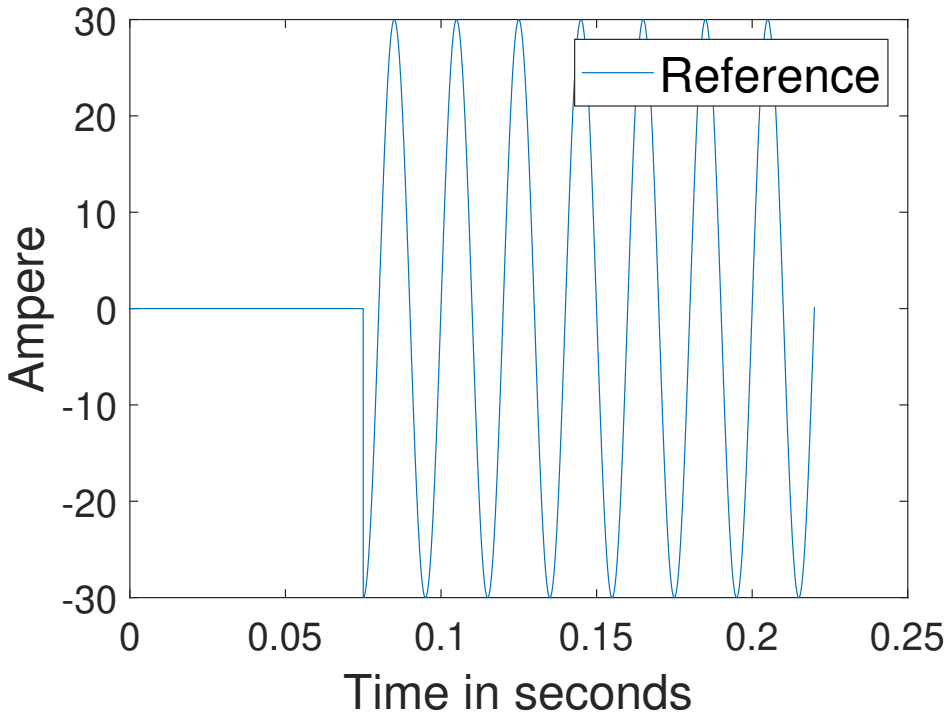

Figure 3.3: The reference used in order to test the step response of the controllers

3.2.3 Case 3

The third test case is based on the steady state test case 1B from section 3.2.1 but with a grid drop at time 125 ms which lasts for 20 ms and then returns to normal. This grid drop is set as it happens instantaneously, which is not true for a real system where this will happen over a very short time. By making the grid drop to be instantaneous, the system will be tested on a case worse than the true worst case.

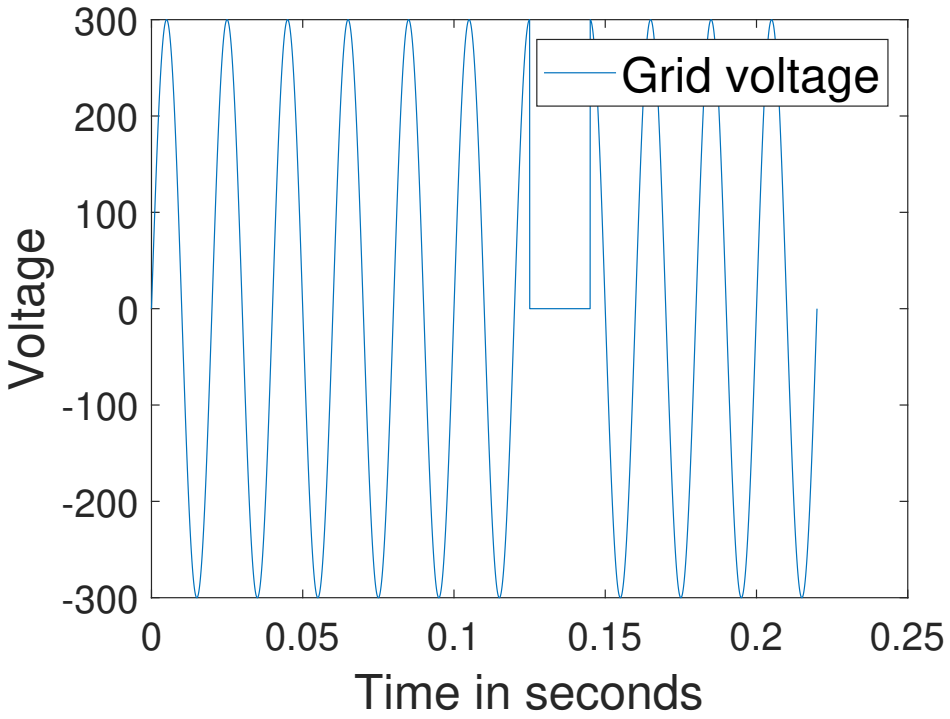

Figure 3.4: This ideal voltage is used to test the controller reaction to grid drops when there is no extra disturbances

3.2.4 Case 4

The fourth test case is based on the steady state test case 3.2.1 but with a phase shift at time 145ms. This phase shift is implemented as being instantaneous and as the largest probable phase shift that occurs in such a system. That is a shift of 1.379 radians. Choosing the most severe type of phase shifts shows the most severe or grave outcome or response from the controllers. The voltage is in Figure 3.5 and the reference current in Figure 3.6. Important to note is that the reference will slowly adapt to the change in voltage phase so that they end up in phase again. This is done by estimating the voltage phase using a PLL.

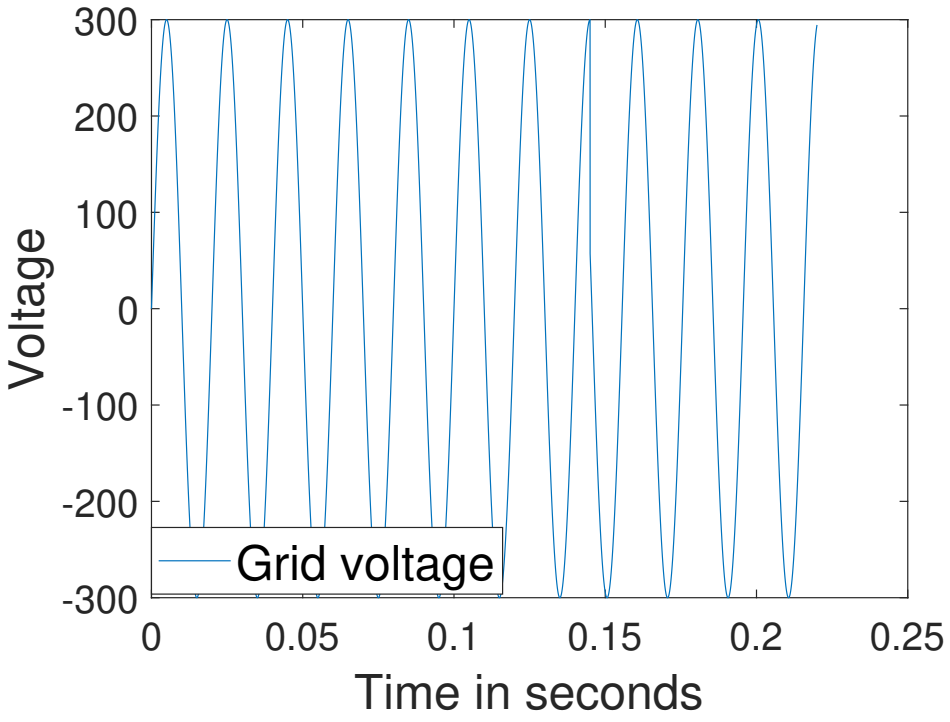

Figure 3.5: The grid voltage when a phase shift is introduced

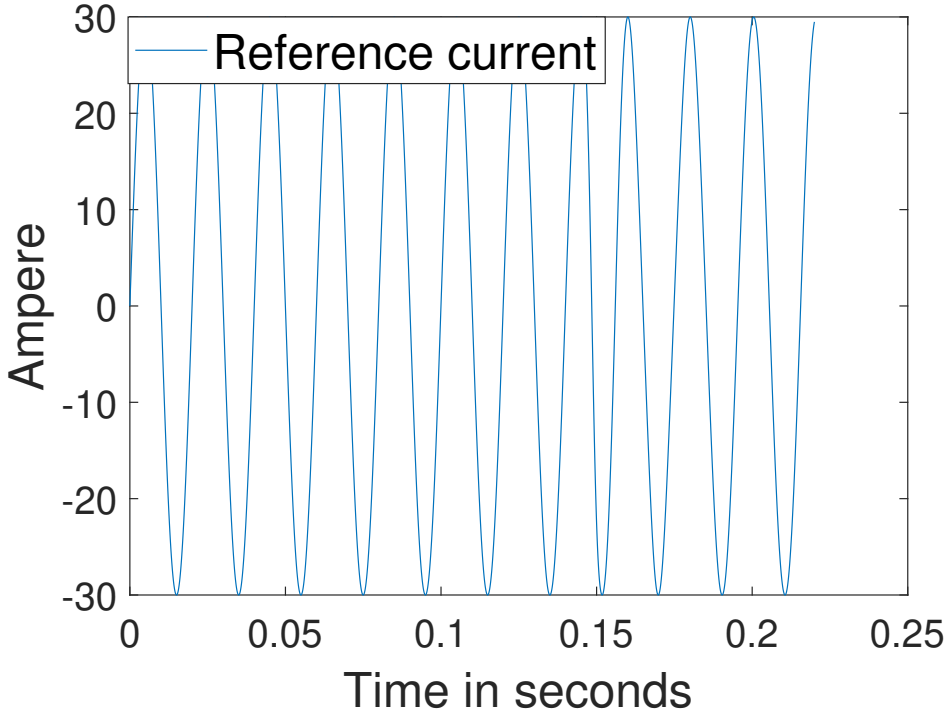

Figure 3.6: The reference is adaptive in order to always end up in phase with the grid and can therefore be seen drifting into place after the phase shift

3.2.5 Case 5

A more realistic scenario then the previous two is that after the drop there is some phase shift. Therefore this test is a mix between the third 3.2.3 and forth 3.2.4 test cases so that when the grid comes back it is shifted. The grid drop occurs at time 125 ms and lasts for 20 ms. The phase shift occurs at time 145 ms and has a shift of 1.379 radians and is shown in Figure 3.7. The reference is the same as in case 4 3.2.4.

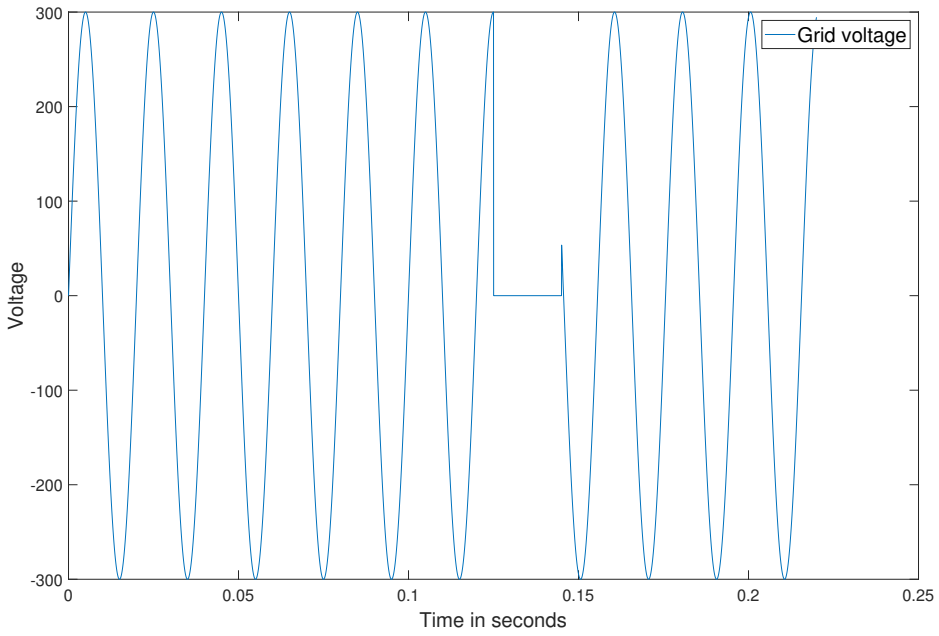

Figure 3.7: This scenario introduces the combination of a grid drop and a phase shift

3.2.6 Case 6

In order to fully understand the characteristics of the controllers that are meant to be tested is it crucial to test these on grids and reference currents that are non-ideal, since this is how the real signals will behave. Therefore will Case 1 3.2.1 be repeated here but with added noise, in order to gain a better understanding of the controllers behaviour in steady state. The noise is added to both the reading and the output of the grid voltage and results in the following Figures 3.8, 3.9.

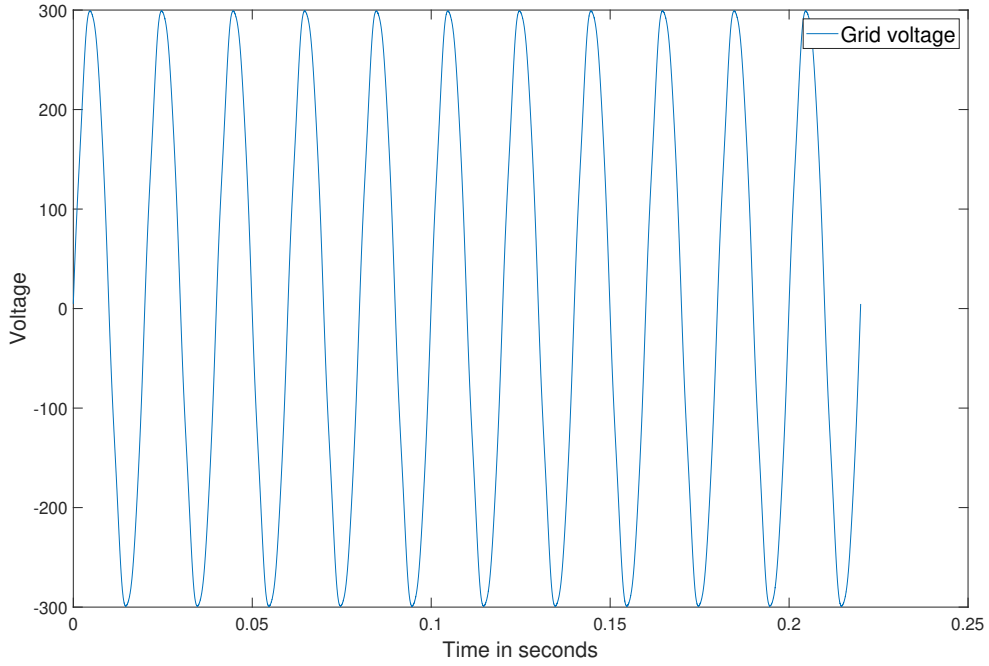

Figure 3.8: The ideal grid now has some introduced noise and harmonic disturbances but not all of it is seen here as some is only introduced when the data is read by the controller

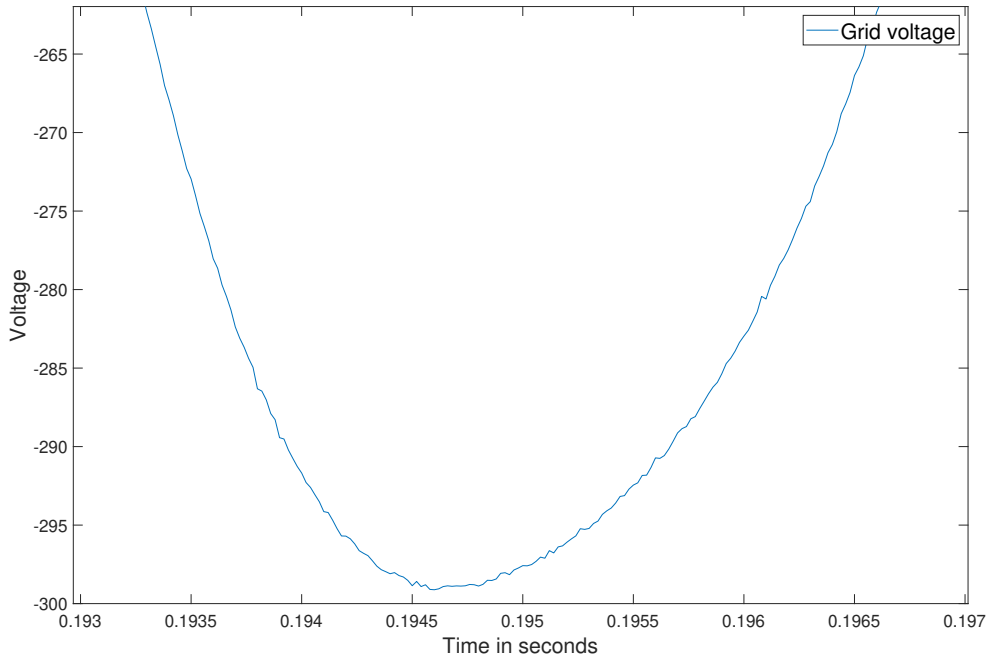

Figure 3.9: A zoomed in version of the grid voltage in order to show the disturbances

3.2.7 Case 7

This case will, as in Case 6 3.2.6, build upon a previous case. This time it will be built upon Case 5 3.2.5 but with the same noise as added in Case 6. This will give a more realistic grid drop where there is added noise that disturbs the readings.

3.2.8 Case 8

Finally all the most crucial disturbances have been added and tested as of Case 7 3.2.7. However since it is impossible to truly take into account every possible problem, the controllers will also be tested on a measured real grid voltage. This includes all noise from the reading instruments, harmonic components, amplitude faults etc and is shown in Figure 3.10. From now on all cases will use this as a standard since this is the real life scenario. The reference if not otherwise stated will be from Case 2 3.3. There was no grid drop in the measured data provided by Aros so that will be added by taking the product of the measured data and a scalar that will switch between 1 and 0.

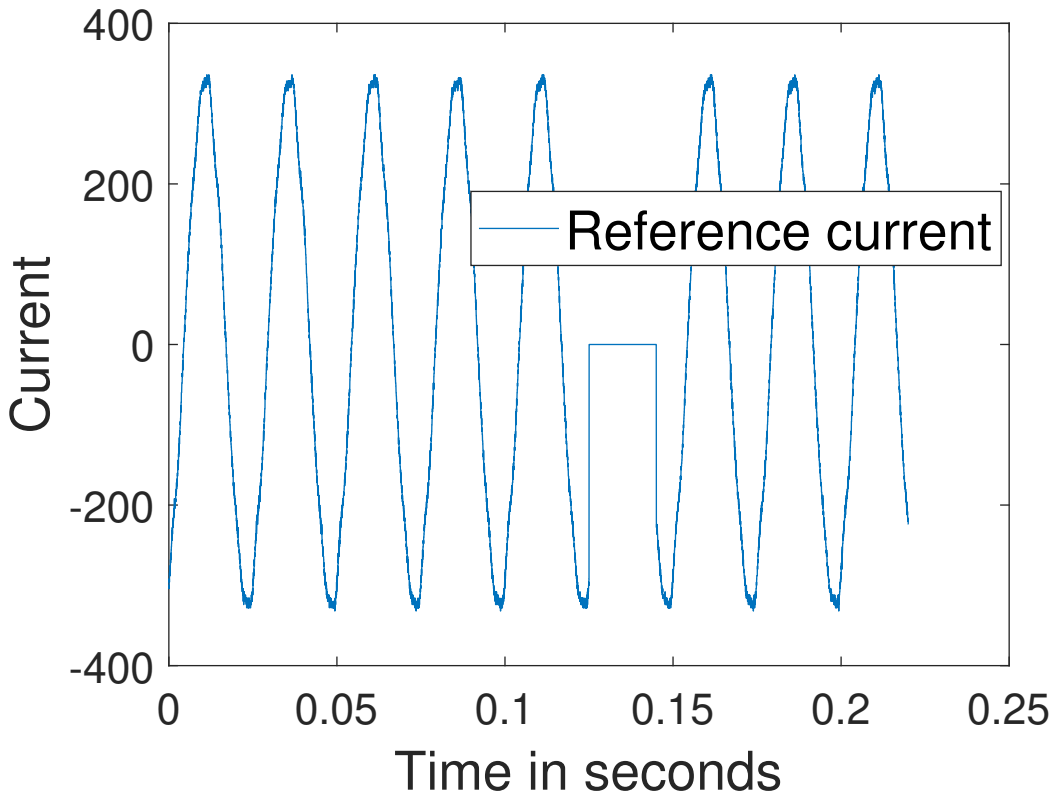

Figure 3.10: The grid voltage from measured data with a added drop at time 125ms lasting until 145ms

4

Results

This chapter will show the results of running the different controllers on the cases set up in chapter **3**. The tests will be split up so that the slow controllers with similar speed are shown together and the the sped up controllers are shown together.

4.1 Result of changing measurement of current from I_1 to I_2

The first test was to see if the results changed drastically when changing the current measurement point from I_1 to I_2. To do this the fastest controller with the most potential for oscillation for each controller type was selected in order to analyse potential oscillation.

4.1.1 Steady state: I_1 and I_2

The first case tested is 3.2.1 and the RMS errors between I_1 and the reference are shown in Table 4.1. It is found that the controllers are stable in steady state, as can be seen in Figures 4.1 and 4.2. Of note is that the I_2 current has a lower amount of high frequency noise than the I_1 current has. This stems from that the L_2 acts as a low pass filter.

Table 4.1: RMS values for I_1 and I_2 in steady state of 30 A while measuring on I_1

Controller type	RMS I_1	RMS I_2
PR With Harmonics	4.6449 A	5.0488 A
PI With Harmonics	3.4061 A	3.8688 A
LQR Fast	2.5881 A	3.2714 A
LQG Slowed down	2.6473 A	3.0838 A

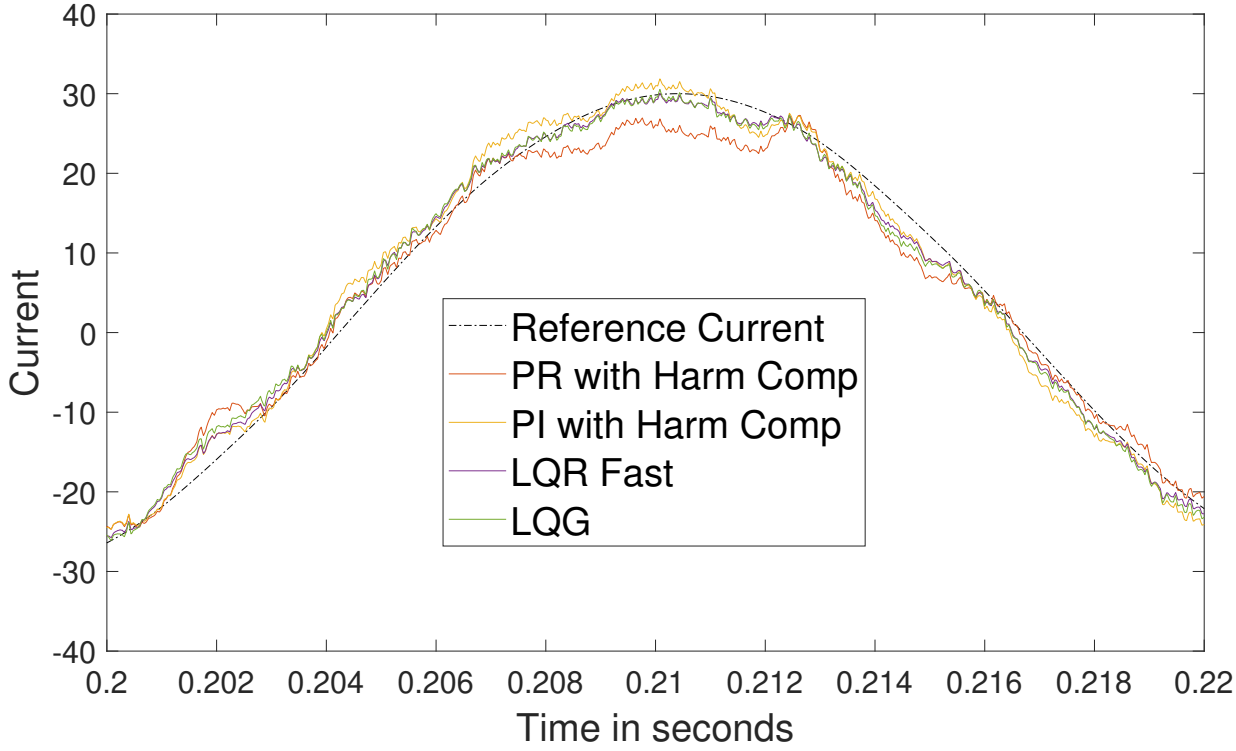

Figure 4.1: Measuring I_1 and viewing I_1 while in steady state of 30 A.

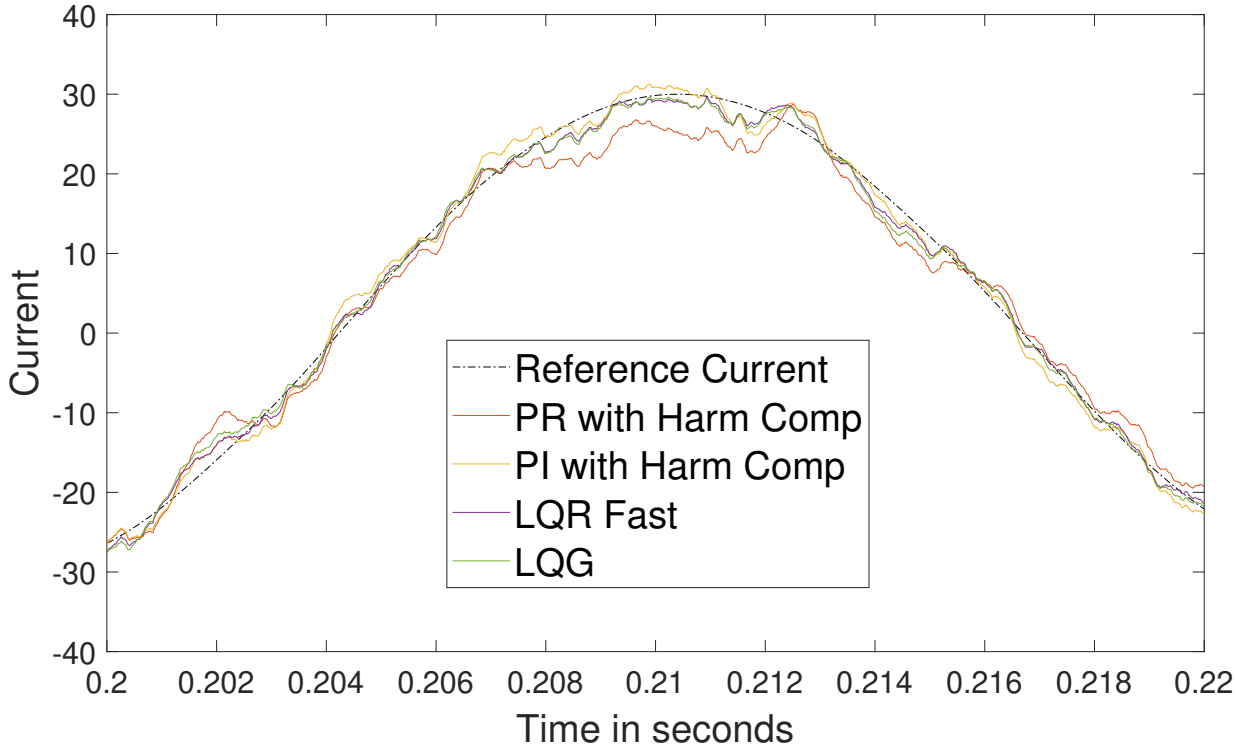

Figure 4.2: Measuring I_1 and viewing I_2 while in steady state of 30 A.

The same test was run again, 3.2.1, but the sensor position was switched from I_1 to I_2. The resulting RMS errors are shown in Table 4.2 and the accompanying Figures 4.3 and 4.4 shows the current behaviour. The results of this test are similar to Table 4.1. The differences are that the RMS error for the I_2 current decreases for the PI and PR when measuring on the I_2 current while it increases for the LQR and LQG. The I_1 RMS error is different, it always decreases when the sensor position is switched to I_2. No major error seems to arise when switching from I_1 to I_2 for the steady state scenario.

Table 4.2: RMS values for I_1 and I_2 in steady state of 30 A while measuring on I_2

Controller type	RMS I_1	RMS I_2
PR With Harmonics	4.3001 A	4.8156 A
PI With Harmonics	2.937 A	3.5858 A
LQR Fast	2.4106 A	3.4009 A
LQG Slowed down	2.3874 A	3.1217 A

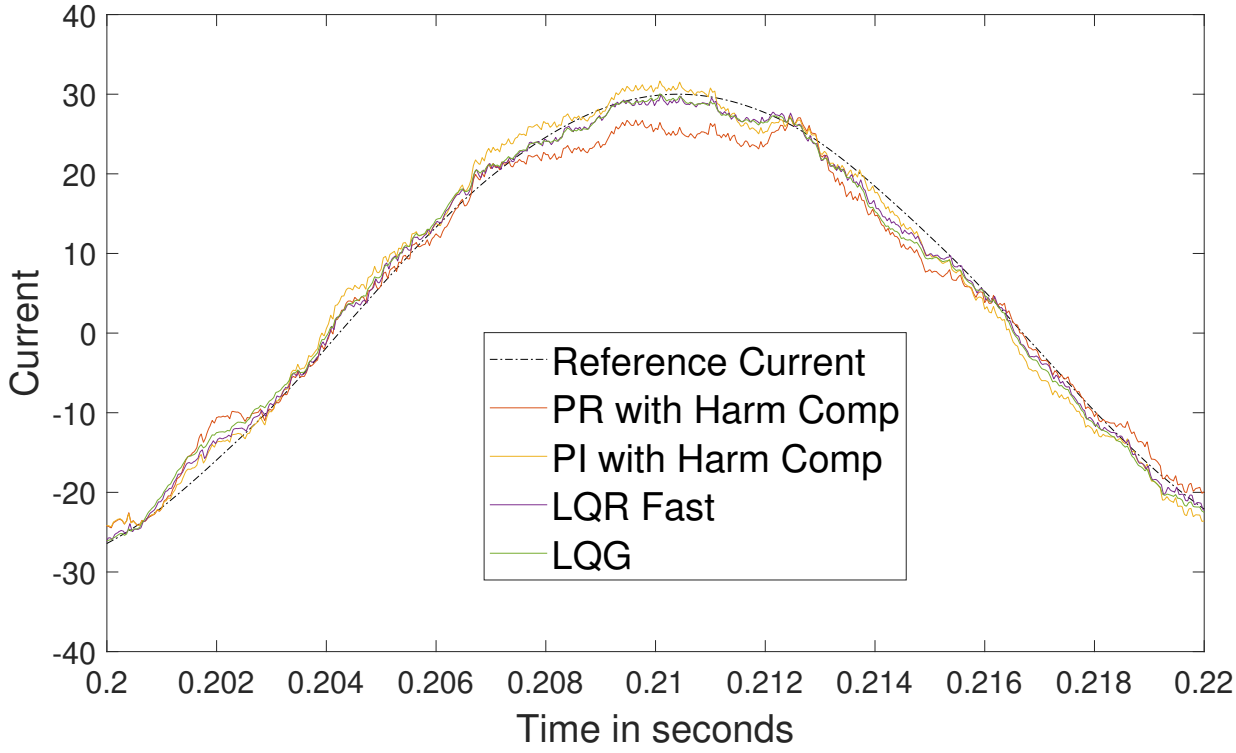

Figure 4.3: Measuring I_2 and viewing I_1 while in steady state of 30 A.

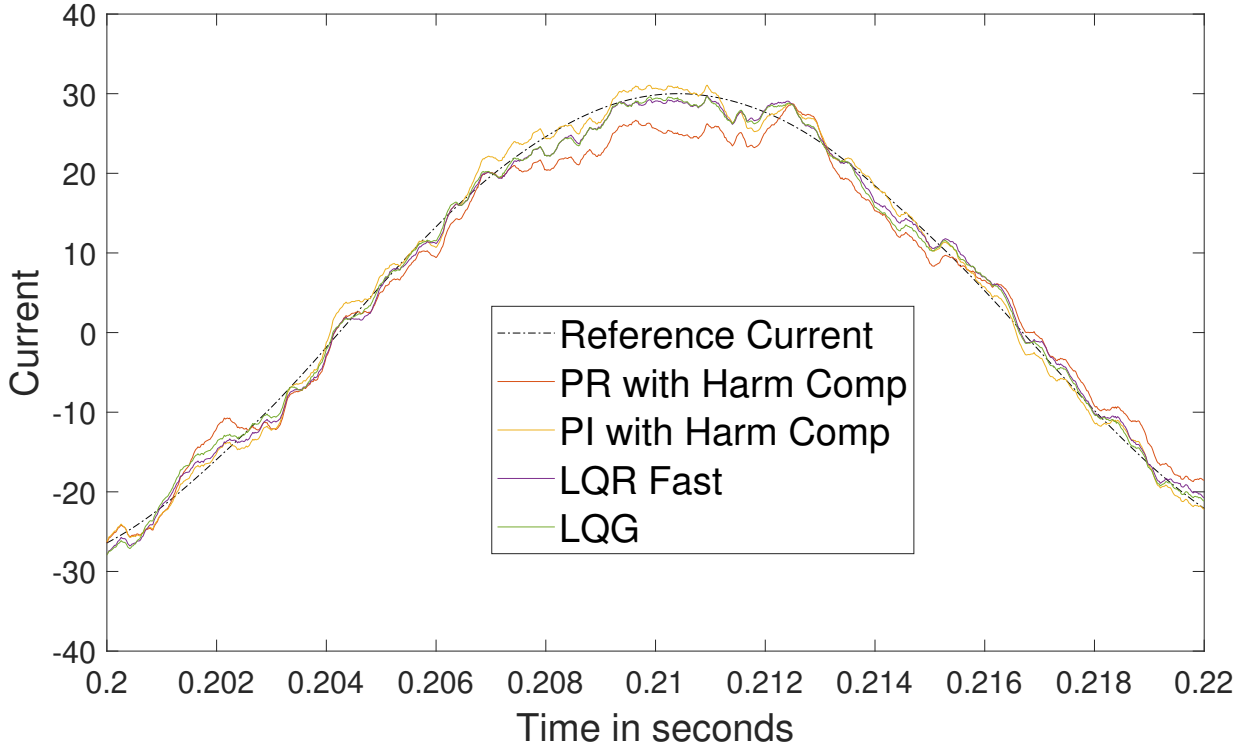

Figure 4.4: Measuring I_2 and viewing I_2 while in steady state of 30 A.

4.1.2 Step: I_1 and I_2

The stability during reference changes were tested using case 3.2.2 and the resulting plots are shown in Figures 4.5-4.8. In these images it seems that no major difference has been introduced. The one thing that appears to change a bit is that the I_1 current becomes a bit smoother in the peak error when measuring on I_2 but the peak errors themselves do not change much in size.

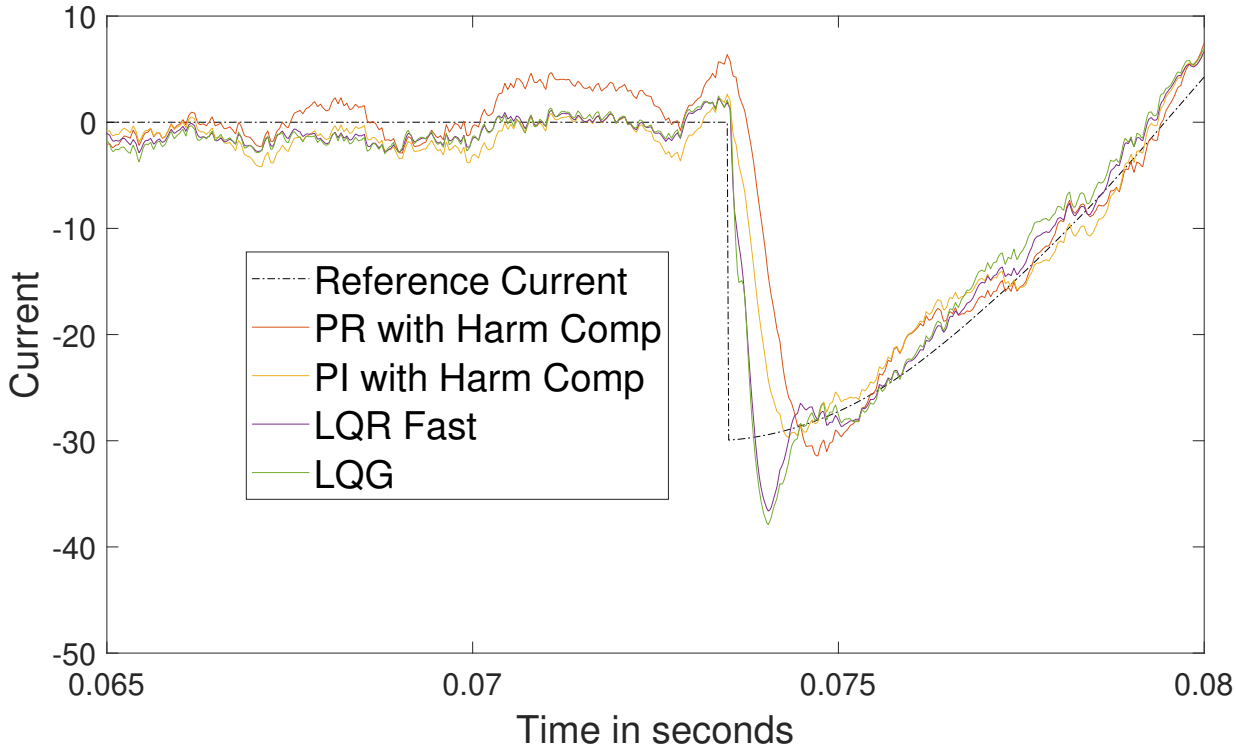

Figure 4.5: Measuring I_1 and viewing I_1 while a reference current step.

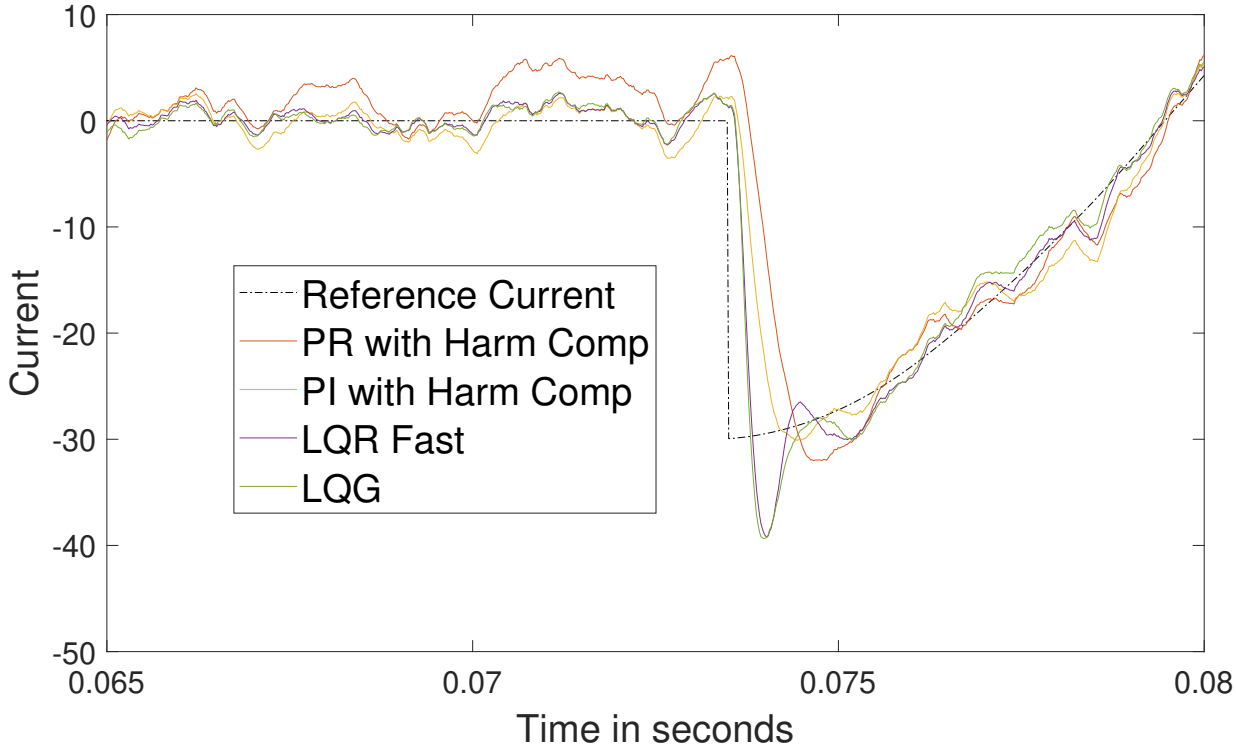

Figure 4.6: Measuring I_1 and viewing I_2 while a reference current step.

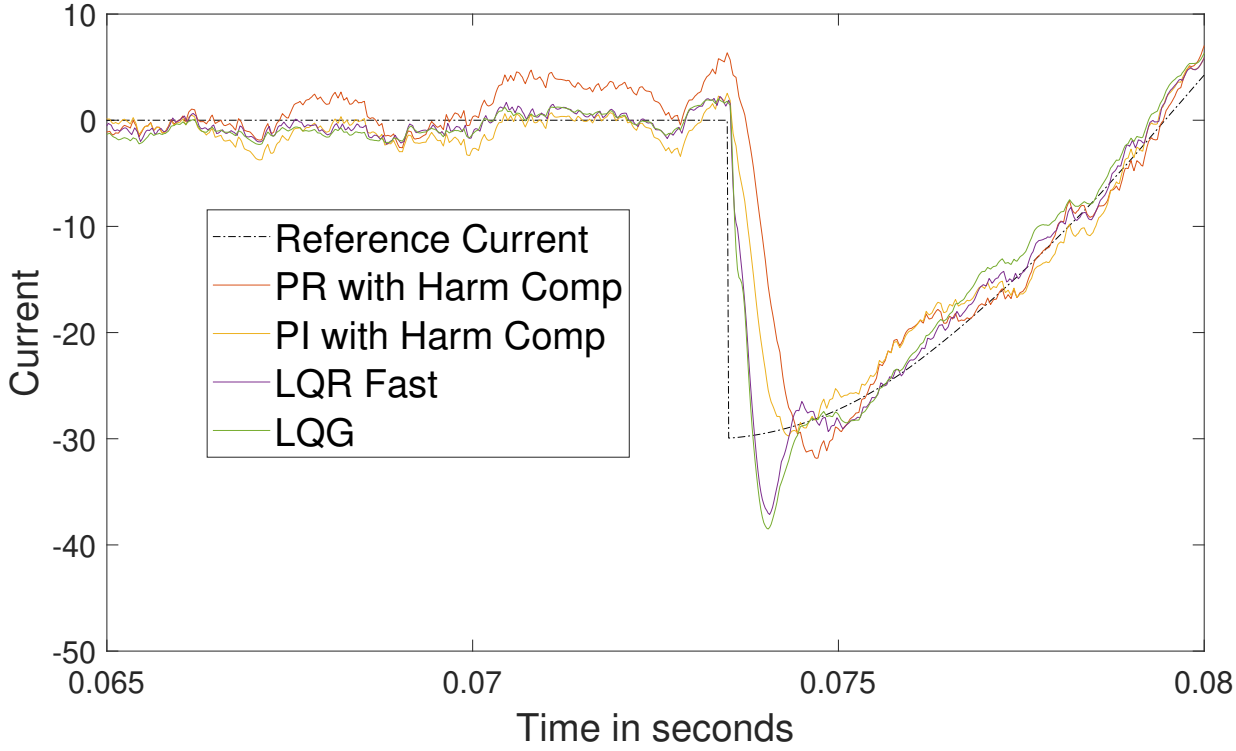

Figure 4.7: Measuring I_2 and viewing I_1 while a reference current step.

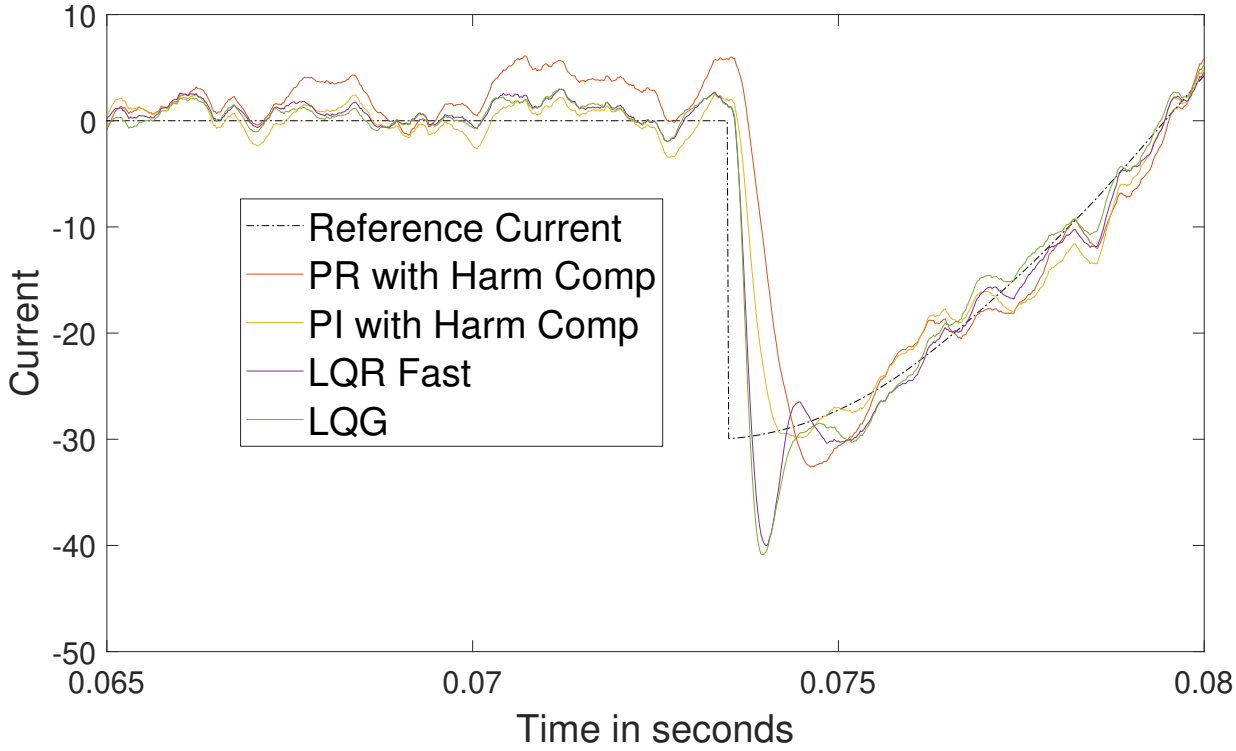

Figure 4.8: Measuring I_2 and viewing I_2 while a reference current step.

4.1.3 Drop: I_1 and I_2

The final stability test to perform when comparing the current sensor position is Case 3.2.3. Tables 4.3 and 4.4 as well as Figures 4.9- 4.12 show the effect that the grid drop has on the controllers behaviours. In this case just as the one with steady state it can be seen that the RMS error for the I_2 current becomes decreases for PI and PR but increases for the LQR and LQG. This means that the peak error increases for the LQR and LQG and decreases for the PI and PR. The I_1 current errors become smaller for all controllers when switching the measurement point from I_1 to I_2.

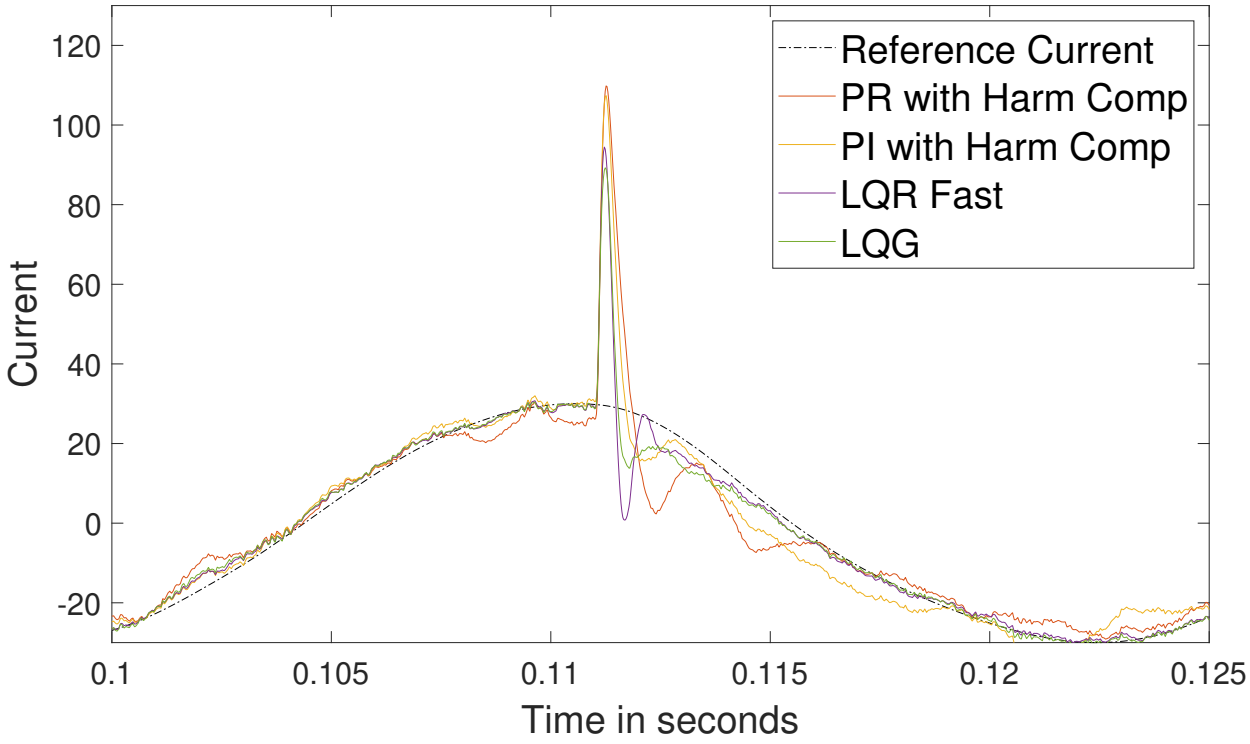

Figure 4.9: Measuring I_1 and viewing I_1 while a grid drop occurs.

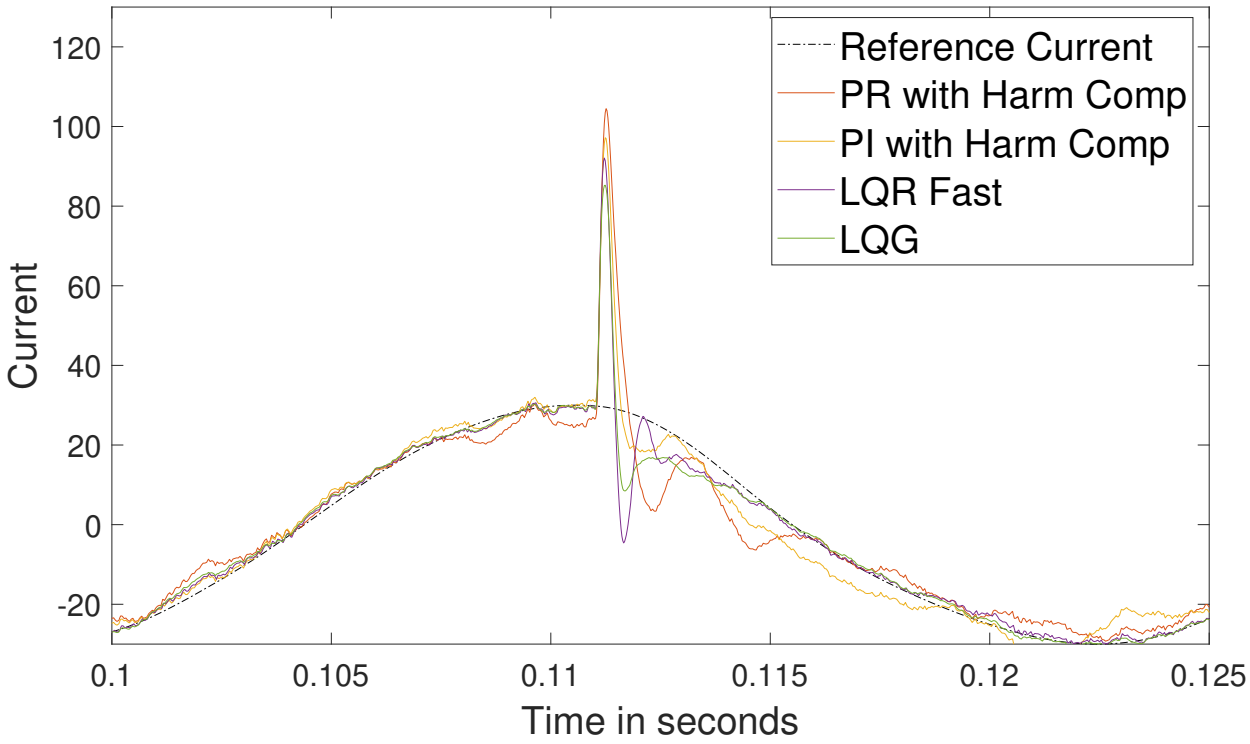

Figure 4.10: Measuring I_2 and viewing I_1 while a grid drop occurs.

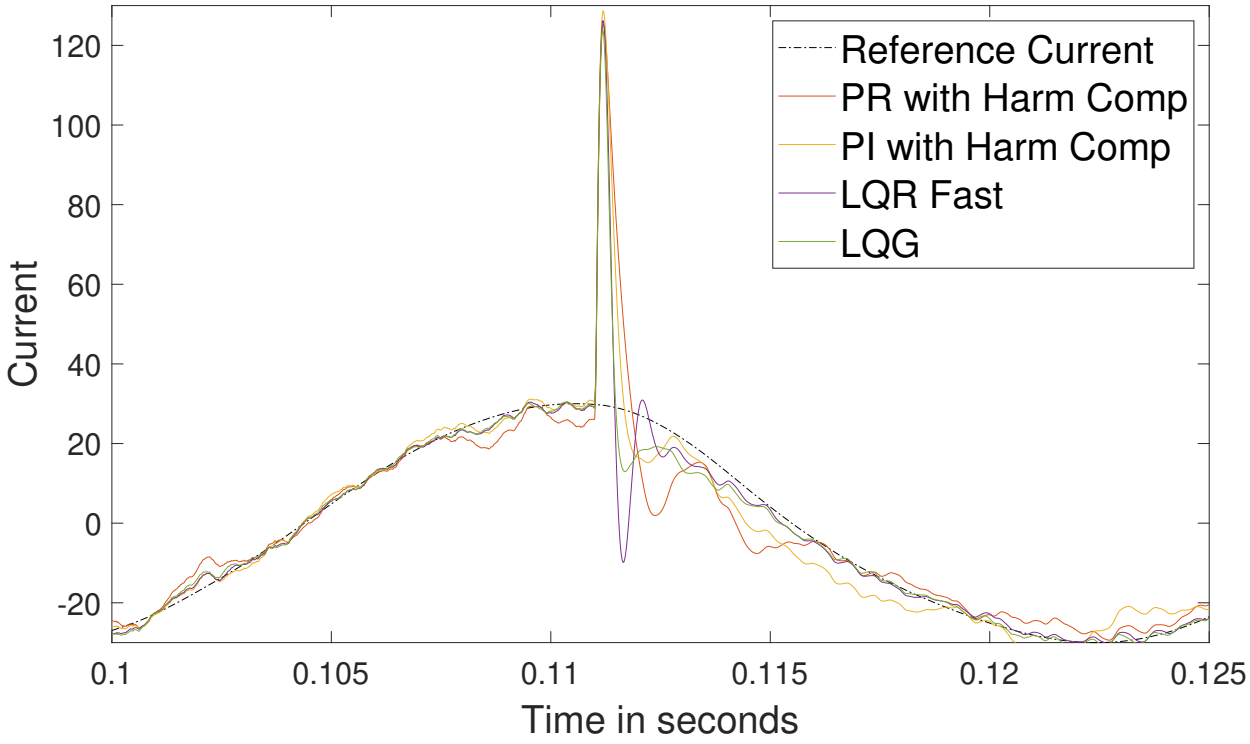

Figure 4.11: Measuring I_1 and viewing I_2 while a grid drop occurs.

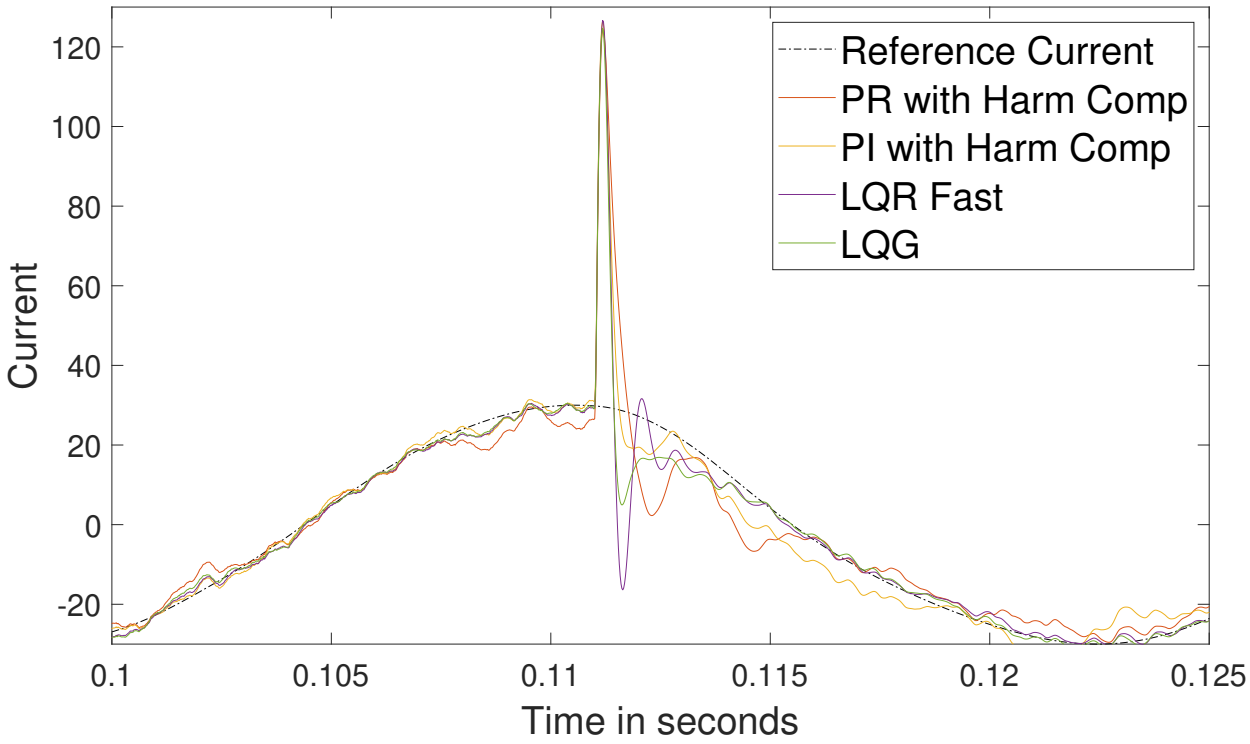

Figure 4.12: Measuring I_2 and viewing I_2 while a grid drop occurs.

Table 4.3: The peak error during a drop when measuring on the I_1 current

Controller type	Peak error on I_1	Peak error on I_2
PR With Harmonics	80.3269 A	95.8325 A
PI With Harmonics	77.893 A	99.1114 A
LQR Fast	64.9031 A	96.5901 A
LQG Slowed down	59.7289 A	94.5542 A

Table 4.4: The peak error during a drop when measuring on the I_2 current

Controller type	Peak error in I_1	Peak error in I_2
PR With Harmonics	74.9788 A	94.705 A
PI With Harmonics	67.6534 A	96.9935 A
LQR Fast	62.5145 A	97.0045 A
LQG Slowed down	55.7235 A	95.0874 A

4.2 Control behaviour of controllers using 1 ms rise time

This section will display the results of the previously mentioned slow controllers working with a 1 ms rise time. These controllers are shown in Table 4.5.

Table 4.5: A table showing all the slow controllers that will be in the results of this section.

Controller
PI (original)
PR
PI with Harmonic compensation slowed down
PR with harmonic compensation slowed down
LQR slowed down

As can be seen in Figure 4.13 is that the PI controllers are the ones that follows the reference around 0 A the closest. The one controller that is able to completely follow the reference current is the PI controller without the harmonic mitigation. Once the harmonic mitigation is added onto the PI controller, a small oscillation occurs. This oscillation would not be noticed in a real grid but is note worthy from an theoretical aspect. The PR controllers both with and without harmonic mitigation as well as the LQR has an oscillation from between 3 to 5 A in amplitude. That is far away from the PI controllers almost perfect steady state following of the reference.

Something similar happens when studying the steady state performance of these controllers when following a 30 A sinusoidal, Figure 4.14, as when following the 0 A, Figure 4.13. The PI controllers are able to follow the reference almost perfectly with no noticeable errors. The controllers using an R term on the other hand are able to follow the basic shape of the reference but always with a delay and some amplitude differences.

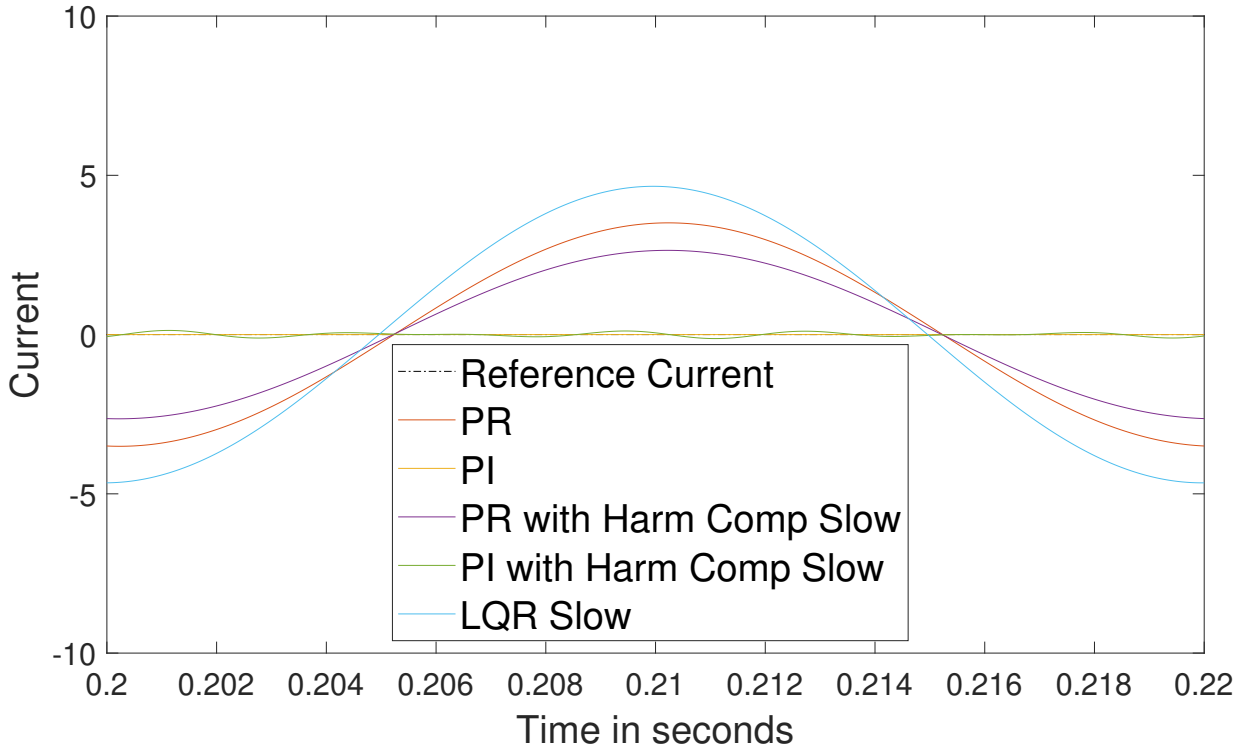

Figure 4.13: Slow controllers: measuring I_2 and viewing I_2 at steady state of 0 A.

Table 4.6: The RMS for steady state of 0 A for the slow controllers

Controller type	RMS I_2
PR	3.0836 A
PI	2.0686 A
PR With Harmonics Slow	2.534 A
PI With Harmonics Slow	2.2127 A
LQR Slow	3.8054 A

Table 4.7: The RMS for steady state of 30 A for the slow controllers

Controller type	RMS I_2
PR	4.2154 A
PI	2.8483 A
PR With Harmonics Slow	3.4518 A
PI With Harmonics Slow	3.0494 A
LQR Slow	4.8353 A

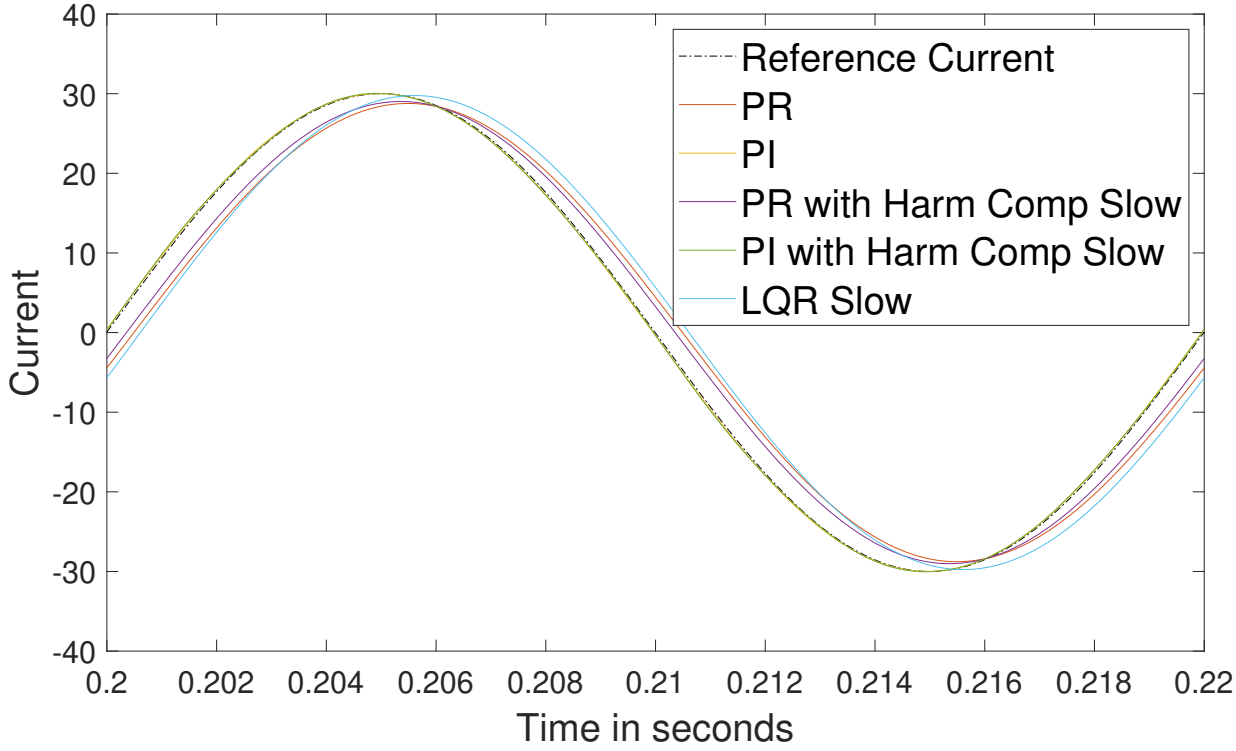

Figure 4.14: Slow controllers: measuring I_2 and viewing I_2 at steady state of 30 A.

Next a step in reference was tested by using test case 3.2.2 and the result is shown in Figures 4.15. This figure show that, while the PI are better at following the reference at steady state, they take a lot longer to end up in steady state than it takes for the controllers with an R-term. All of these controllers are slow in their response to the step and no oscillation occurs. The controllers end up rather far away from the reference for some time before returning to the steady state.

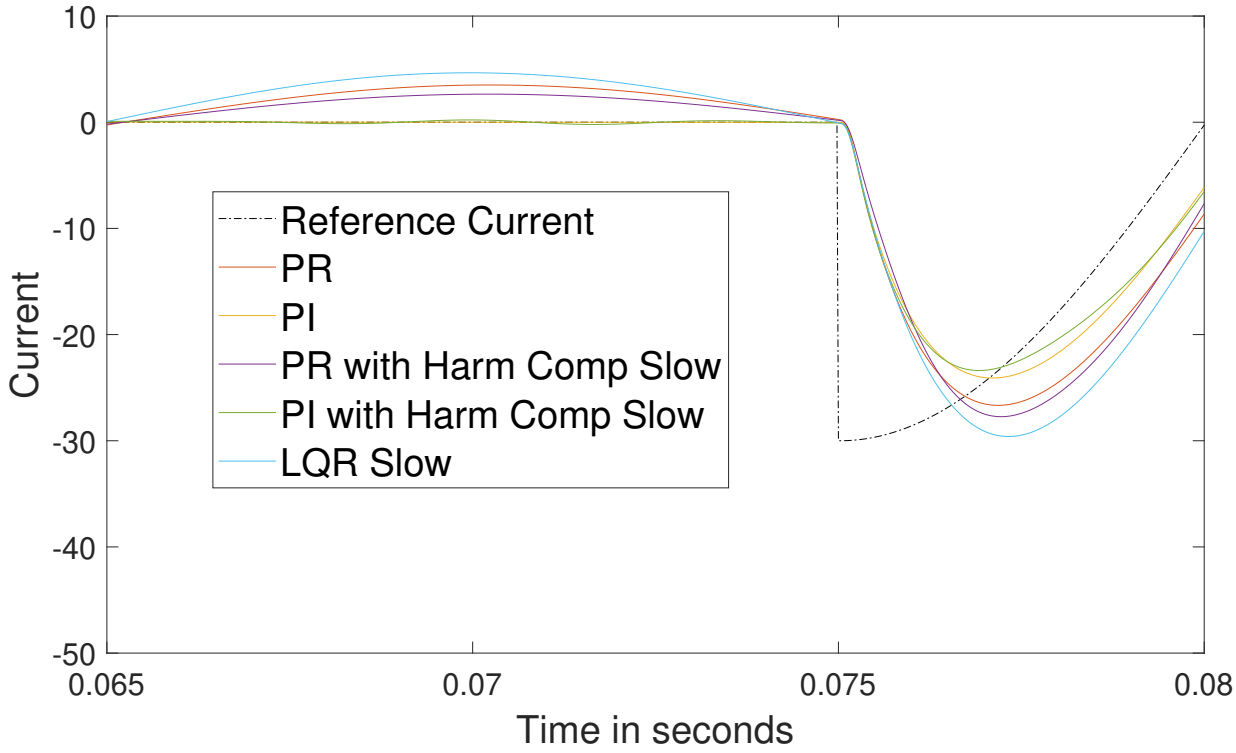

Figure 4.15: Slow controllers: measuring I_2 and viewing I_2 at reference step.

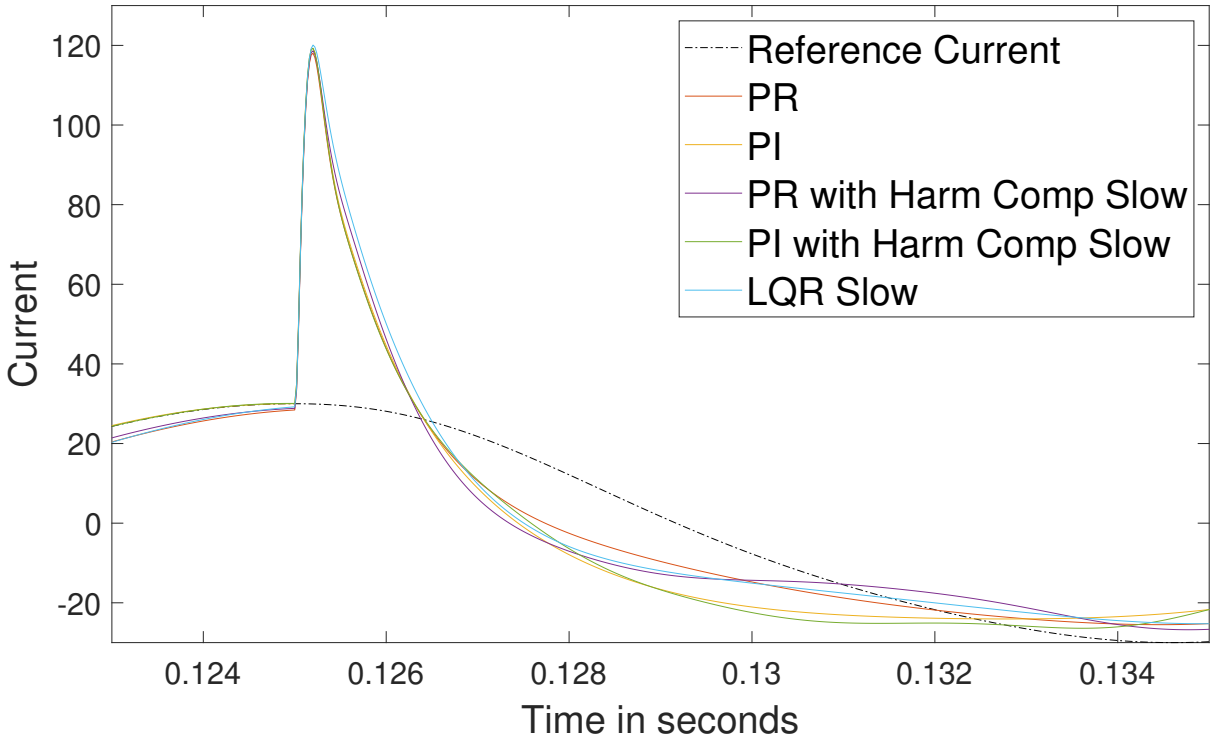

Figure 4.16: Slow controllers: measuring I_2 and viewing I_2 at grid drop.

Table 4.8: The peak error between the reference and the I_2 current when a grid drop occurs for slow controllers when using the ideal grid.

Controller type	Peak error I_2
PR	90.3914 A
PI	91.6877 A
PR With Harmonics Slow	90.1437 A
PI With Harmonics Slow	93.7297 A
LQR Slow	91.0803 A

At the occurrence of a grid drop, as seen in Figure 4.16, all of the controllers reach roughly the same amplitude peak in the spike of current. The differences lies in the behaviour afterwards when the signals are supposed to return to steady state. Just as for the step response case the PI controllers are slow at returning to the steady state. Otherwise the behaviour of the PR, LQR and PI controllers are mostly similar in their response to the change.

Figure 4.17 showcases the response when running the slower controllers on test case 4 from chapter 3.2.4. The controllers all behave almost the same as for the grid drop case. The large difference is that the controllers take a longer time to compensate for the large error and to get back to steady state. These changes arise from the fact that the grid is still connected and keeps on changing, unlike in the grid drop case.

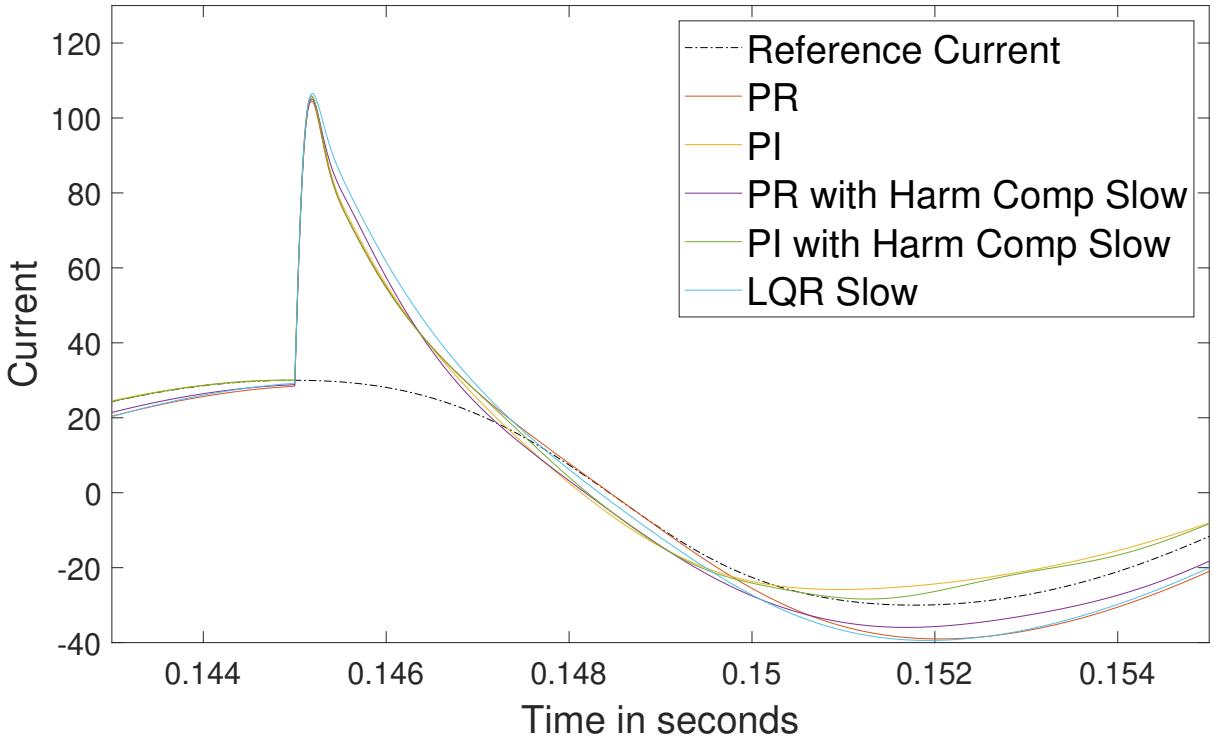

Figure 4.17: Slow controllers: measuring I_2 and viewing I_2 with phase shift.

Case 5 from chapter 3.2.5 combines the phase shift with the grid returning from a drop. The result of this test is shown in Figure 4.18 and shows a very small jump in the current. The jump is small since the grid returns but the shift ensures that the grid is at almost 0 volt when the change occurs. The recovery is similar to that of the phase shift case.

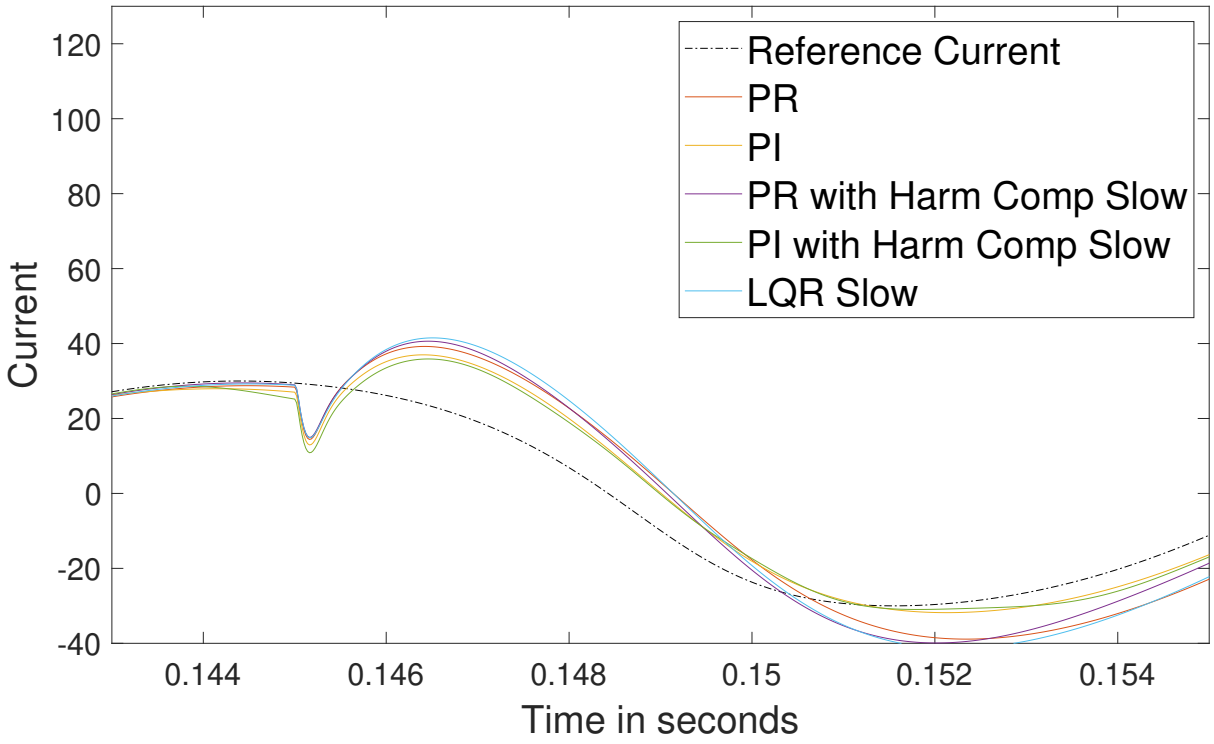

Figure 4.18: Slow controllers: measuring I_2 and viewing I_2 with phase shift and drop.

Finally the steady state and grid drop are tested again but for the more realistic case with the measured grid and read disturbances. The steady state is shown in Figure 4.19 and the drop is shown in Figure 4.21. The general behaviour for both these cases are the same as when the ideal grid was used.

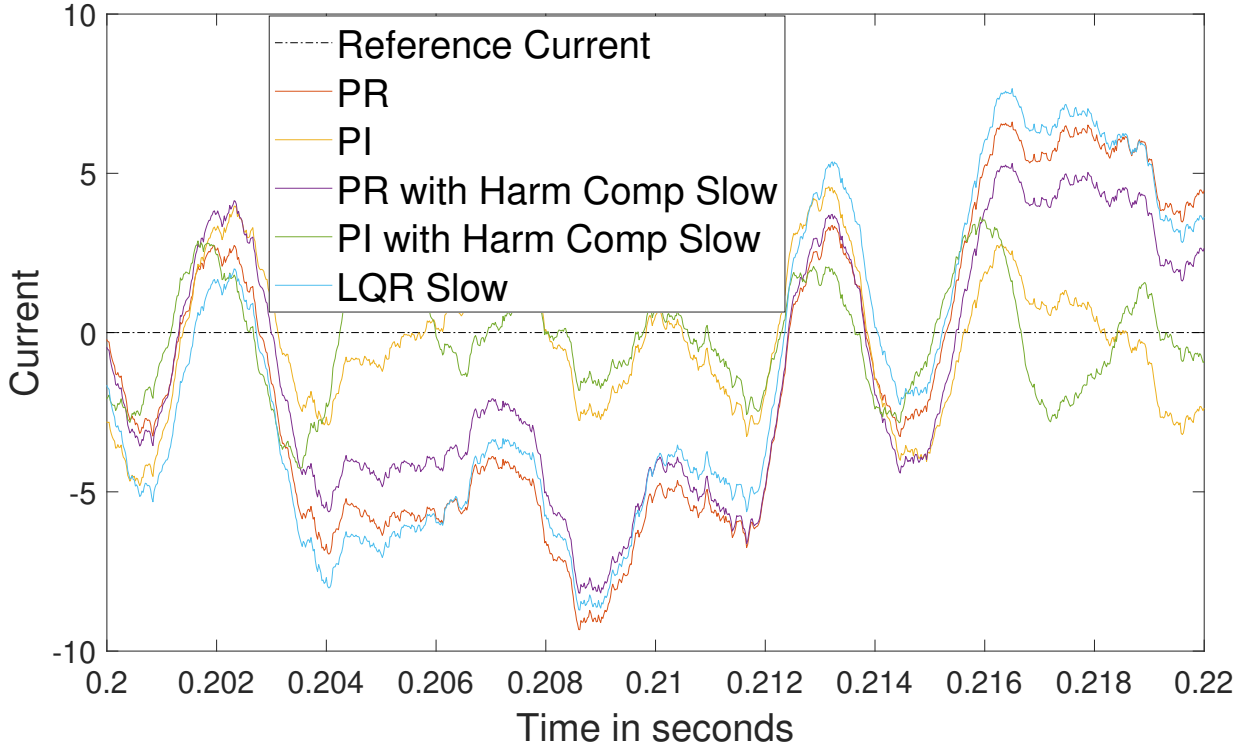

Figure 4.19: Slow controllers: measuring I_2 and viewing I_2 at steady state 0 A. Using measured grid data.

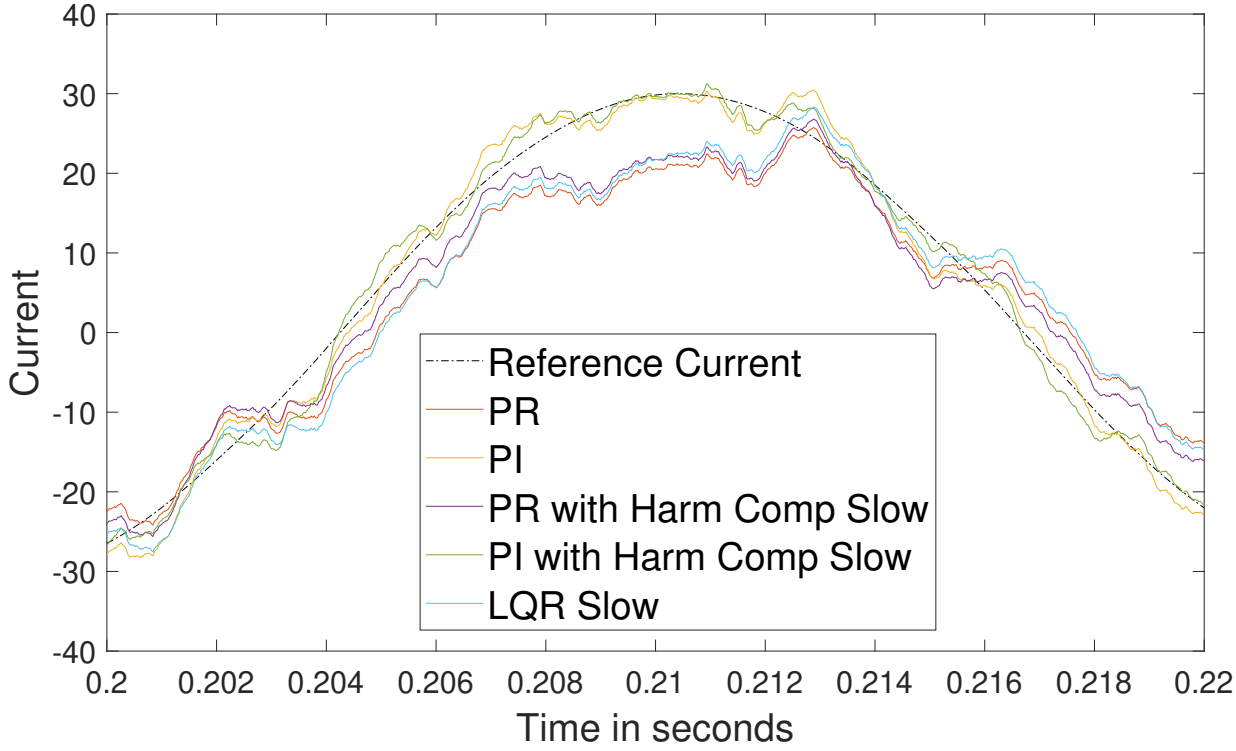

Figure 4.20: Slow controllers: measuring I_2 and viewing I_2 at steady state 30 A. Using measured grid data.

Table 4.9: The RMS error between the reference and the I_2 current during a steady state reference of 30 amp while using the measured grid.

Controller type	RMS I_2
PR	8.0735 A
PI	5.343 A
PR With Harmonics Slow	7.2366 A
PI With Harmonics Slow	5.356 A
LQR Slow	7.8103 A

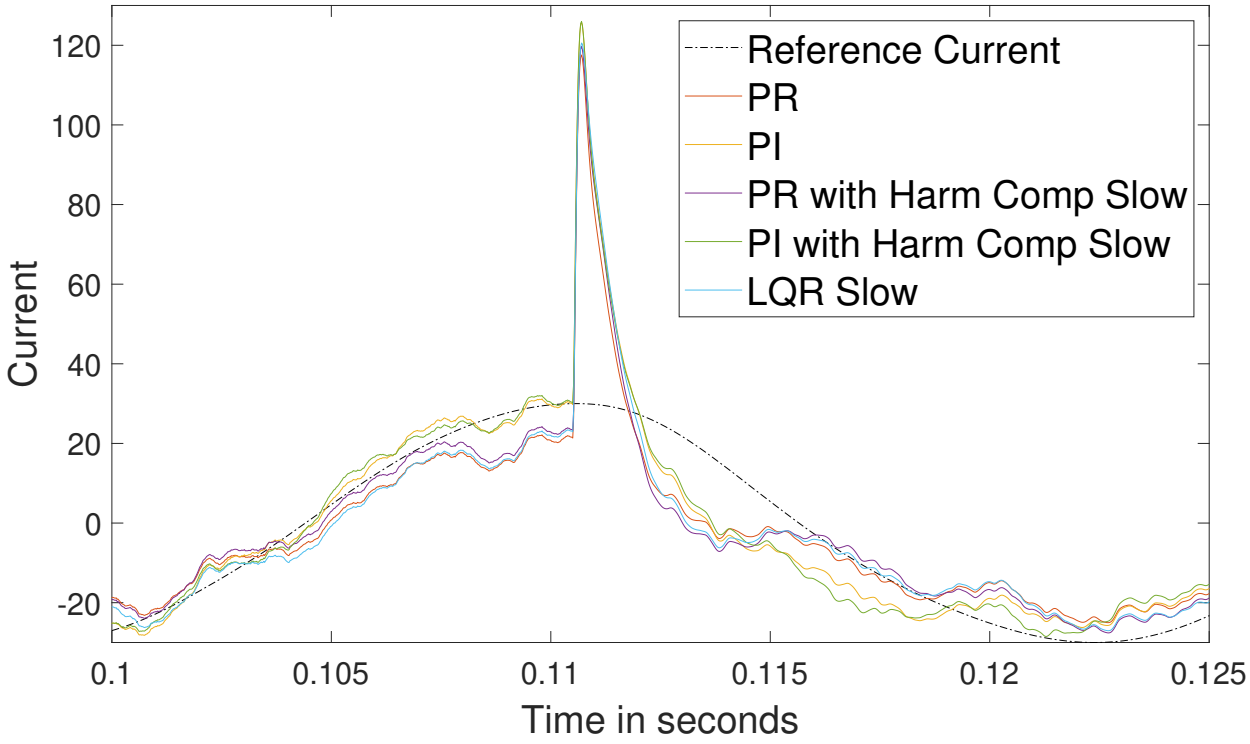

Figure 4.21: Slow controllers: measuring I_2 and viewing I_2 with drop of grid. Using measured grid data.

4.3 Control behaviour of controllers using at most 0.6 ms rise time

This section will do the same as the previous one but the focus will be shifted on to the faster controllers. These are controllers that have a rise time of between 0.25 to 0.6 ms. They do not all have the same speed because some of the controllers become unstable at the faster speeds. With that in mind the controllers where speed up while trying to minimise the loss of stability.

Table 4.10: A table showing all the fast controllers that will be in the results of this section.

Controller	Rise Time
PI with harmonic compensation	400 μs
PR with harmonic compensation	560 μs
LQR Fast	280 μs
LQG	260 μs

When evaluating the steady state behaviour of the faster controllers, as seen in Figure 4.22, with a reference signal of 0 A the PI controller with harmonic mitigation appears to follow the reference without any apparent oscillations. The remaining controllers oscillates around the reference current, where the PR with harmonic compensation has the largest amplitude. The slow controllers, as seen in Figure 4.13, oscillates with a much larger amplitude than their faster counterparts does. However there is to be said that the oscillations still occurs, no matter the speed of the controller, although the faster controllers appear to have a reduced amplitude.

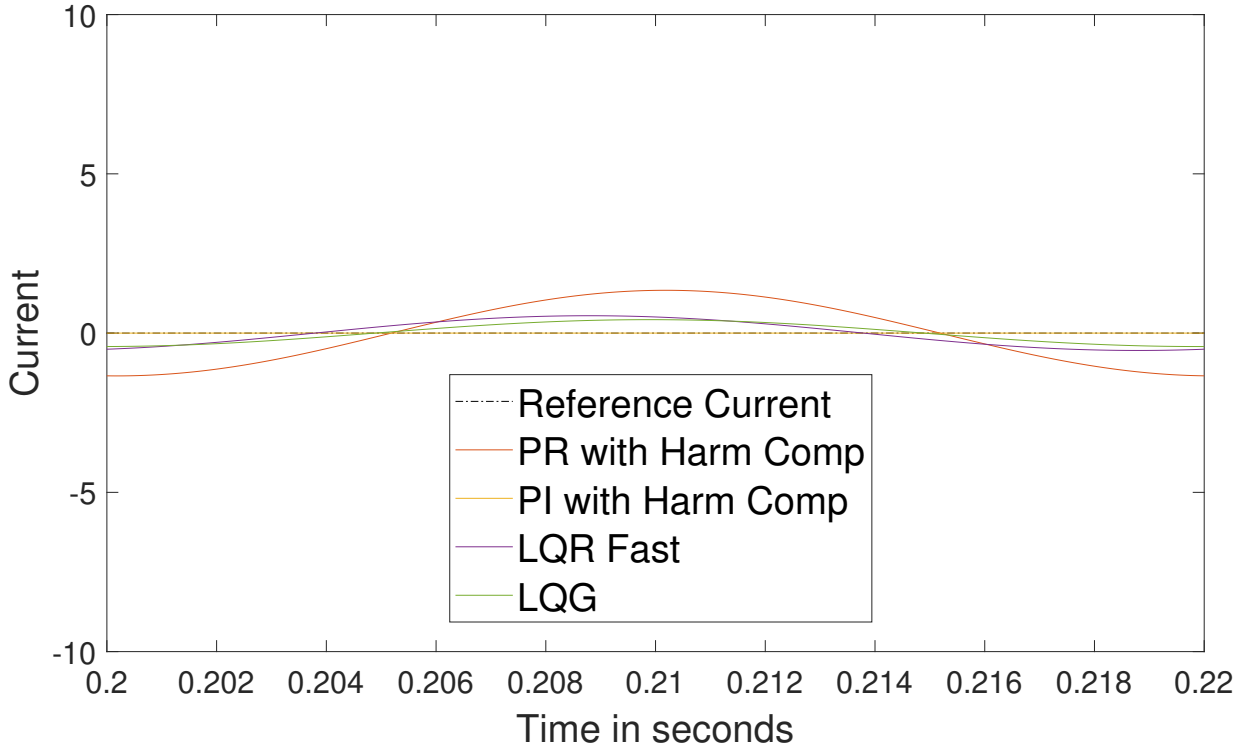

Figure 4.22: Fast controllers: measuring I_2 and viewing I_2 at steady state of 0 A.

Table 4.11: The RMS error when running the fast controllers on the measured grid and using a reference of 0 A sinusoidal.

Controller type	RMS I_2
PR With Harmonics	1.325
PI With Harmonics	1.288 A
LQR Fast	0.58346 A
LQG Slowed down	0.51635 A

The fast controllers appears to be able to follow the reference current of 30 A quite well without any significant shift as seen in Figure 4.23, however this is not true for the PR with harmonic compensation. It still follows the reference somewhat accurately but is clearly not as strong as the other controllers. The reduced shift of the signals can be seen when comparing Figure 4.14 and Figure 4.23. It is worth to note that when the faster LQR and LQG are used they are able to follow the 30 amp reference closely even though they use an R term.

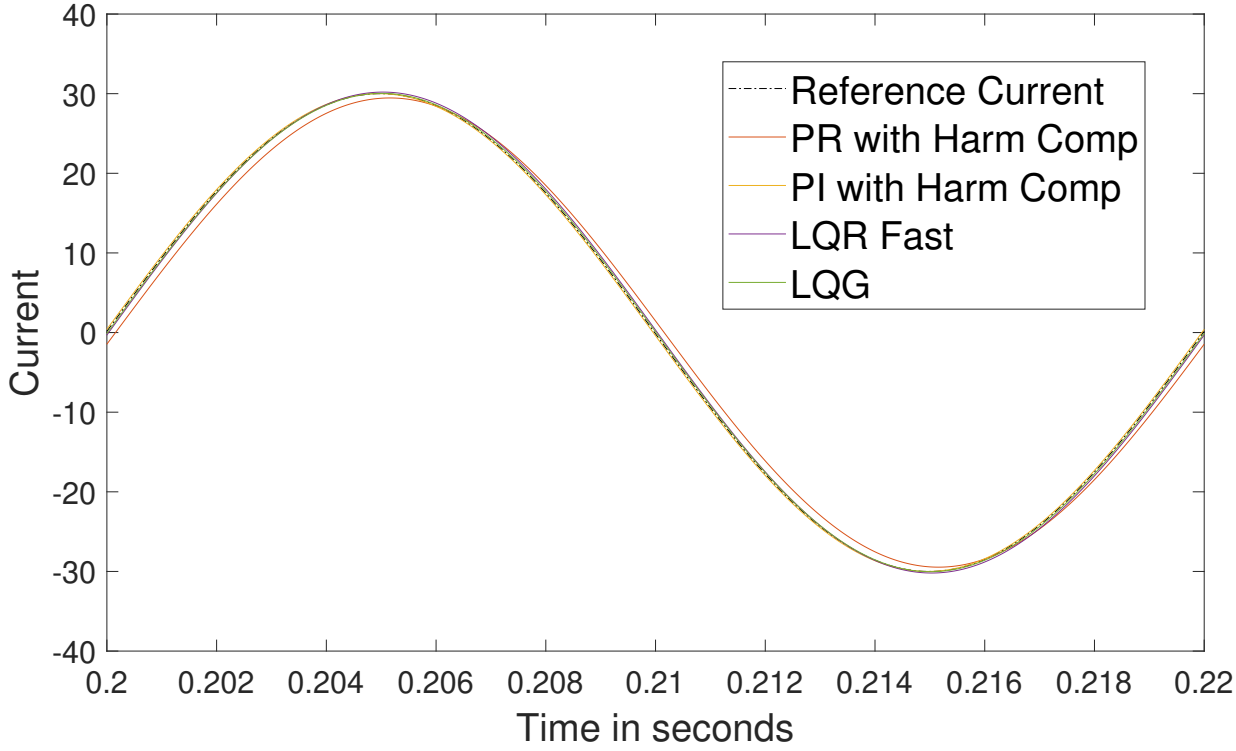

Figure 4.23: Fast controllers: measuring I_2 and viewing I_2 at steady state of 30 A.

Table 4.12: The RMS error when running the fast controllers on the measured grid and using a reference of 30 A sinusoidal.

Controller type	RMS I_2
PR With Harmonics	1.7613 A
PI With Harmonics	1.7526 A
LQR Fast	0.66753 A
LQG Slowed down	0.53656 A

The step response of the fast controllers are shown in Figure 4.24. The LQR and LQG appears to have a significant undershoot and the LQR has a little bit of oscillation, however these controllers are quick to converge to steady state and they follow it closely. The PI and PR with harmonic mitigation are the controllers which has the least amount of undershoot, however these continues to oscillate and are slower than the LQG and LQR to converge to the steady state.

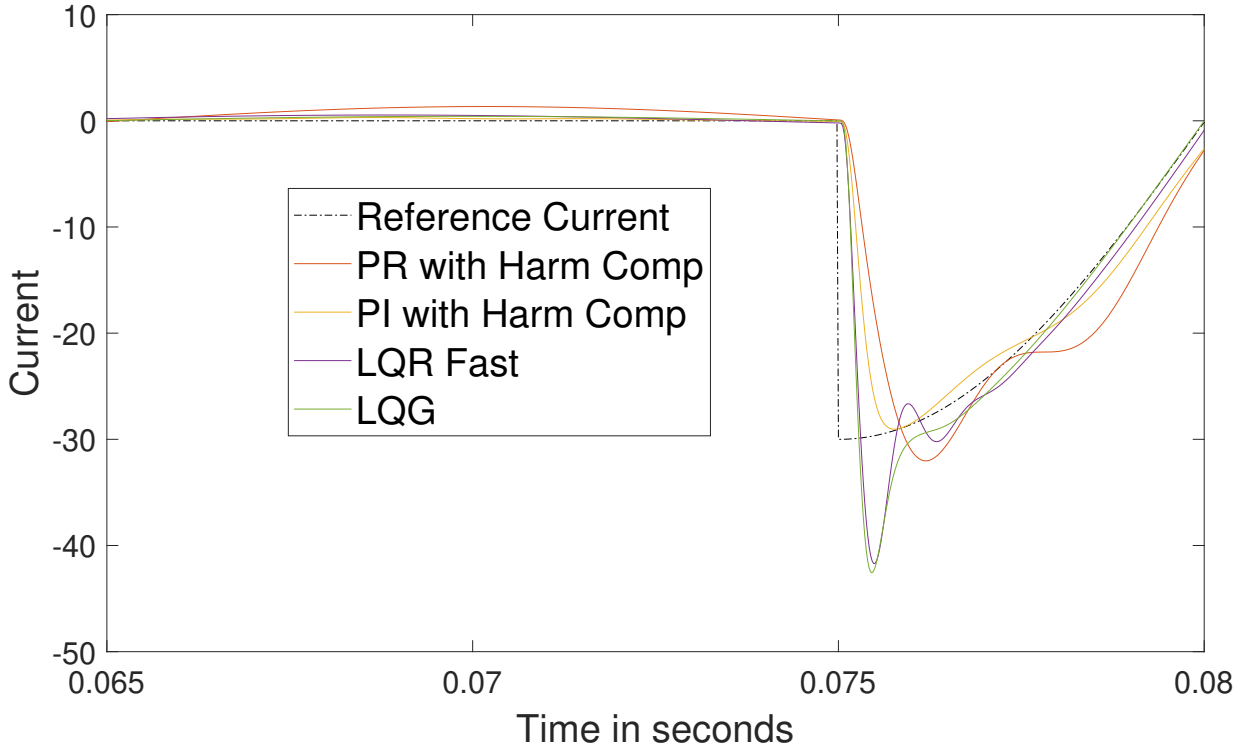

Figure 4.24: Fast controllers: measuring I_2 and viewing I_2 at reference current step.

The fast controllers when run on test case 3 from chapter 3.2.3 produce Figure 4.25. In it, all controllers are shown to get the same peak error but that the LQR and LQG quickly managed to return to steady state while the other controllers struggled to do this. While all controllers undershoots, the LQR does that the most and it also oscillates even if it is weak. The LQG on the other hand is faster than the LQR and does not oscillates at all.

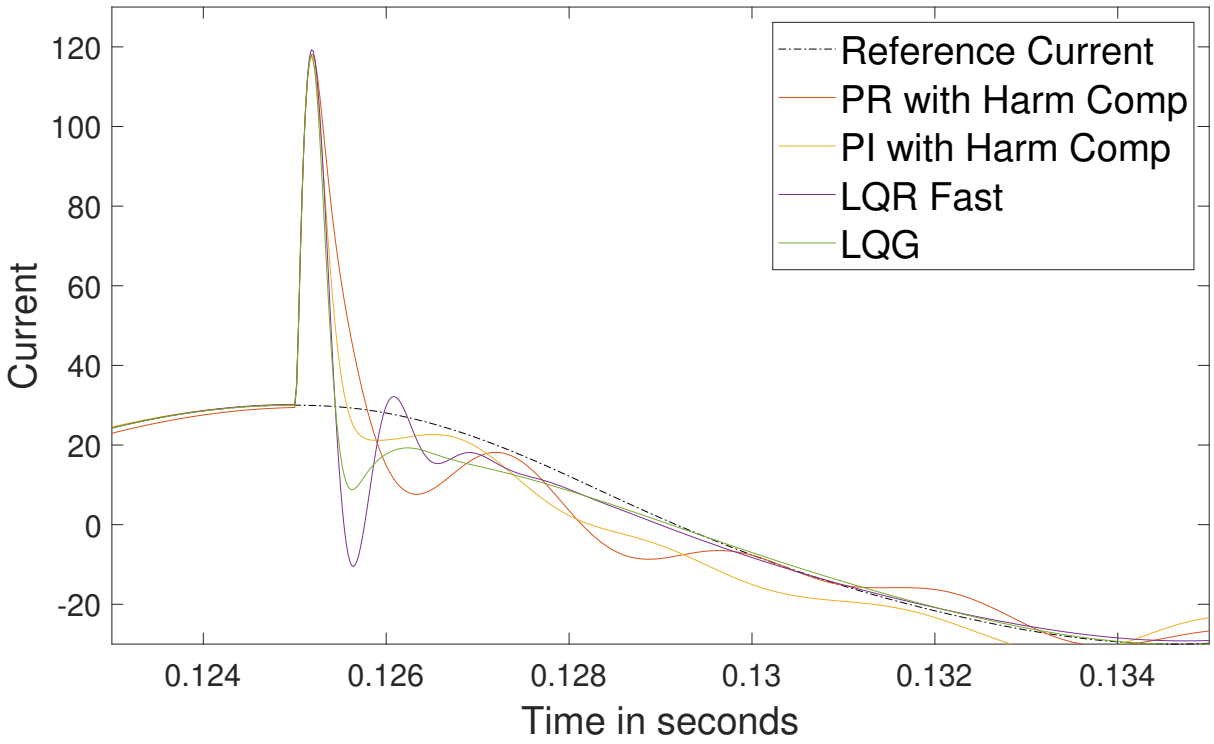

Figure 4.25: Fast controllers: measuring I_2 and viewing I_2 at grid drop.

Table 4.13: The peak error between the reference and the I_2 current when the grid experiences a drop and the measured grid is used.

Controller type	Peak error I_2
PR With Harmonics	88.9806 A
PI With Harmonics	90.7517 A
LQR Fast	89.3054 A
LQG Slowed down	88.033 A

When the phase shift occurs it appears to be less straining on the system, Figure 4.26, than when the grid dropped, Figure 4.25. The overall performance is similar in the two cases but the controllers goes faster towards steady state.

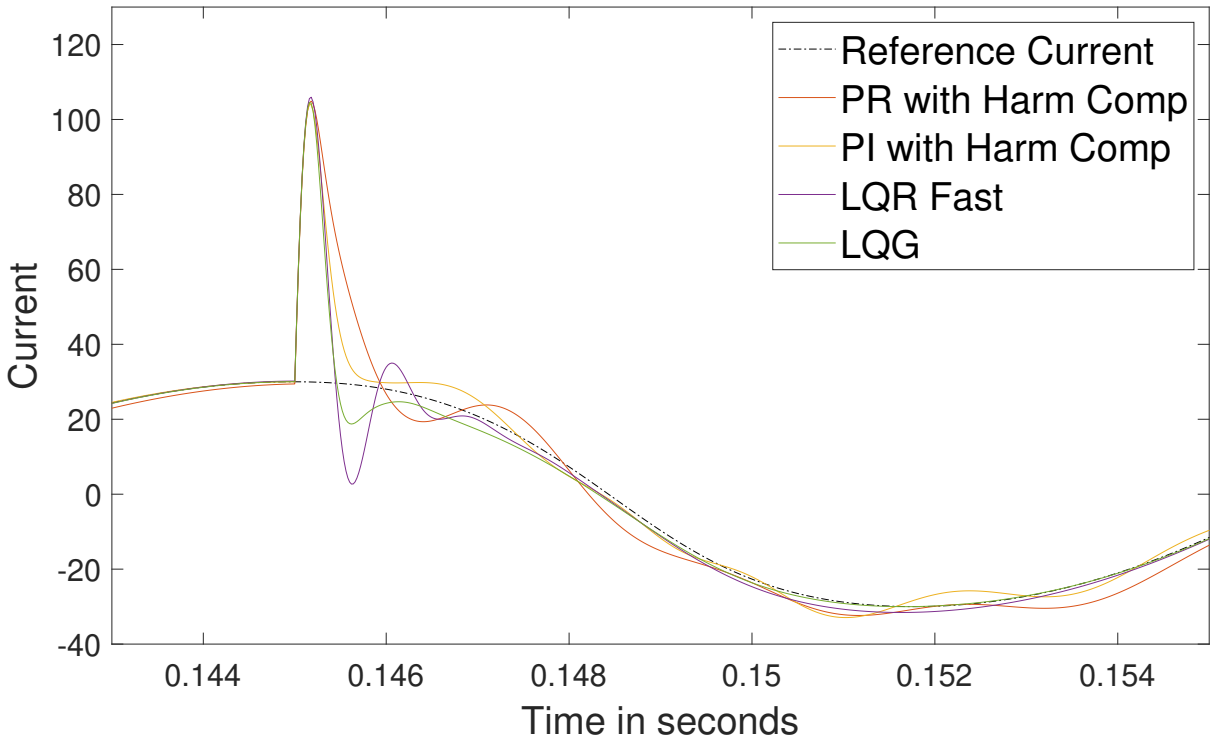

Figure 4.26: Fast controllers: measuring I_2 and viewing I_2 with phase shift.

When combining the phase shift with the grid drop recovery and running the fast controllers on it, Figure 4.27 is derived. This figure shows that the PI is not able to recover during the 20 ms when the drop occurs. Just as in the slow case the error spike is very low but it takes a long time for the controllers to recover. Here the same is seen as before in that the LQR and LQG are able to rather quickly return to steady state. While the PR is fast at recovering it is not able to closely follow the reference in steady state. The PI on the other hand is slow at recovering but follows the reference closely.

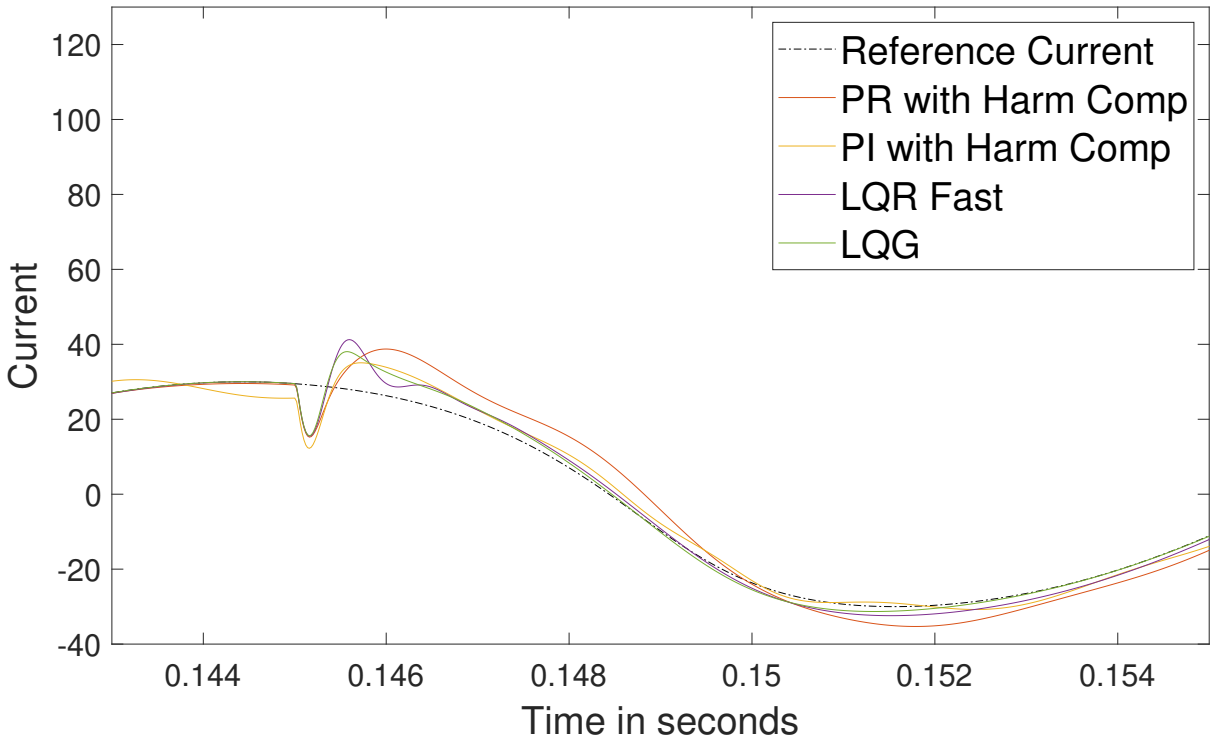

Figure 4.27: Fast controllers: measuring I_2 and viewing I_2 with phase shift and drop.

When the more realistic case is used for the fast controllers not much differs from what was previously seen. The Figures 4.28 and 4.30 both show that, while the signals become more noisy, the controllers still follow the reference closely. When comparing this with the slow controllers as seen in figure 4.19 and 4.21 it is clear that the faster controllers are able to mitigate a lot of the errors that seep through the slower controllers while still being faster at reacting to large changes. This is especially true for the recovery time. While the PI from the slow controllers is able to follow the steady state almost perfectly it needs a lot of time to get there. The LQG is able to do the same but without the long delay in recovery.

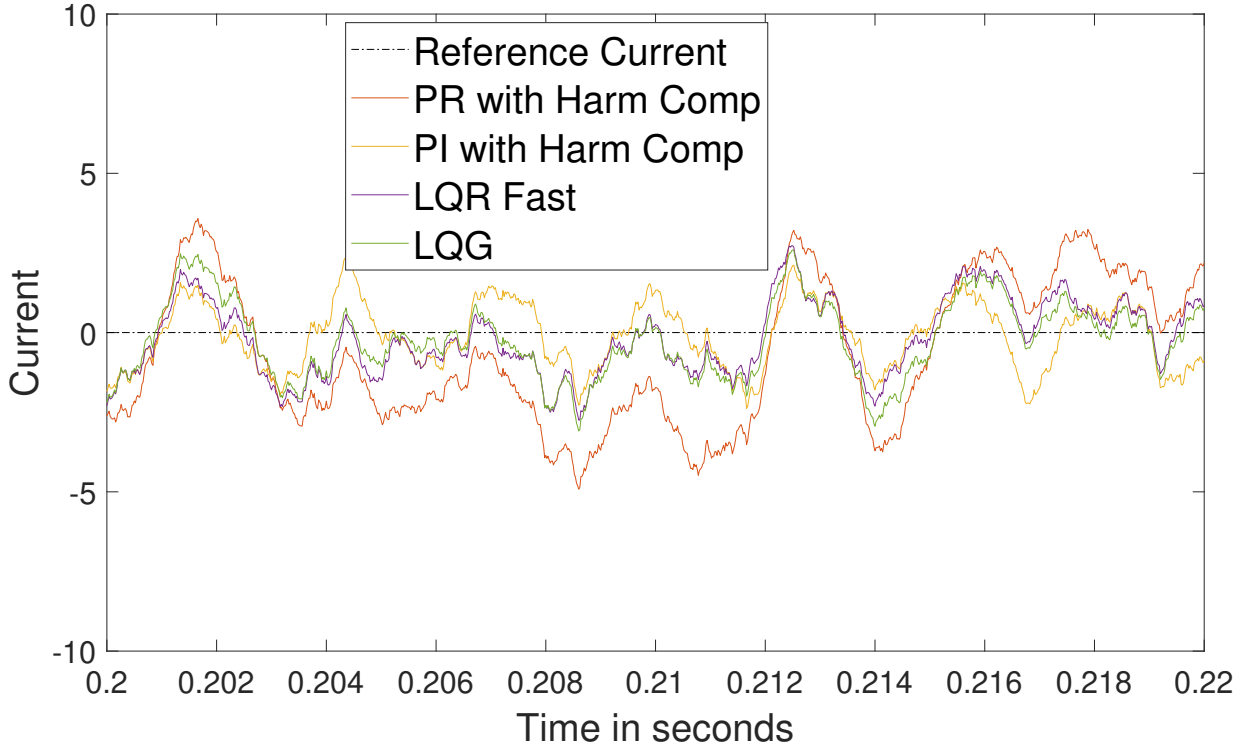

Figure 4.28: Fast controllers: measuring I_2 and viewing I_2 at steady state 0 A. Using measured grid data.

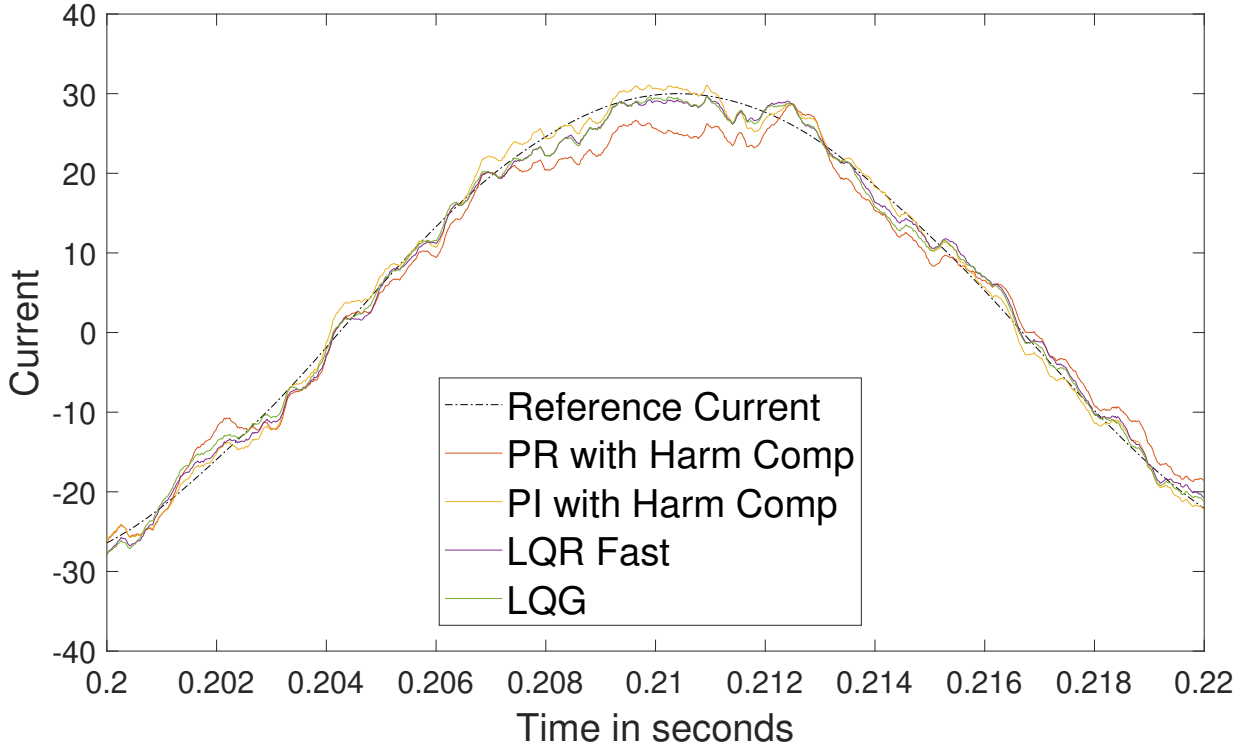

Figure 4.29: Fast controllers: measuring I_2 and viewing I_2 at steady state 30 A. Using measured grid data.

Table 4.14: The RMS error between the reference and the I_2 current when following the 30 A reference and using the measured grid.

Controller type	RMS I_2
PR With Harmonics	4.8156 A
PI With Harmonics	3.5858 A
LQR Fast	3.4009 A
LQG Slowed down	3.1217 A

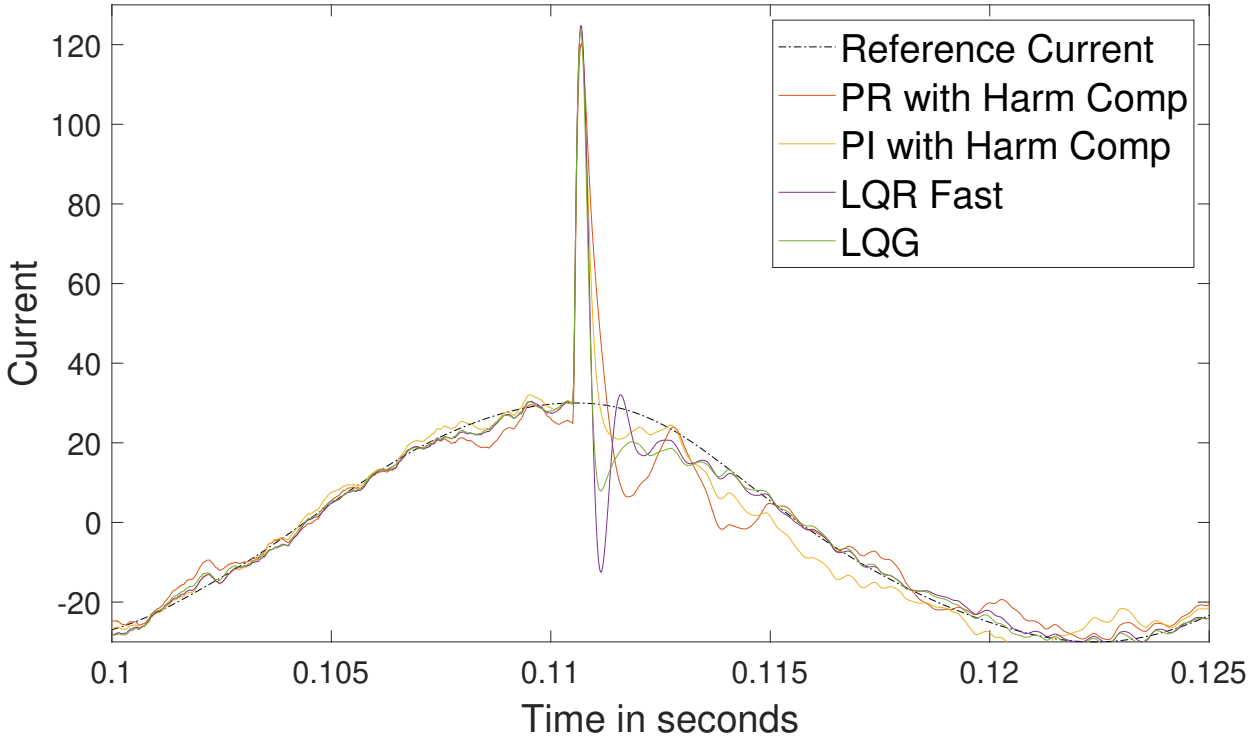

Figure 4.30: Fast controllers: measuring I_2 and viewing I_2 with drop of grid. Using measured grid data.

4.3.1 Fast controllers on weak grid inductance

The grid inductance L_2 has been divided by 4 in this case to illustrate the control behaviour on sensitive grids. When the fast controllers are run on a strong grid, when the grid impedance is low, then the currents acts more erratically. The system becomes more sensitive and as seen in Figure 4.31 the controllers creates more oscillations. None of the oscillations are large enough to create major problems but show a clear decrease in performance. Notably the LQR is the controller that seems to be the least affected by the strong grid.

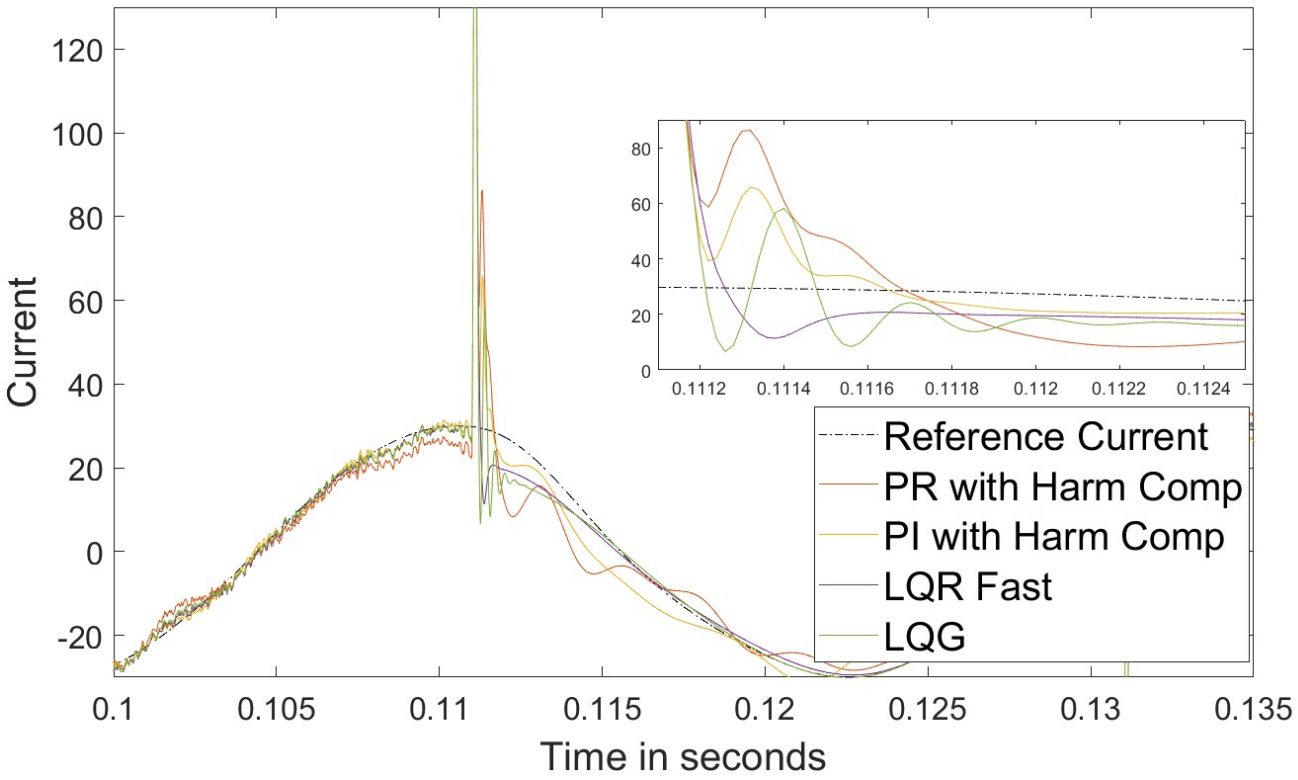

Figure 4.31: Fast controllers using a weak grid inductance with a drop in grid voltage

4.4 Adding one and two step ahead Smith prediction

This section will investigate the error performance and stability of using prediction. The Smith predictor has a one step ahead as well as a two step ahead version and both will be used and compared with the original controllers.

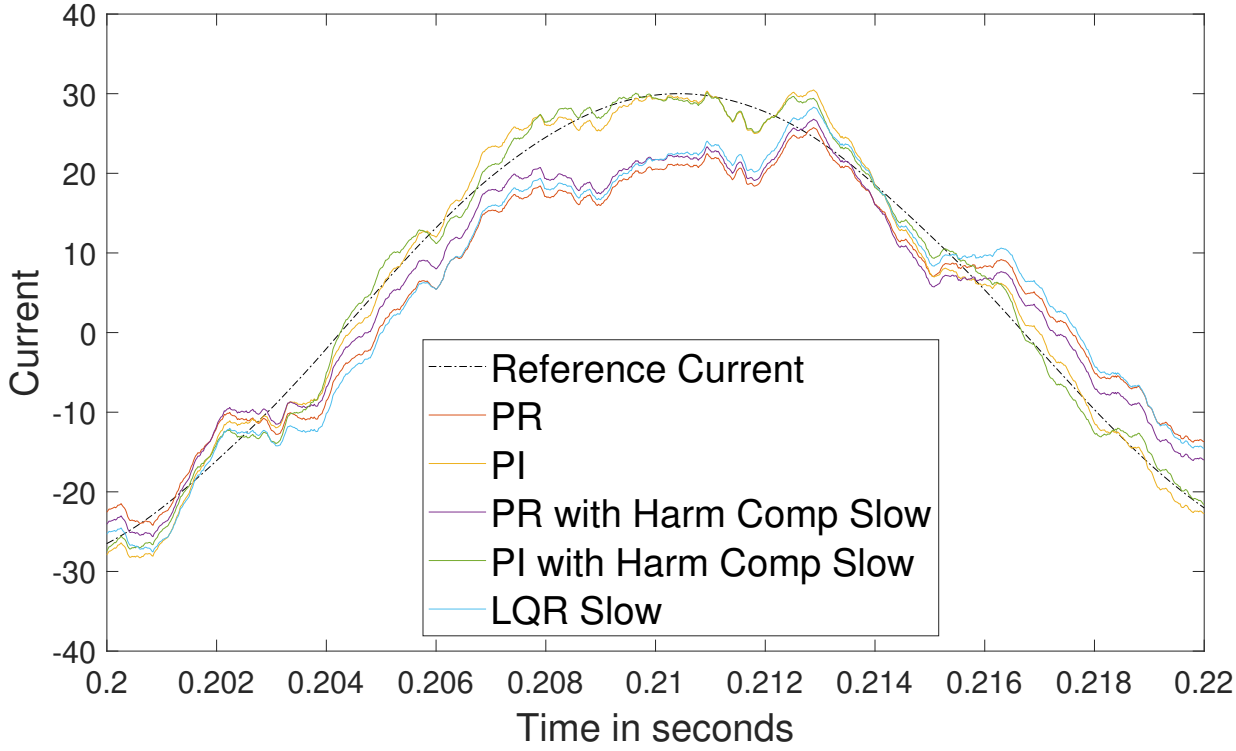

Figure 4.32: Slow controllers: one step ahead prediction with steady state 30 A. Using measured grid data.

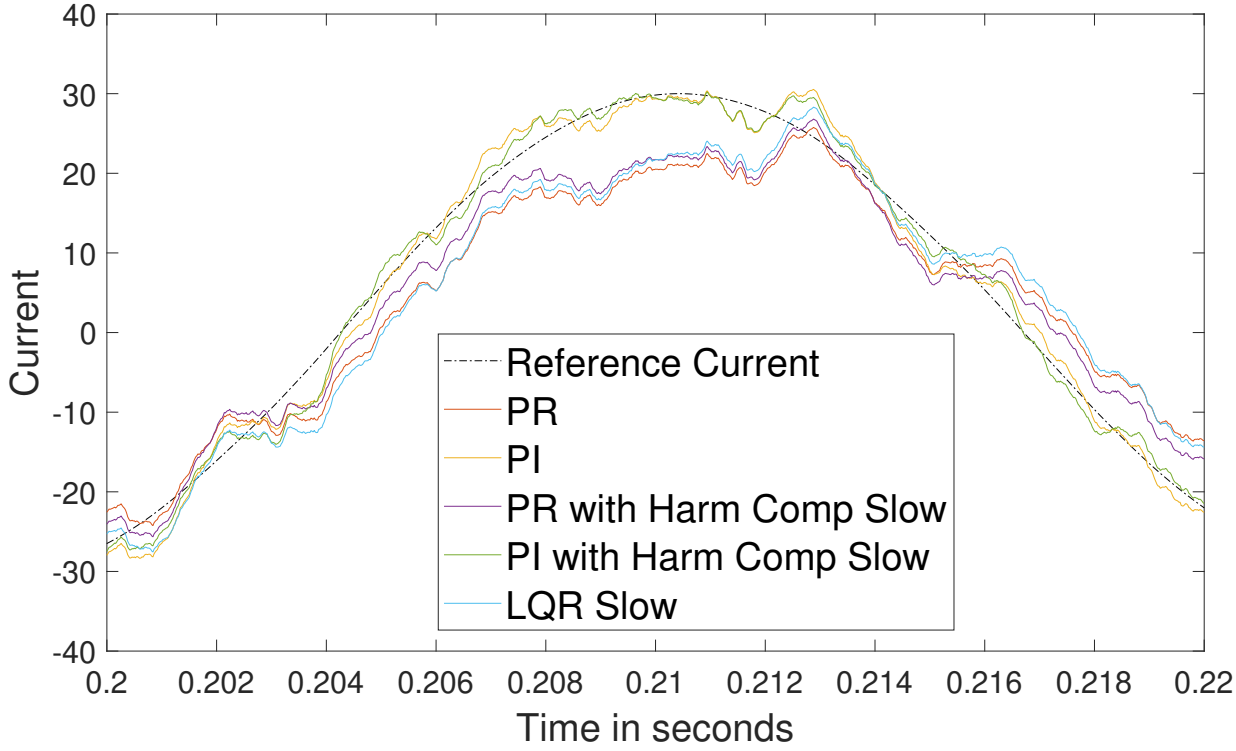

Figure 4.33: Slow controllers: two step ahead prediction with steady state of 30 A. Using measured grid data.

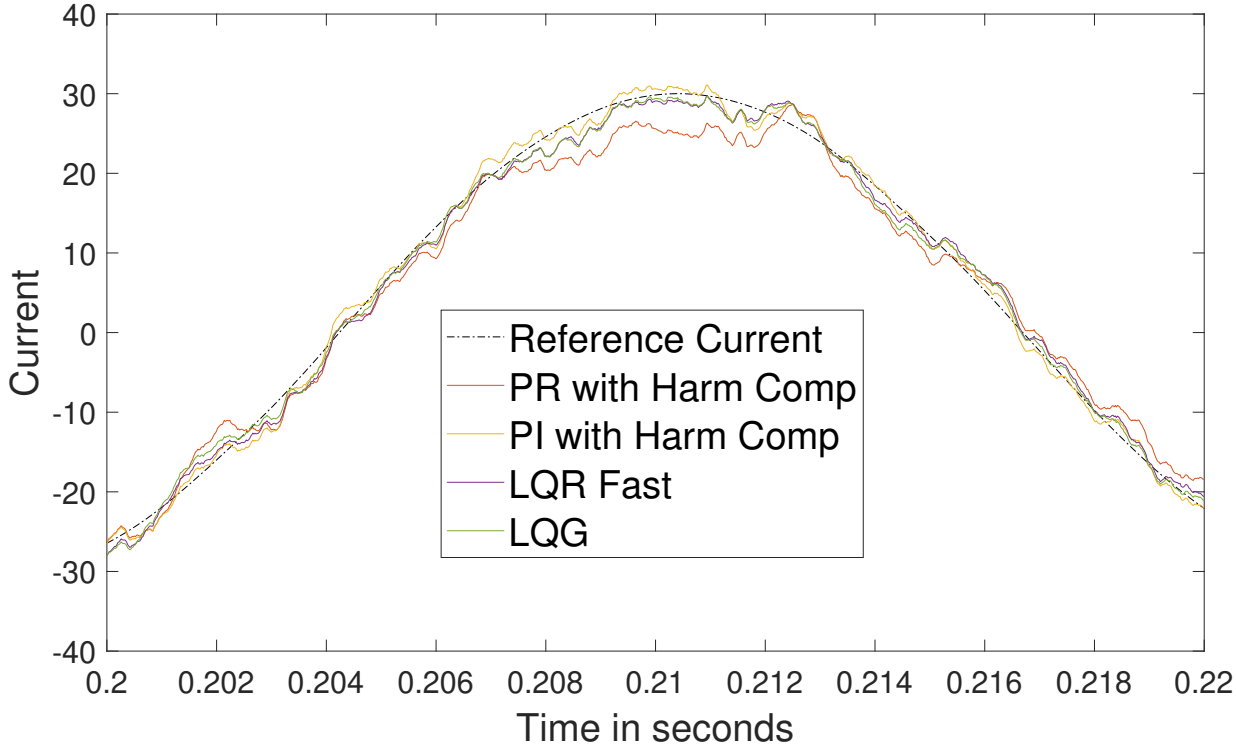

Figure 4.34: Fast controllers: one step ahead prediction with steady state of 30 A. Using measured grid data.

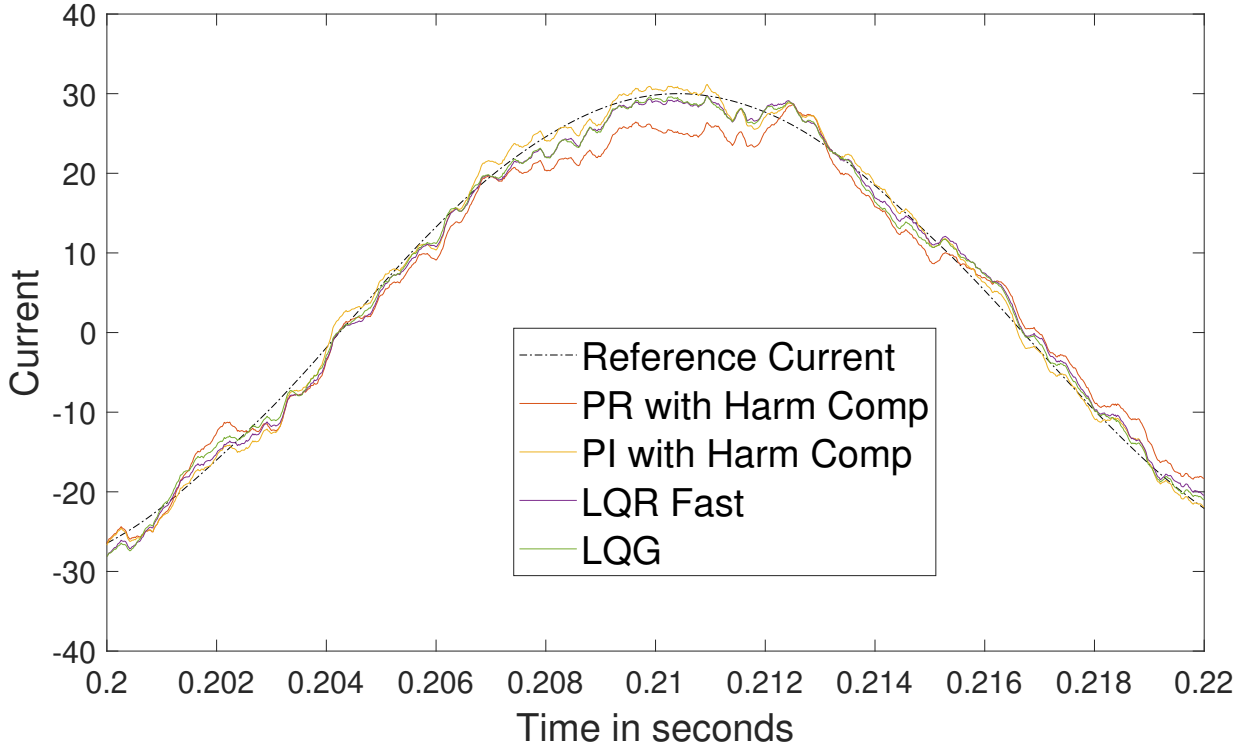

Figure 4.35: Fast controllers: two step ahead prediction with steady state of 30 A. Using measured grid data.

The use of several steps ahead does not appear to have an improvement on the controllers while in steady state with a reference current of 30 A, as seen in Figures 4.20, 4.32 and 4.33 as well as in Figures 4.29, 4.34 and 4.35. Using prediction does not appear to have made an obvious improvement on either oscillations or amplitudes.

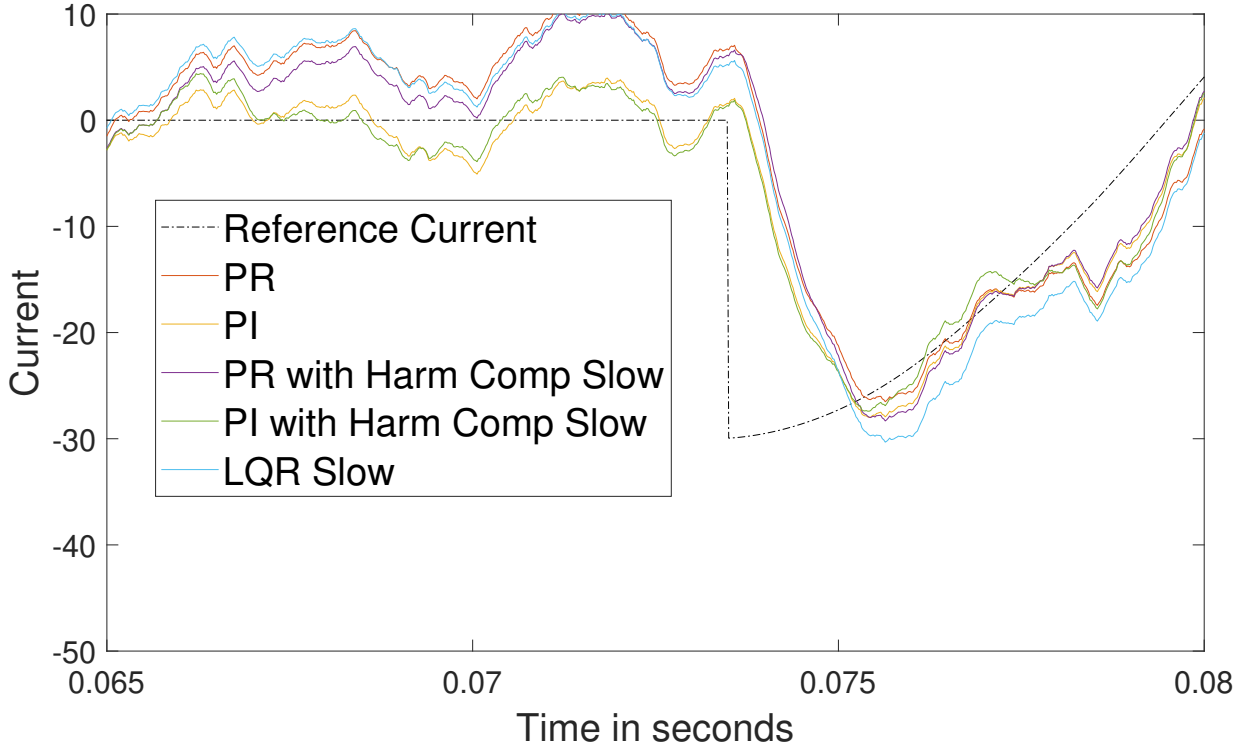

Figure 4.36: Slow controllers: one step ahead prediction with reference step. Using measured grid data.

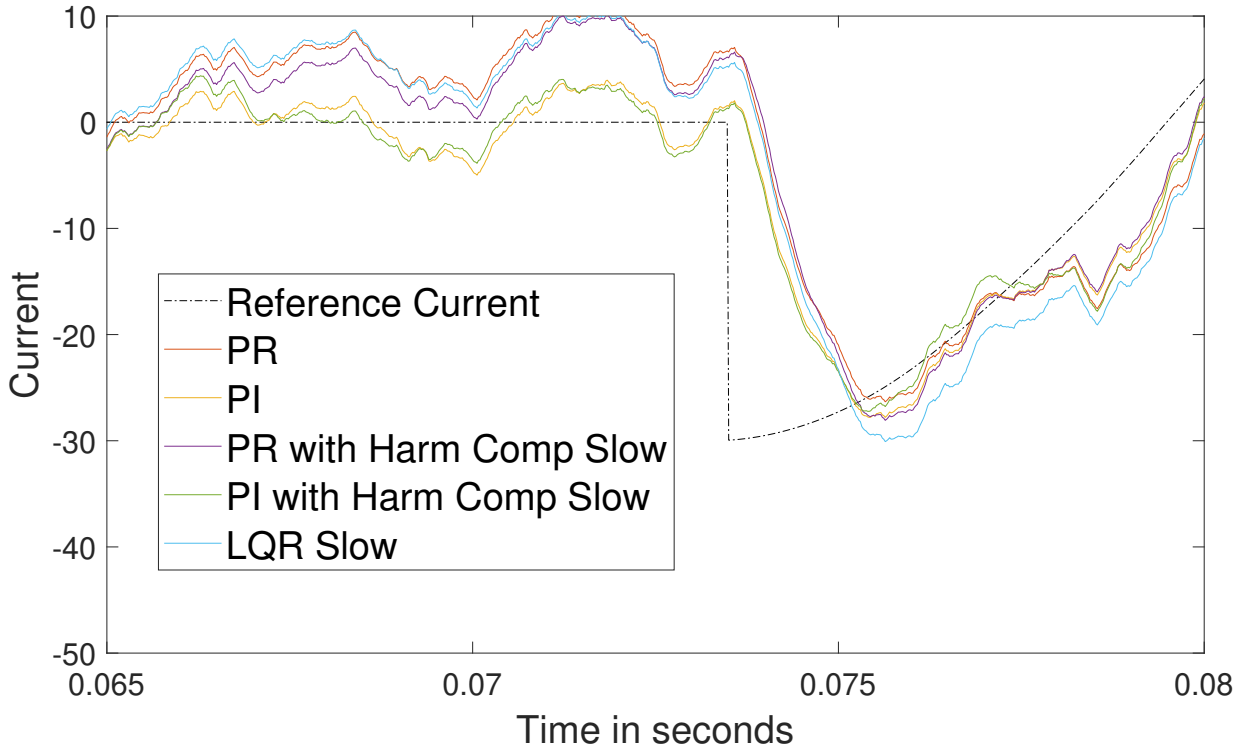

Figure 4.37: Slow controllers: two step ahead prediction with reference step. Using measured grid data.

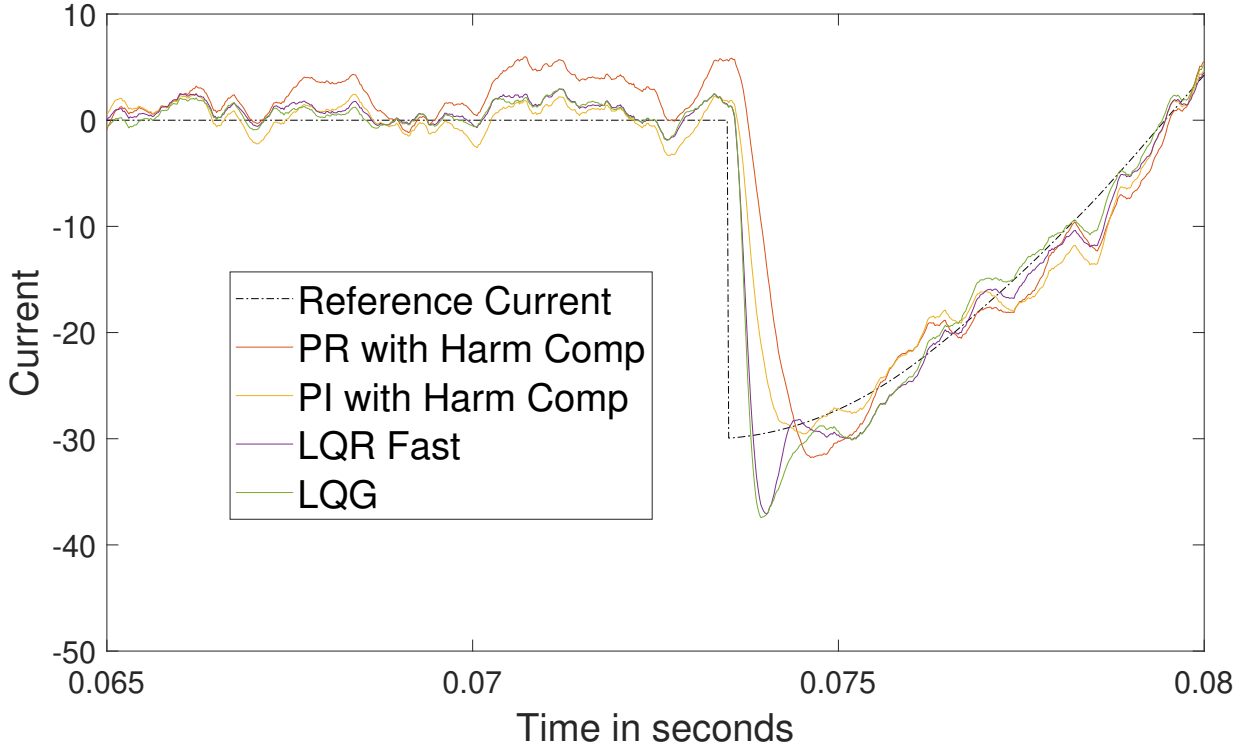

Figure 4.38: Fast controllers: one step ahead prediction with reference step. Using measured grid data.

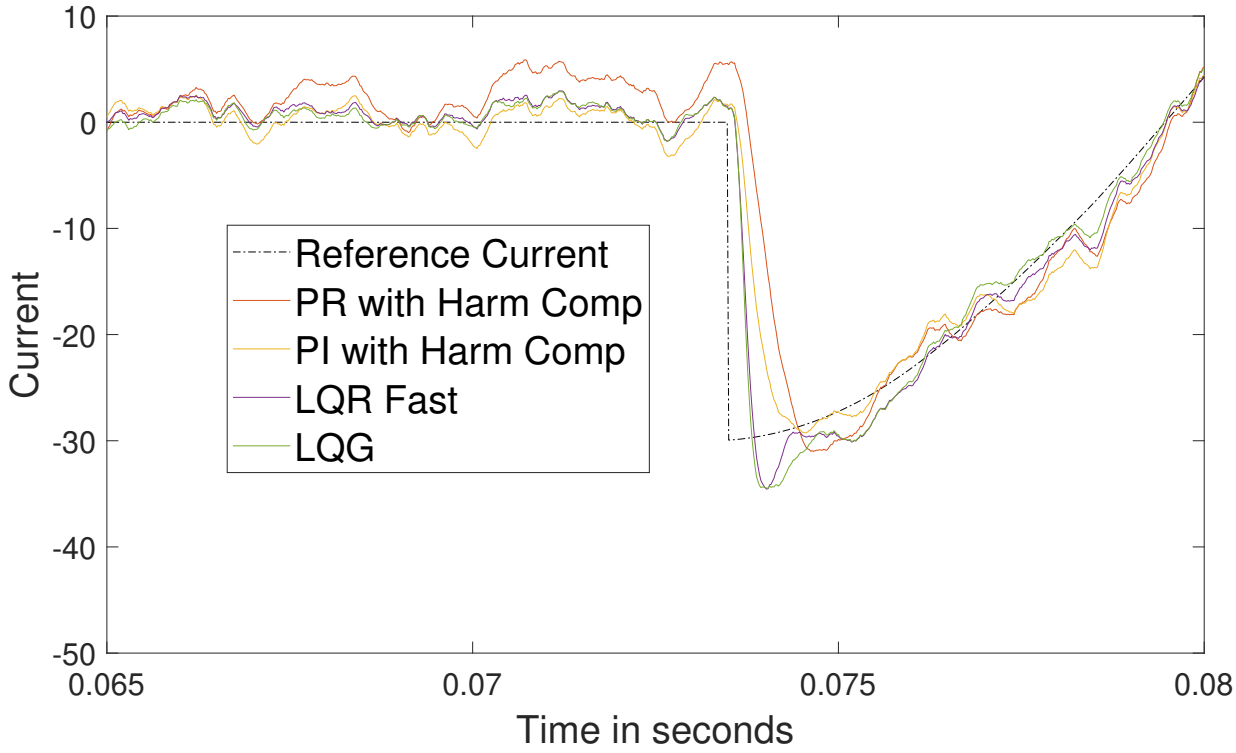

Figure 4.39: Fast controllers: two step ahead prediction with reference step. Using measured grid data.

Using prediction does appear to have made an improvement once subjected to a change in the reference current, which can be deduced by studying Figures 4.15, 4.36 and 4.37 as well as in Figures 4.24, 4.38 and 4.39. All of the controllers have a reduced undershoot when using prediction, where an increase in steps leads to a greater error reduction.

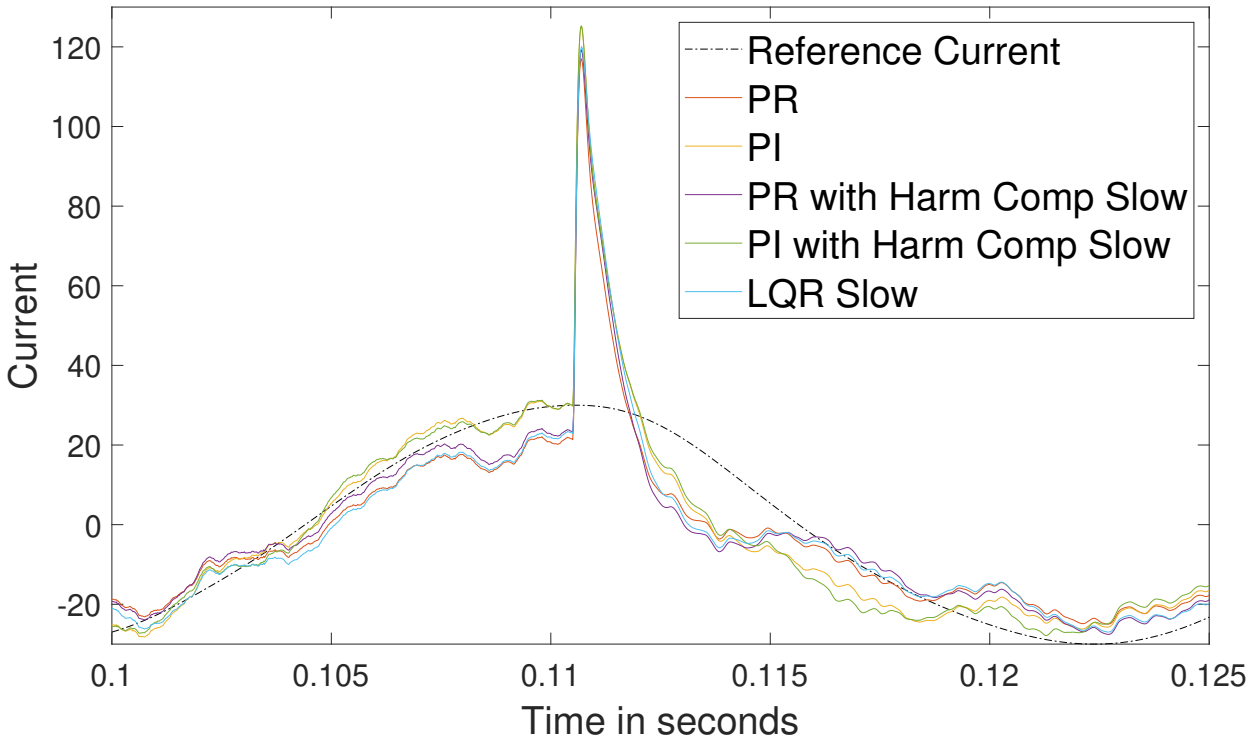

Figure 4.40: Slow controllers: one step ahead prediction with grid drop. Using measured grid data.

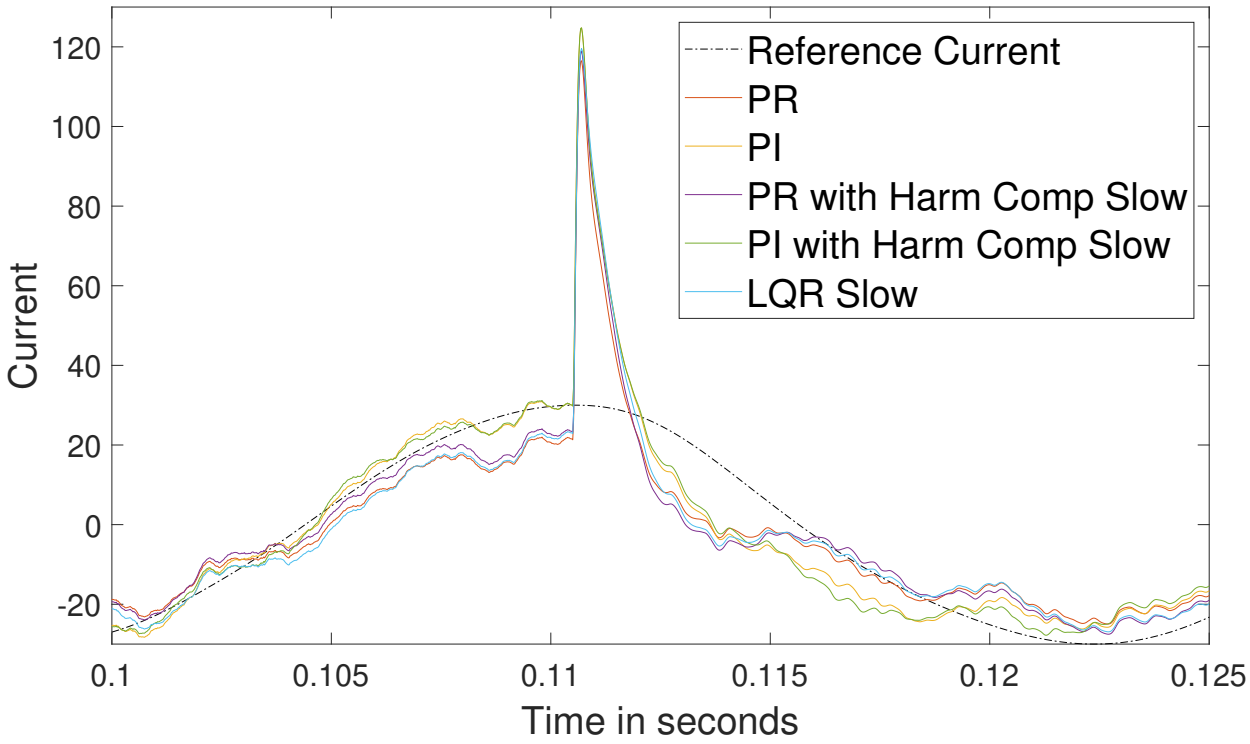

Figure 4.41: Slow controllers: two step ahead prediction with grid drop. Using measured grid data.

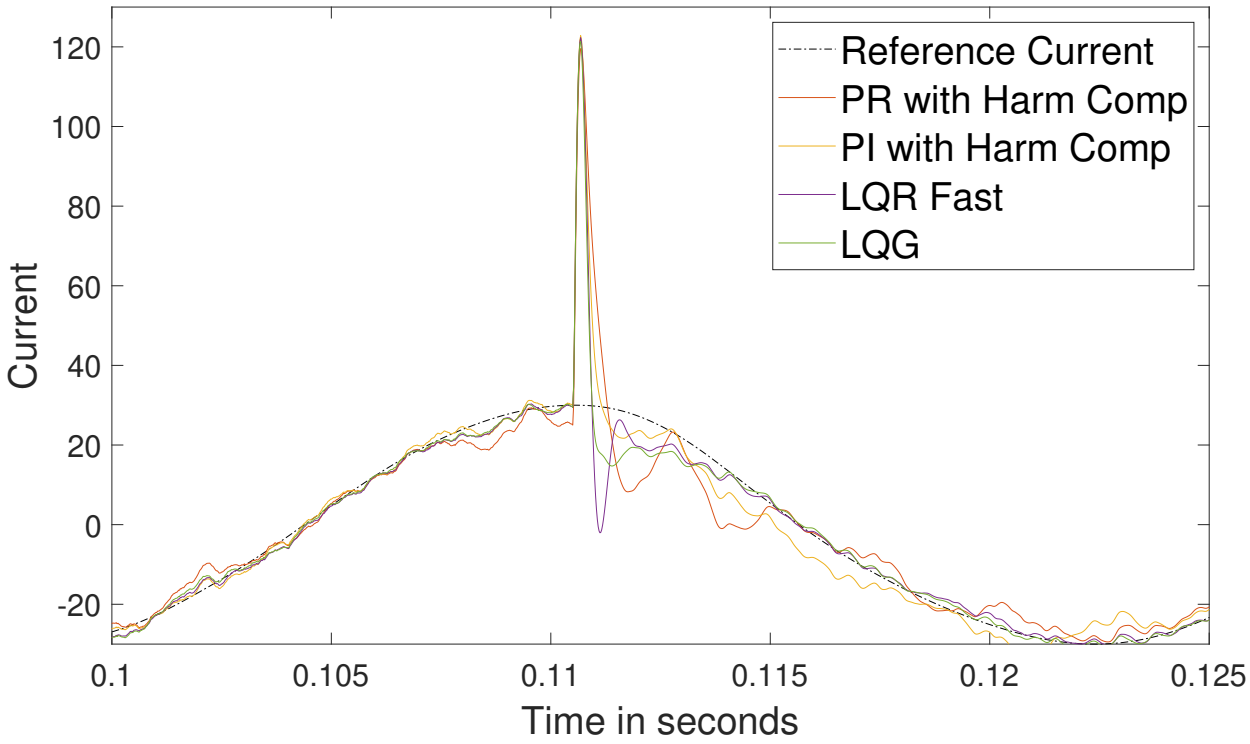

Figure 4.42: Fast controllers: one step ahead prediction with grid drop. Using measured grid data.

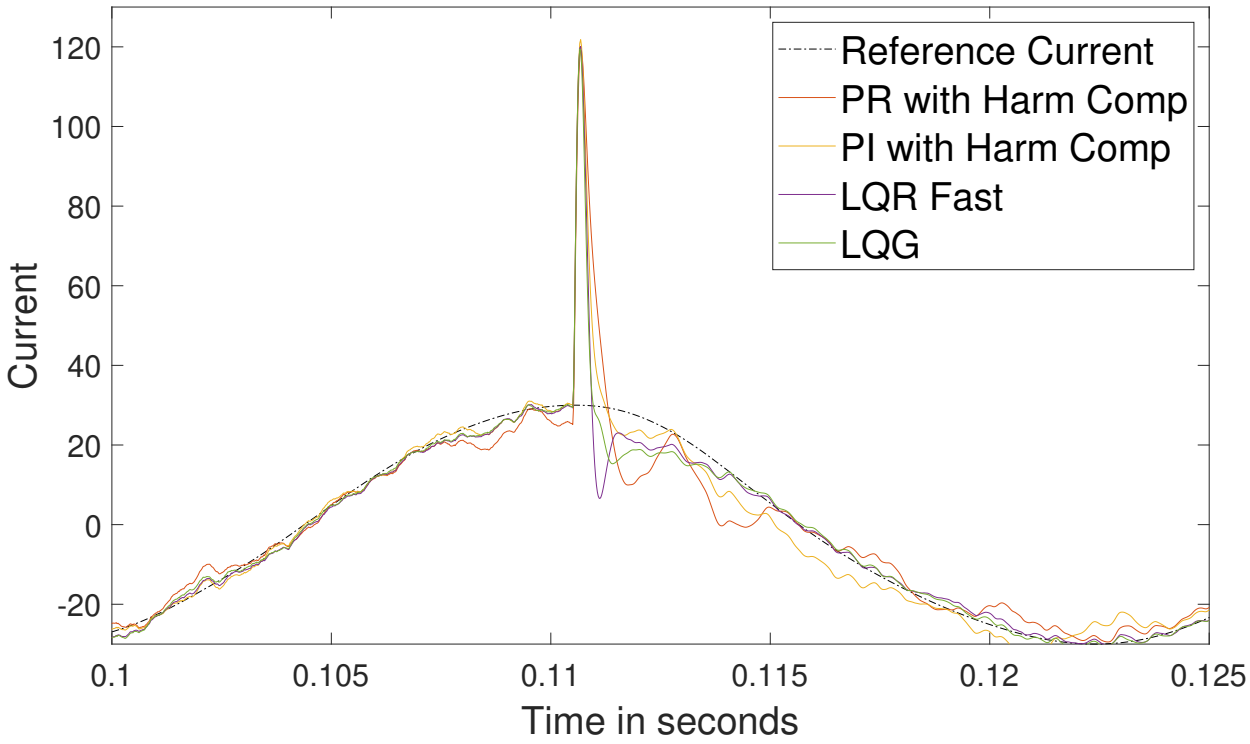

Figure 4.43: Fast controllers: two step ahead prediction with grid drop. Using measured grid data.

When the controllers are exposed to a drop in grid voltage it is clear that the LQR and LQG benefits the most from the prediction, which can be seen in Figures 4.16, 4.40 and 4.41. The undershoot is reduced to a greater extent for the LQR than for the PI and PR with harmonic mitigation, however the undershoot was larger for the LQR than for the rest. There is no apparent improvement for the slow controllers when using prediction, the improvement is seen when fast controllers are faced with a change, such as a grid drop or a step change in the reference current.

4.5 Worst case scenario applied to the fastest controllers

Since the fastest controllers are the most unstable, it is important to ensure stability for these controllers even in the worst possible cases. The base for this test will be Case 8 from chapter 3.2.8. Adding prediction often (and notably in this case) makes a system faster and more accurate in its behaviour but it also becomes more unstable if it estimates wrong or reacts to strongly. Therefore the two step ahead Smith predictor will be used in this test. In addition, the scenario that makes the system most reactive is when the grid (L_2) induction is small. Therefore L_2 will have one fourth of its normal value given in Table 2.1.

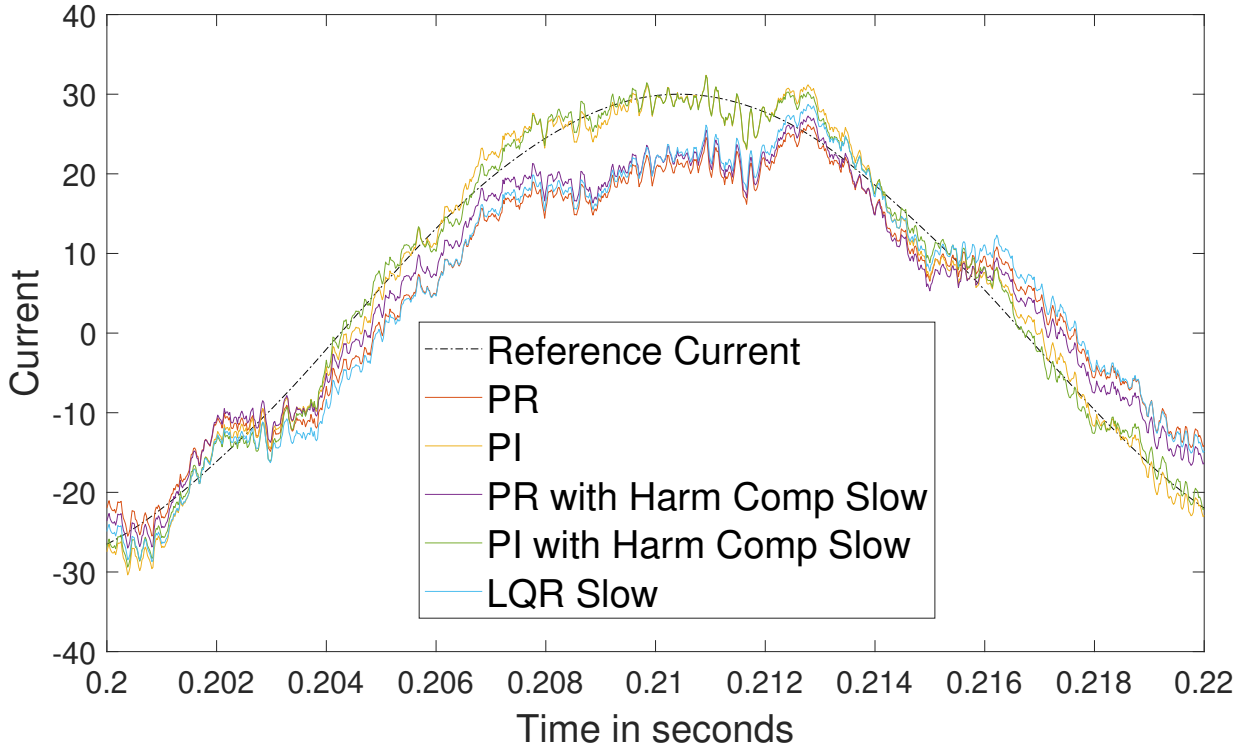

Figure 4.44: Slow controllers: worst case steady state of 30 A

Table 4.15: The RMS error between the reference and the I_2 current for the worst case when following a 30 A reference.

Controller type	RMS I_2
PR	9.044 A
PI	7.7018 A
PR With Harmonics Slow	8.6554 A
PI With Harmonics Slow	7.7404 A
LQR Slow	9.2018 A

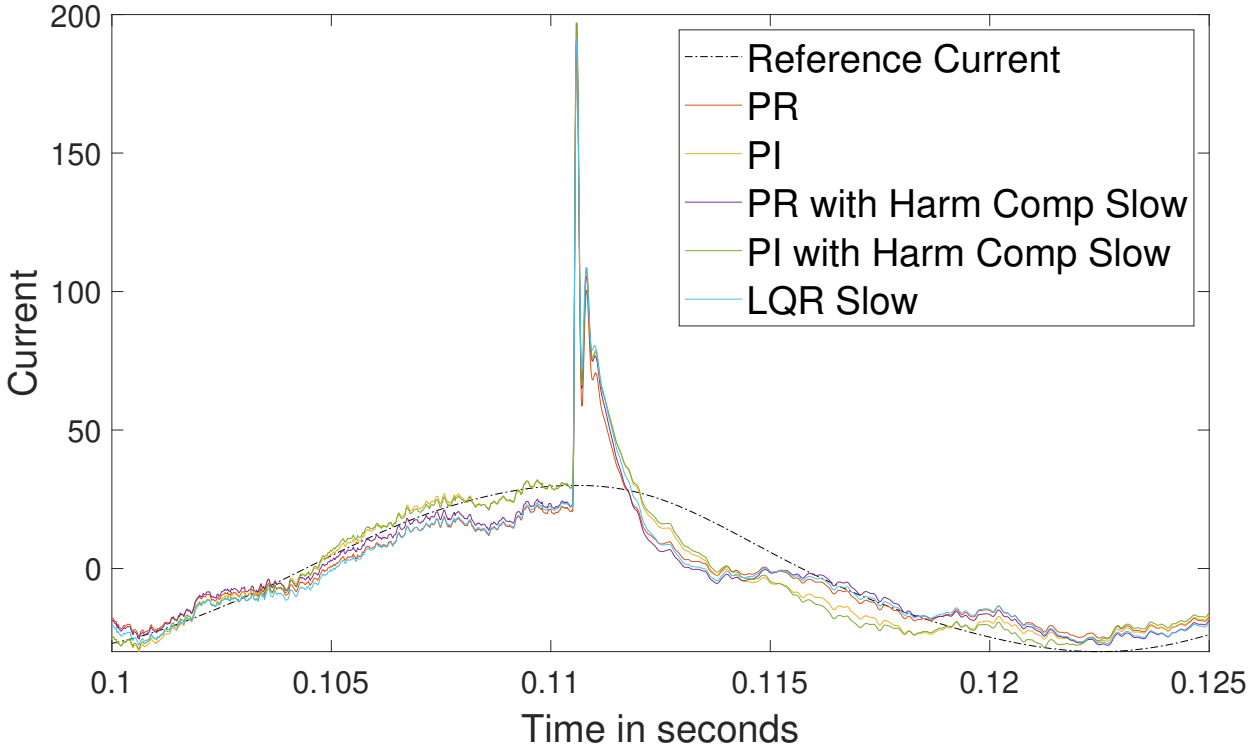

Figure 4.45: Slow controllers: worst case grid drop

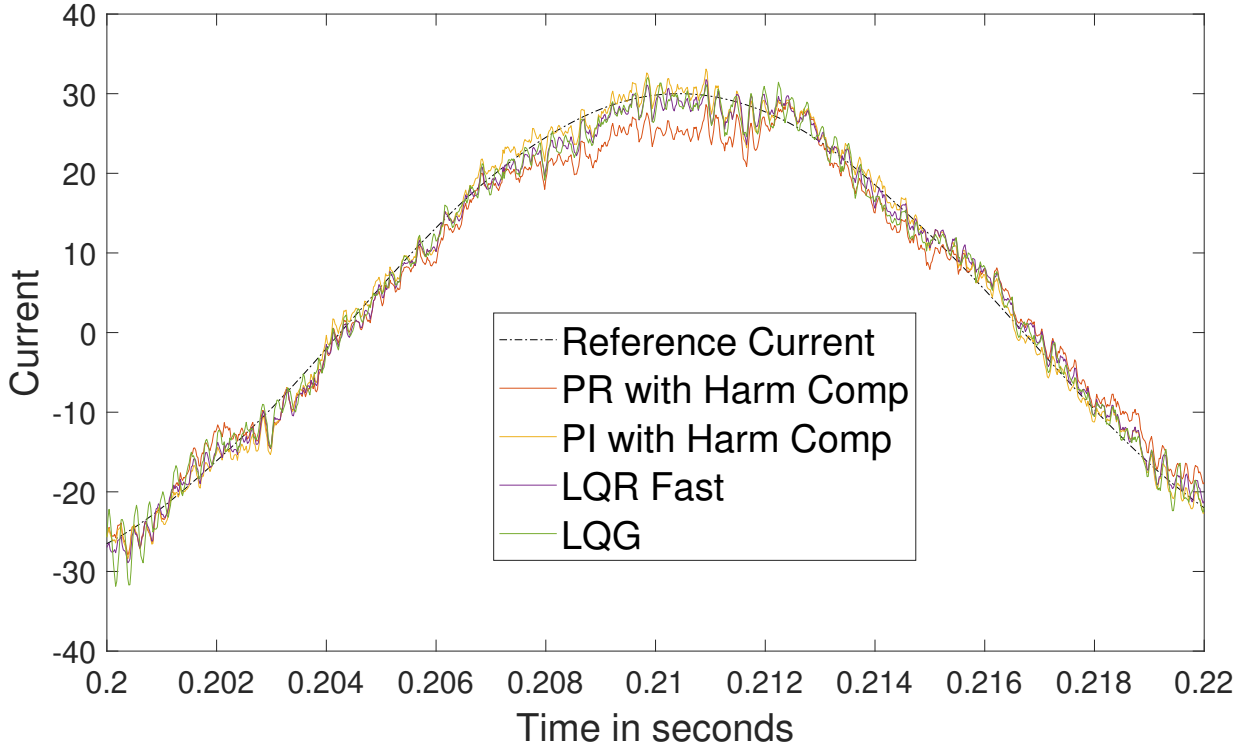

Figure 4.46: Fast controllers: worst case steady state of 30 A

Table 4.16: The RMS for steady state of 30 A for worst case

Controller type	RMS I_2
PR With Harmonics	6.359 A
PI With Harmonics	5.6036 A
LQR Fast	5.062 A
LQG Slowed down	6.9427

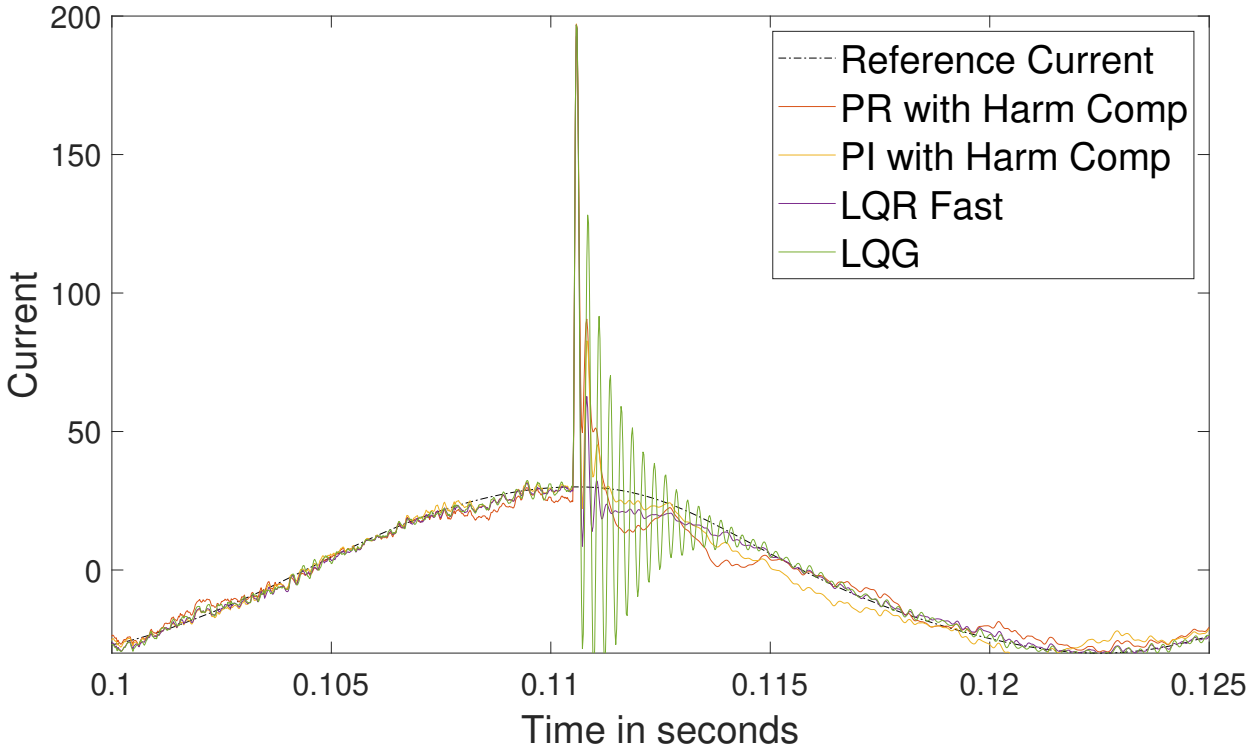

Figure 4.47: Fast controllers: worst case grid drop

The LQG oscillates heavily when faced with drop in the worst case scenario as seen in Figure 4.47. It is the model based controllers that appear to struggle the most with the worst case scenario, since they are designed with another L_2 and R_2 in mind. All of the controllers appears to have larger peak errors when faced with a grid drop in the worst case scenario as well as increase in oscillations overall, even in steady state. The slow controllers gain a second error peak when there is a grid drop, as seen in Figure 4.45.

Controller	Steady state	Overshoot	Recovery
PI slow			
PI harmonic compensation slow			
PR slow			
PR harmonic compensation slow			
LQR slow			

Figure 4.48: The results of the test cases for slow controllers, where green signifies a good result, yellow a slightly worse and red is meant to signify an underperforming controller.

Controller	Steady state	Overshoot	Recovery	Strong grid	Strong grid + prediction
PI harmonic compensation fast					
PR harmonic compensation fast					
LQR fast					
LQG					

Figure 4.49: The results of the test cases for fast controllers, where green signifies a good result, yellow a slightly worse and red is meant to signify an underperforming controller.

5
Conclusion

In this chapter are the conclusions discussed based on the results shown in chapter 4. Potential future work as well as ethics and sustainability are discussed in this chapter as well.

5.1 Evaluating I and R

When choosing integrator action there are several aspects to consider regarding the choice of using R with AC signals as opposed to using I with DC signals. The R-term underperforms when the proportional term is weak. The reason is that the controller is unable to reach the correct amplitude and instead falls short. Additionally, the control action is not able to compensate for the delays in the system and therefore the current is always out of sync with the reference. The I-term does not share these weaknesses with the R-term. It is able to accurately follow the desired reference in steady state. However it does take a longer time for the I-term to reach its steady state than it does for the R-term, shown clearly in Figure 4.16. The R-term is also unable to perfectly keep the current at zero when that is desired while the I-term does not have any problem with doing so and this is illustrated in Figure 4.13.

Other differences arise when the controllers are speeded up and noise is introduced. When the controllers are faster, the R-terms weaknesses are mostly mitigated. The controller is able to follow the reference much closer than before in regards to both amplitude and phase. When the noise is added, the error from the R-term is less prevalent than the errors that arise from the grid and measurements. With stronger controllers the R-term is instead at an advantage compared to the I-term because it reaches its steady state faster and is thereby able to avoid the current deviating from the reference for a long period of time.

5.2 Evaluating P and LQR/LQG

While the simple implementation of the P-term is great it is also that, very simple. It only takes the error of the current and applies a constant to it. The LQR instead uses the I_1 and I_2 errors together with the V_c which gives it more depth in its response. When the Kalman filter is added transforming the LQR into an LQG it is even better as seen in Figure 4.30. It is able to make faster changes with less oscillations and overshoots. The LQG and LQR are model based and does therefore experience larger decreases in performance than the P-term does when the model

does not match reality. It does however not worsen the controllers to the point of being worse than the P-based controllers. The example where the model based controllers decrease the most in performance is when the grid inductance is weak and prediction is used. In this scenario the LQG decreased the most in performance and the LQR the second most as seen in Figure 4.47. LQG is however still better in many regards than the other alternatives. The best part of using the LQG is that it is very fast at returning to its steady state. Even if it gets similar peak errors as P it is able to stabilise much quicker. Part of this is because the LQE uses information both about the LQR and the R term in order to more accurately estimate the true states, thereby limiting oscillation.

5.3 Evaluating harmonic compensation

Harmonic compensation is not beneficial with slower controllers, due to that the R-term needs to follow the reference and cannot spare resources for harmonic mitigation. If an optimal R-term is used to follow the reference and then a harmonic mitigator is added the rise time of the controller will be speeded up. When these mitigators are used and the rise time is to remain the same, then the R-term used to follow the reference needs to be tuned down leading to a worse performance in the overall aim of following the reference. If instead the rise time of the controller is unlimited, then there is no draw back of using a properly tuned harmonic mitigator since there will still be an optimally tuned R-term for the base frequency.

Additional harmonic compensator terms are sometimes completely unnecessary. One of these cases are when a model based controller such as the LQR and LQG is used. These controllers are able to remove the harmonic components without additional R-terms.

For the PI case, the compensators does not have a great effect. There is no major error added by the mitigation, but the harmonics are not greatly reduced either. The strongest harmonic mitigation for the PI seems to come from a stronger tuning of the controller and not anything specifically made for the reduction of harmonic components.

5.4 Evaluating the Smith predictor

There are two Smith predictors in this case, the one and the two step ahead predictions. Both of these versions are better than not using either in regards to peak error mitigation and overall RMS error mitigation. While in steady state no significant change is noticeable when using prediction as seen in Figures 4.14, 4.32 and 4.33 as well as in Figures 4.23, 4.34 and 4.35. The two step ahead predictor eliminates peak errors even further than the one step ahead predictor. Problems arise if the LQR, and especially the LQG, is used on a weak grid. In this specific situation the controllers become more unstable and starts oscillating heavily. The LQR is able to mitigate most of these problems but the oscillation is still present as seen in

Figure 4.47. The advantages are believed to overcome the disadvantages but some components may be damaged during heavy oscillation. For those systems it may be unwise to use the LQR/LQG with prediction without first estimating the L_2 in order to overcome the oscillation problems with a change to the SS model.

5.5 Choosing the best controller

At faster speeds the LQG is the best choice, because it has the fastest convergence towards steady state but manages to also have a very low overshoot and oscillation. The exception to this is when the prediction is used with the model based controllers and the grid inductance is weak. In this case too much instability is introduced which means that the prediction should not be used in tandem with the model based controllers.

If the model based controllers are too computationally heavy to implement then the P-based models are an apt choice. Specifically a PI with harmonic compensation is to be preferred over a PR since it follows the reference more accurately even though it requires more time to reach steady state. However if the outer loop, that has been disregarded in this thesis, is able to compensate for the amplitude problems of the PR, then the PR is the preferred choice. The PR does not suffer from convergence problems and is therefore better if the amplitude is not of concern.

It is not preferable to use an LQG for the longer rise time. The problem is that for the Kalman filter to work optimally the rise time needs to be fast and no solution was found to make it work with a rise time around 1 ms. In this scenario it would be better to instead choose the original PI controller. Any controller using the R-term is unable to match the steady state reference both in amplitude and in phase. The actual current lags the reference current which is not desired. Even if the amplitude were to be correct, the phase mismatch with the reference (and therefore also the grid) would lead to a poor power factor. The PI on the other hand does not have that problem. It is able to follow the reference at steady state and, while slow, it is able to handle the grid drops without any major problems.

5.6 Choosing I_1 or I_2

The desire to change from measuring I_1 to measuring I_2 was one of monetary cost. To be able to measure I_1 there was a need to measure quickly so that the square wave output from the PWM could be correctly measured in order to estimate the sinusoidal current that ends up in the system. The benefit of measuring I_2 is that it only has sinusoidal signals and therefore cheaper components may be used since fewer measurements are needed. In addition it is I_2 that gives the actual output in the system and is the current of interest. There is also a positive increase in performance for the currents when measuring on I_2, especially for the I_1 current which got much lower peak errors. However the I_2 current was a mixed bag where some controllers got a bit worse and some a bit better, the change was however

minimal and the important change occurred in I_1.

5.7 Future work

There are a lot of aspects that needs to be analysed in order to truly understand what is the best type of controller for the system. For example, the real system has another control loop of voltage instead of the simplified version addressed in this report. In addition, the PWM has been simplified away so there may be an even larger impact when switching from reading I_1 to reading I_2 than discussed in this report.

There is also the problem of computational loads on the CPU. It has not been analysed how many clock cycles each control scheme requires. Some control schemes may be very low on computational cost and might be able to run prediction at the same or lower cost than running another control scheme without prediction. These differences may change which controller is preferable at what stage.

A model predictive controller could be used instead of the now separated control and prediction schemes. A robust controller could be used otherwise, because a correctly implemented robust controller is guaranteed to be stable. Another way to mitigate grid drop interference is to connect a battery or a strong capacitor and let it unload when the grid drops. This leads to slower change in grid voltage, which means that the controllers can follow the reference easier. These are some control schemes that could be of use to further investigate in the future.

The results in this report are from simulations which may not properly reflect the real world. Everything should be tested on hardware because results may vary in reality. In addition, the monetary cost of using and implementing the investigated control schemes in this report has not been evaluated. This means that some controllers may be less cost effective which may change the final choice of which controller to implement.

5.8 Ethics & sustainability

This report centers around the LCL grid current control which for instance is used in the extraction of renewable energy sources such as solar panels. Therefore the improvement of the power efficiency and overall performance of the control scheme may very well help fight climate change on some level. In addition the reduction of oscillation in the system will decrease the wear and tear on the components in the chip, meaning that it will be usable for a longer time which in turn reduces the need for replacements. However, all electronics does have a high impact on the climate in regards to extracting, creating and shipping materials as well as finished components. Furthermore many metals are extracted under dubious circumstances and with questionable working conditions and labor forces. The control scheme in itself increases the lifetime of the components, however it may also increase the amount

of components used due to its efficiency and possible increase in sales.

While the technologies and techniques that where gathered during this thesis on its own helps the world with cleaner extraction of renewable energy, one needs to keep in mind from where the material and components come from and how they were extracted.

Bibliography

[1] L. Harnefors *Control of Power Electronic Converters and Variable-Speed Drives*. Compendium, 2002.

[2] D. Chädström and F. Karlsson, Conversations, January-May 2023.

[3] T. C. Wang, Z. Ye, G. Sinha, and X. Yuan, *"Output Filter Design for a Grid-interconnected Three-phase Inverter"* in Proc. of IEEE 34th Annual Power Electronics Specialist Conference (PESC 03), 2003, pp. 779–784.

[4] P. V. Brennan *Phase-Locked Loops: Principles and Practice*, 1st ed. Houndmills, Basingstoke, Hampshire, United Kingdom: MACMILLAN PRESS LTD, 1996. [Online]. Available: https://link-springer-com.proxy.lib.chalmers.se/book/10.1007/978-1-349-14006-0, Accessed April 27, 2023.

[5] Ang, K.H. and Chong, G.C.Y. and Li, Y. (2005) *"PID control system analysis, design, and technology"*. IEEE Transactions on Control Systems Technology 13(4):pp. 559-576.

[6] Q. C. Zhong and T. Hornik *CONTROL OF POWER INVERTERS IN RENEWABLE ENERGY AND SMART GRID INTEGRATION*. Chichester, West Sussex, United Kingdom: John Wiley & Sons, Ltd, 2013. ch 15, pp 251-258.

[7] B. Lennartsson *Reglerteknikens grunder* Lund, Sweden : Studentlitteratur AB, 2000

[8] Q. C. Zhong and T. Hornik *CONTROL OF POWER INVERTERS IN RENEWABLE ENERGY AND SMART GRID INTEGRATION*, 1st ed. Chichester, West Sussex, United Kingdom: John Wiley & Sons, Ltd, 2013. ch. 16, pp. 259-268.

[9] J.M.C. Geldenhuys, H. du Toit Mouton, A. Rix and T. Geyer, "Model Predictive Current Control of a Grid Connected Converter With LCL-Filter" in *Proceedings of the 2016 IEEE 17th Workshop on Control and Modeling for Power Electronics (COMPEL)*,Trondheim, Norway, 27–30 June 2016. pp. 1-6. [Online]. Available: https://www.researchgate.net/publication/307573009_Model_predictive_current_control_of_a_grid_connected_converter_with_LCL-filter, Accessed on: 2023-03-15.

[10] T. Glad and L. Ljung *Control Theory: Multivariable and Nonlinear Methods* London, United Kingdom : Taylor & Francis, 2000.

[11] J.E. Normey-Rico and E.F. Camacho *Control of Dead-time Processes* London, United Kingdom : Springer-Verlag London Limited 2007. pp 131-163

DEPARTMENT OF ELECTRICAL ENGINEERING
CHALMERS UNIVERSITY OF TECHNOLOGY
Gothenburg, Sweden
www.chalmers.se

CHALMERS
UNIVERSITY OF TECHNOLOGY